2023

Light-inducible tools for control of bacterial gene expression and antibiotic resistance

BOSTON UNIVERSITY

COLLEGE OF ENGINEERING

Dissertation

LIGHT-INDUCIBLE TOOLS FOR CONTROL OF BACTERIAL GENE EXPRESSION AND ANTIBIOTIC RESISTANCE

by

MICHAEL BRIAN SHEETS

B.S., Franklin W. Olin College of Engineering, 2017
M.S., Boston University, 2020

Submitted in partial fulfillment of the

requirements for the degree of

Doctor of Philosophy

2023

Approved by

First Reader

Mary J. Dunlop, Ph.D.
Associate Professor of Biomedical Engineering

Second Reader

John T. Ngo, Ph.D.
Associate Professor of Biomedical Engineering

Third Reader

Wilson W. Wong, Ph.D.
Associate Professor of Biomedical Engineering

Fourth Reader

Joe W. Larkin, Ph.D.
Assistant Professor of Biology
Assistant Professor of Physics

Fifth Reader

Alexander A. Green, Ph.D.
Assistant Professor of Biomedical Engineering

ACKNOWLEDGMENTS

I have been incredibly fortunate to have the support of so many while doing the work described here. First, I would like to thank my advisor, Dr. Mary J. Dunlop. I could not have asked for a better scientific, professional, and personal mentor. Thank you for your guidance, project planning, experimental troubleshooting, mentorship ideas, writing advice, figure design tips, organizational skills, and being a kind and compassionate role model. I would also like to thank my committee, Dr. John T. Ngo, Dr. Wilson W. Wong, Dr. Joe W. Larkin, Dr. Alexander A. Green for their valuable input on my work and thought-provoking conversations.

My lab-mates, mentors, and mentees have taught me so much. I am especially grateful to Dr. Imane El Meouche, Dr. Nicholas Rossi, Dr. Nathan Tague, Dr. Ariel Langevin, Dr. Tiebin Wang, Dr. Xi Wen, Dr. Nadia Sampaio, Dr. Jonghyeon Shin, Dr. Jean-Baptiste Lugagne, Dr. Razan Alnahhas, Dr. Virgile Andreani, Dr. Heidi Klumpe, Caroline Blassick, Cristian Coriano-Ortiz, Hellen Huang, Owen O'Connor, Eric South, Chris Kuffner, and Dr. Mark Aronson. There has never been a dull moment in the lab and offices, and you all have made the process of research truly enjoyable. Thank you for the lab lunch conversations, game nights, project advice, and sharing in the highs and lows of scientific discovery.

My path to BU was made possible by so many teachers and mentors along the way. I am lucky to have been guided by Dr. Jean Huang in microbiology and excitement for the unknown, Dr. Alisha Sarang-Sieminksi in biological design and passion for making a difference, Dr. Jon Adler for text analysis and the power of a story, and Dr.

Janna Bednenko and the team at Tetragenetics for an understanding of industrial biotechnology and how to choose the right microbe. I would not have found this field if not for the biotechnology club started by Dr. Rebekah Ravgiala, and the tireless educational efforts and accomplishments of Dr. Natalie Kuldell. I have been so lucky to work the entire BioBuilder team, and it has fundamentally shaped me as a researcher, an educator, and a person.

Finally, thank you to my friends & family for your tireless support and boundless enthusiasm. To my grandparents, Ed & Jeanne Dery and Stuart & Madeline Sheets, thank you for your kindness and shaping me into the person I am today. To my parents, Brian and Kelly Sheets, and my brother Andrew, I am forever grateful for all you have done for me. Thank you for encouraging me at every turn, and always caring about me. To David, thank you for coming on this journey with me. You make any day brighter and make me happier than I thought possible. Here's to the next thousand adventures.

Thank you, all.

LIGHT-INDUCIBLE TOOLS FOR CONTROL OF BACTERIAL GENE EXPRESSION AND ANTIBIOTIC RESISTANCE

MICHAEL BRIAN SHEETS

Boston University College of Engineering, 2023

Major Professor: Mary J. Dunlop, Ph.D., Associate Professor of Biomedical Engineering

ABSTRACT

Antibiotics and their corresponding resistance genes act as a tool to control bacterial survival. Antibiotic resistance is used to select for desired engineered cells, and study how pathogens acquire resistance to continue infection. Here, we develop tools to control the expression of antibiotic resistance genes using light. To accomplish this, we use optogenetics, the regulation of cellular behavior using light as a direct and programmable input for gene expression. We develop an optogenetic recombinase in *Escherichia coli* through split-protein engineering techniques, and characterize the behavior of our best candidate in detail: a split Cre recombinase that responds to blue light. We apply this optogenetic system to control the expression of resistance genes for four antibiotics: ampicillin/carbenicillin, kanamycin, chloramphenicol, and tetracycline. By varying the expression levels of these genes, we tune the concentrations at which bacteria can survive before and after light exposure. We then apply this system to improve production of fatty acids. Finally, we make progress toward characterizing the impact of resistance activation timing on bacterial survival. This work creates tools that are broadly useful for spatiotemporal control of bacterial survival, and enables precise studies on how bacterial resistance spreads at the single-cell level.

TABLE OF CONTENTS

LIST OF TABLES

LIST OF FIGURES

CHAPTER 1. Introduction

Bacteria are highly optimized input-output processors, interacting with their environment in a variety of ways. Microbes have evolved ways to sense and respond to chemicals, heat, magnetism, electricity, pressure, osmolarity, salinity, and light. For any physical, chemical, or biological process, there is likely an organism that has found a niche which requires sensing and responding to it. Light is particularly important to sense for many organisms which rely on photosynthesis or have day/night cycles. The field of synthetic biology has utilized many of these sense-and-response systems, and applied them to report gut health,[1] sense environmental contaminants,[2] or improve microbial bioproduction.[3]

The very first example of an engineered organism was an *Escherichia coli* strain engineered to be resistant to kanamycin, fifty years ago in 1973.[4] Ten years later, early examples of engineered genetic control involved using the small molecule isopropyl beta-D-thiogalactoside (IPTG) to activate gene expression through derepression of LacI.[5] Here, we build on this early research as well as recent advances in light-induced gene regulation, protein engineering, and antibiotics to engineer optogenetic control of antibiotic resistance. This work focuses first on developing effective and well characterized optogenetic gene regulation using recombinases. We then apply these systems to improve metabolic engineering and study the development of antibiotic resistance.

1.1. Optogenetics

Light is a particularly useful tool in gene expression, due to its ability to be precisely controlled in time and space, ability to interface with computational setups, and orthogonality to most other small molecule or metabolic cell processes. Tools using light for cellular control have expanded greatly in recent years, showing much promise to enable a greater understanding of complex and single-cell processes, as well as regulate gene expression for engineering goals.

1.1.1. Optogenetic control systems

Optogenetics has proven to be valuable across all domains of life. Much of optogenetics to-date has focused on neural applications, with single-neuron control using light enabling a wide variety of new findings in neuroscience. In particular, optogenetics has enabled research on how activation or silencing of single neurons impacts their circuits and contexts.[6,7] Many of these tools rely on light-activated ion channels, including microbial rhodopsins. These have been applied to enable whole-brain functional connectivity mapping[8] and further understanding of social behavior, spatial learning, and memory.[9,10]

In the past two decades, there has been an increasing interest in applying light regulation to gene control in bacteria.[11–14] Systems which rely on small-molecule inducers of gene activation are still the standard in synthetic biology, and often used to regulate gene expression.[15] However, light has key advantages for genetic control. Light can be precisely controlled in time, where it can be added and removed from a culture much more easily than a small molecule. Light can also be tightly controlled in space,

and can be applied to individual cells through a digital micromirror device (DMD)[16] which projects light through the microscope objective for spatially patterned illumination, allowing for temporally-programmable, micron-scale control.[17–19]. It is also relatively inexpensive to apply to bulk cultures, and has minimal toxicity and interference with native chemical pathways. Overall, optogenetics shows great promise as a tool for understanding biological systems and for controlling genetic and metabolic expression.

The first optogenetic control strategy in *E. coli* used the *Synechocystis* phytochrome Cph1 fused to the native *E. coli* EnvZ histidine kinase. This system used red light to turn off the *ompC* promoter regulated *lacZ*, creating a black pigment output only in the absence of red light.[20] Since then, a panoply of optogenetic tools in bacteria have been developed (Figure 1-1). Many of these focus on light-inducible promoters, such as blue light-sensitive EL222,[21] pDusk/pDawn,[22] and BLADE (Vvd-AraC),[23] or two-component systems like the red-green sensitive CcaSR.[24,25] Light-oxygen-voltage (LOV) domains form the core of many blue light-sensitive proteins, notably AsLOV2.[26,27] A modified AsLOV2 domain is used in LOVtag, a degradation tag made accessible to the Clp protease machinery under blue light.[28] Another common strategy is to use photodimers to create light-inducible split proteins. This has been applied successfully to the T7 RNA polymerase in *E. coli*[29] as well as Cas9 in mammalian contexts,[30] and can theoretically be applied to many proteins with known split sites. Overall, these approaches provide complimentary ways to regulate gene expression using light, with each system fitting a specific context or application. For example, the CcaSR system has been applied to understand the benefit of colanic acid on the *Caenorabditis*

elegans gut through colanic acid producing *E. coli*,[31] and multiple optogenetic systems have been used to understand and regulate the role of cyclic-di-GMP in biofilm formation and biofouling.[17,32,33]

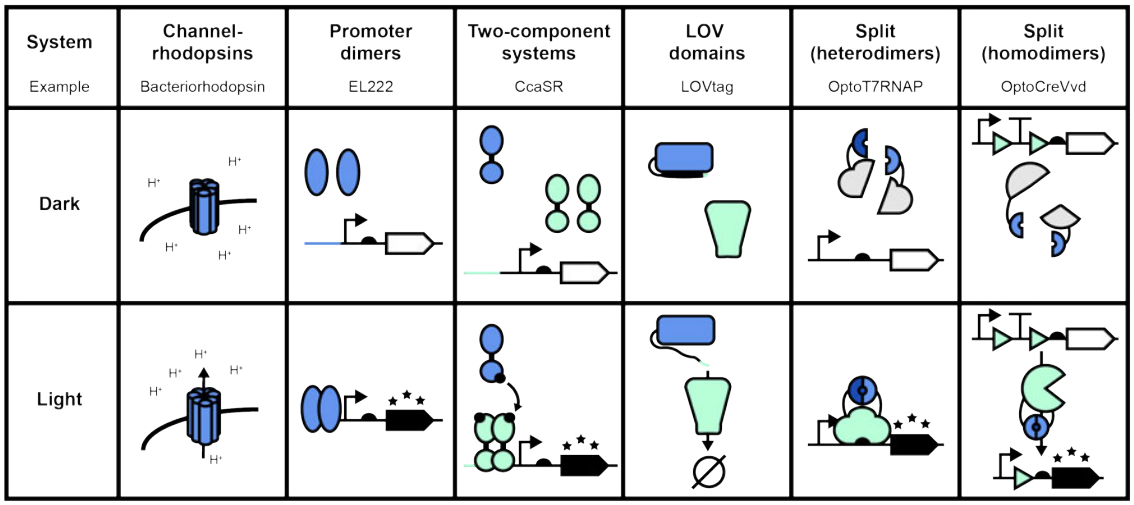

Figure 1-1. Classes of optogenetic systems.

Behavior of common optogenetic systems in the dark and light. Channelrhodopsins are closed in the dark, and act as a proton pump when exposed to light. DNA-binding dimers change conformation on exposure to light and can activate (or repress) promoters. Two-component systems have one component that is activated by light, and phosphorylates a secondary promoter-activating domain. LOV domains contain a Jα helix which is tightly folded in the dark, and unfolds in response to light. Heterodimers are distinct proteins which bind (or unbind) to each other on light exposure, and can be used to bring together fragments of other proteins to restore function. Homodimers are identical proteins which bind (or unbind) on light exposure, and can also be used to bring together fragments of other proteins to restore function.

1.1.2. Optogenetic recombinases

One tool that has shown great promise for gene regulation is the optogenetic recombinase. Recombinases are proteins which recognize short DNA sequences and invert or remove the DNA sequence between them. Tyrosine recombinases do this by forming a tetramer around two recognition sites, breaking DNA strand pairs to create a Holliday junction, then re-ordering the target sequences with half of each original

recognition site. Two tyrosine recombinase tools most commonly used for engineered gene regulation are Cre/*lox* and Flp/FRT. Cre recombinase is native to the P1 bacteriophage, and recognizes the 34 base pair *lox* site. Flp recombinase is native to *Saccharomyces cerevisiae*, and recognizes the 48 base pair FRT (Flippase Recognition Target) site. Both have been used extensively across biological systems for lineage tracing,[34] gene delivery, gene silencing,[35] genetic circuits and computation,[36] signal amplification,[37] and more.[38]

Light-inducible recombinases have proven to be a valuable tool in mammalian and yeast cells.[39,40] These systems have been used to understand the casual relationship between dopamine neuron firing and positive reinforcement in mice[41] and control activation of CAR-T cell therapeutics.[40,42] In yeast, these systems have been used to create artificial consortia,[43] enable genome shuffling,[44] and control carotene production.[45] However, there had not been a functional optogenetic recombinase developed for regulation of gene expression in bacteria.

1.1.3. Optogenetics in metabolic engineering

Using light to control gene expression is a promising strategy to improve product yields in metabolic engineering.[46,47] Gene regulation is extremely important for bioproduction, as many metabolic targets are costly to make or toxic for cells, encouraging the growth of "cheater" cells that do not produce the compound of interest. Bioproduction often uses a growth phase followed by a production phase, where cells are grown to near-stationary phase before the metabolic system of interest is induced.[48] Small molecules are often used as an inducer, but can be expensive and cannot be removed

from a culture once added. Light as an activator can be applied to bioreactors without the need for costly small-molecule inhibitors, will not interfere with downstream purification processes, and can be turned on and off at any point in the growth or production phase. However, light does face its own issues in bioreactor contexts, particularly with issues of light penetration in dense cultures, and the cellular burden placed by the optogenetic systems themselves.[47] Intense illumination in the blue and ultraviolet wavelengths can cause cell toxicity,[49] and could cause cultures to overheat. Even with these limitations, optogenetic regulation has already shown value in metabolic engineering.

Light induction has been applied to bioproduction in a variety of promising ways. One strategy used blue light-sensitive EL222 and red light-sensitive BphS to control the cell cycle length in *E. coli*, which they used to improve acetoin and poly(lactate-co-3-hydroxybutyrate) production.[50] Similarly, EL222 has been used to repress the central metabolism through CRISPRi, increasing muconic acid production.[51] Another strategy involved the use of blue light-sensitive YF1/FixJ to regulate *lacI* expression, which was used to control production of melvalonate and isobutanol.[52] The clustering of light-inducible dimers has been used to create synthetic organelles which regulate the violacein pathway.[53] In mixed cultures, optogenetic control of co-culture dynamics has also been promising, including the use of FixJ to regulate a toxin-antitoxin system, controlling the *E. coli* growth rate in a yeast co-culture to improve production of isobutanol and naringenin.[54] Additionally, use of optogenetics and fluorophores enables closed-loop computational supervision, which is highly programmable for applications like co-culture control and shows promise for regulating metabolic systems.[55,56] As novel optogenetic

systems are created and improved, the control they provide continues to boost metabolic engineering yields across product types.

1.2. Antibiotic resistance

Bacteria have evolved antibiotics and resistance genes to counteract them long before humans used either. The discovery of antibiotics transformed the medical practice, and extended the average human lifespan by twenty-three years.[57] The later discovery of antibiotic resistance genes has been foundational to synthetic biology, allowing selection of bacteria with desired genes or phenotypes. However, these resistance genes in pathogenic contexts are a severe threat to human health and our current medical system.

Cells generally develop genetic resistance in two primary ways: through the mutation of the antibiotic target which nullifies the effect of the antibiotic, or by the acquisition of a separate resistance gene. The ease of transfer of resistance genes is primary to both their use as a tool and their clinical concern. When used in synthetic biology, their portable nature enables them to be placed on plasmids with other genes of interest and used to select for the acquisition of the entire plasmid, or for integration of multiple genes into the chromosome. Yet, this portability also allows resistance genes to spread between pathogenic strains and allows cells to acquire multiple resistances, making many of these genes a serious clinical issue.

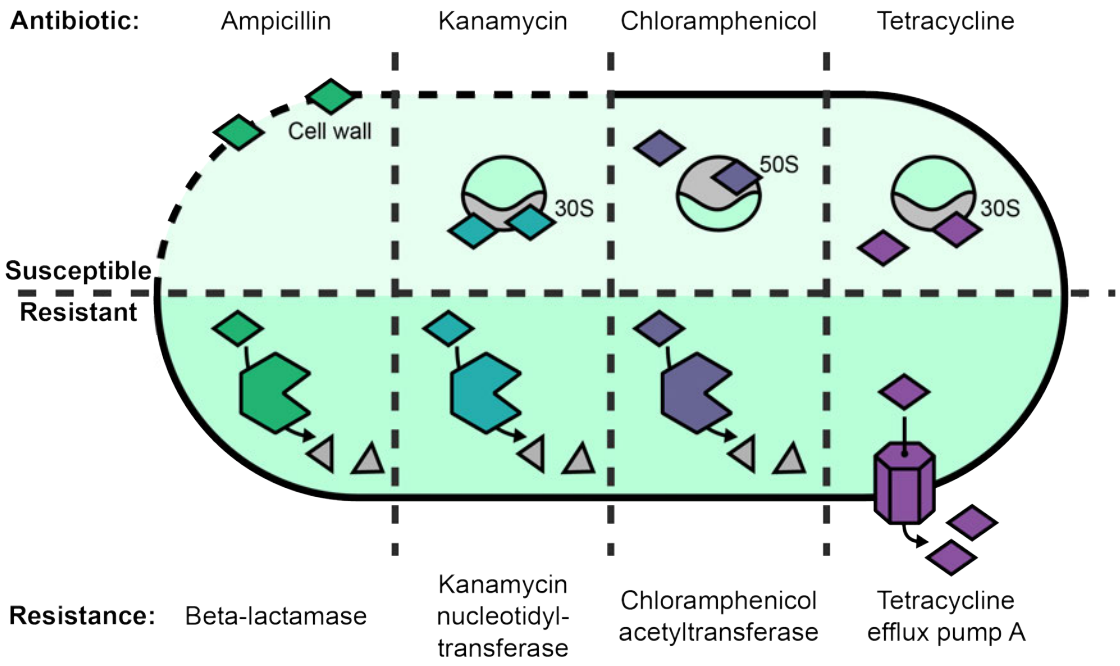

Figure 1-2. Examples of antibiotic resistance genes.

Ampicillin is a bactericidal beta-lactam antibiotic that interferes with the cell wall biosynthesis. The beta-lactamase enzyme cleaves ampicillin. Kanamycin is a bactericidal aminoglycoside that binds the 30S ribosomal subunit, inactivated by the kanamycin nucleotidyltransferase enzyme. Chloramphenicol is a bacteriostatic antibiotic that interferes with the 50S ribosomal subunit, inactivated by the chloramphenicol acetyltransferase enzyme. Tetracycline is a bacteriostatic antibiotic that interferes with the 30S ribosomal subunit, and is exported by the tetracycline efflux pump A.

1.2.1. Antibiotic resistance as a tool

Nearly all work done in bacterial synthetic biology relies on antibiotics. When recombinant DNA is introduced to cells on a plasmid or chromosomally, an antibiotic resistance gene is used as a standard to select for correct uptake of the DNA of interest. Portable resistance genes act as an easily standardized way to select for genetically modified cells of interest, and can be more convenient than selection-based approaches by ensuring cells require the DNA of interest to grow. Orthogonal resistance genes can also be used to select for uptake of multiple genetic constructs in the same cell. A few of these resistance genes are often used as standard in synthetic biology, and have been

popularized by plug-and-play plasmid collections like BglBricks,[58] to the point where most labs will have plasmids containing these resistance genes and the corresponding antibiotics on hand (Figure 1-2).

However, there has been little work done to-date enabling inducible control of resistance genes. An analogous recent development is creation an inducible origin of replication, another key plasmid component.[59] This novel method of control is useful across synthetic biology, and furthered research from biological data storage[60] to whole-cell riboswitch diagnostics[61] to decoupling growth and production phases in metabolic engineering.[62] Similarly, control of resistance genes can enable novel applications. Tunable expression of antibiotic resistance has been applied in synthetic evolution and protein production approaches.[63] When coupled with optogenetics, light-controlled resistance has been shown to enable setpoint control in bacterial co-cultures.[55] For these and other applications, we need systems that enable tight regulation of resistance gene expression. Additionally, inducible control of different classes of antibiotics can allow for selection regardless of other plasmid selection markers being used, or multiplexed control requiring multiple conditions to be met for cell survival. Antibiotic resistance is a key tool in synthetic biology, and enabling novel ways to control resistance in space and time can expand our regulation of cellular processes across application areas.

1.2.2. Antibiotic resistance as a threat

When penicillin was discovered in 1928, it fundamentally altered how humans interact with our microbes. Deaths due to infection fell drastically, and the ability to prevent harmful microbial growth enabled new surgical practices, with confidence that

surgery was much less likely to cause a fatal infection. However, human use and overuse of antibiotics has caused an increased spread of antibiotic resistant bacteria.[57] A recent meta-analysis found that antibacterial resistance was responsible for 1.27 million deaths in 2019 alone, with *E. coli* as a pathogen of particular concern.[64] Multidrug-resistant species have often been found in healthcare and agricultural facilities where regular mixing of many species occur, but in recent years have increasingly been found in communities beyond these settings.[65,66] Additionally, novel antibiotics are being developed at a plummeting rate. Relatively few new antibiotics are in the clinical pipeline, and even fewer of these have novel mechanisms.[67] This is in part due to the large costs of bringing a new drug to market and "last resort" usage of novel antibiotics to preserve their efficacy, along with scientific and technical challenges.[68]

With the current state of antibiotic discovery, it is increasingly important to discover how bacteria become resistant to antibiotics, and how single instances of resistance acquisition can lead to a problematic resistant infection. Bacteria can acquire genetic resistance in two primary ways: vertically through evolution and inheritance of native genetic systems so that antibiotics no longer prevent cell growth, or horizontally through acquisition of foreign genetic material that enables resistance.

1.2.3. Horizontal gene transfer across scales

Acquisition of antibiotic resistance through horizontal gene transfer (HGT) is the main mechanism through which resistance genes are spread, and as such, is a major public health concern.[69] The molecular mechanics of HGT via conjugation, transformation, and phage transfer have been well studied, and our current understanding

extends to how they operate *in vivo*.[70,71] Similarly, the large-scale genomic impact of resistance spread through HGT has been extensively characterized, revealing how HGT has contributed to surging resistance to multiple classes of antibiotics on a global level.[72,73] However, the single-cell dynamics associated with expression of newly acquired resistance genes have been much less well defined. In particular, little is known about what antibiotic exposure conditions allow an individual cell to move from a susceptible to resistant phenotype, and how these individual events ultimately lead to resistance at the community level. This is a significant gap, because studies that reveal events associated with initial acquisition of resistance can inform the types of treatment plans that would best prevent and combat different types of clinically resistant infections.

The significance of when individual gene acquisition events lead to resistance has been highlighted recently in a small number of studies that hint at the importance of timing for different antibiotics and species. Notably, recent work in this area has shown that even after tetracycline exposure, acquisition via conjugation of the *tetA* efflux pump gene can confer phenotypic resistance in *Escherichia coli*.[74] This is in part due to the AcrAB-TolC efflux pump, which weakly exports tetracycline, allowing just enough cellular function for a small amount of TetA expression, which then acts as a positive feedback loop allowing the cell to achieve a resistant phenotype. However, this phenomenon appears to be antibiotic specific. For example, another recent study on HGT and multispecies interactions suggests that gene acquisitions after antibiotic exposure do not result in phenotypic resistance to kanamycin.[75] Additionally, time-lapse microscopy from this work highlights that not all successful resistance gene acquisitions led to long-

term cell survival. The contrast is interesting because it is unclear whether and how the antibiotic class and resistance mechanism affect survival and community proliferation. Further, drug efflux pumps are also known to have inconsistent levels of impact on different antibiotics, further highlighting the potential for heterogeneity in gene acquisition time and conditions.[76] The spatiotemporal control enabled by optogenetics is well suited to unpack the spatial and temporal conditions that lead from resistance acquisition to proliferation. This creates the framework for a thorough understanding of how individual gene acquisition events can lead to resistance in a single cell, and how survival of single resistant cells leads to bacterial population-level resistance.

1.3. Summary

This thesis contains five chapters covering the development and application of an optogenetic recombinase in *E. coli*. In **Chapter 2**, we developed a novel optogenetic recombinase, OptoCreVvd2. In the process, we test multiple recombinases and photodimers, and use protein split sites found computationally, rationally, and from literature. We then thoroughly characterize the light activation conditions needed and temporal dynamics of our best candidate, a highly functional split optogenetic recombinase.

Using this system in **Chapter 3**, we enable optogenetic activation of antibiotic resistance genes. We focus on resistance genes for four common antibiotics: ampicillin, kanamycin, chloramphenicol, and tetracycline. To enable inducible survival for each antibiotic, we tune resistance expression levels by varying genetic elements including the

copy number, promoter, ribosome binding site, and protein itself. We ultimately create four inducible resistance systems for different resistance genes across antibiotic classes. We characterize a subset of these systems through single-cell time lapse microscopy, and further apply them to improve octanoic acid production through light-induced production coupled with antibiotic-mediated selection of producers.

In **Chapter 4**, we begin to apply these light-inducible resistance systems to study how the activation timing of resistance acquisition impacts bacterial survival. We couple each inducible resistance gene previously developed with a fluorescent reporter, to enable an improved understanding of when cells begin to express resistance genes and how this translates to phenotypic resistance. We further discuss how this system can be used to understand the impact of resistance gene acquisition on bacterial survival. Here, we also discuss the development of a two-fluorophore Cre "stoplight" reporter which can be used to better characterize future Cre induction systems, and a red-light inducible split Cre recombinase.

In **Chapter 5**, we detail notable but nonfunctional systems we created and characterized, including recombinases, reporters, and a split resistance protein. We detail light-inducible recombinases which did not perform as well as OptoCreVvd2, and various reporter architectures tested in the development of inducible resistance. We also discuss an attempt at developing a split beta-lactamase enzyme.

This thesis is both about the tools we developed and the findings those tools enabled. Our hope is that these tools will continue to be useful for applications across the realm of bacterial gene regulation, both similar to and beyond what we have done here.

Additionally, we hope that the findings here about how antibiotic resistance can be applied as a regulation tactic in metabolic engineering, and when bacterial gene acquisition leads to strain proliferation, will inform these fields moving forward.

CHAPTER 2. Light-inducible recombinases for bacterial optogenetics

2.1. Disclosure & Copyright Statement

This chapter is a modified version of "Light-Inducible Recombinases for Bacterial Optogenetics" by Michael B. Sheets, Wilson W. Wong, and Mary J. Dunlop, 2020. Reprinted with permission from *ACS Synthetic Biology* 9, 2, 227–235.

2.2. Abstract

Optogenetic tools can provide direct and programmable control of gene expression. Light-inducible recombinases, in particular, offer a powerful method for achieving precise spatiotemporal control of DNA modification. However, to-date this technology has been largely limited to eukaryotic systems. Here, we develop optogenetic recombinases for *Escherichia coli* which activate in response to blue light. Our approach uses a split recombinase coupled with photodimers, where blue light brings the split protein together to form a functional recombinase. We tested both Cre and Flp recombinases, Vivid and Magnet photodimers, and alternative protein split sites in our analysis. The optimal configuration, OptoCreVvd, exhibits strong blue light-responsive excision and low ambient light sensitivity. For this system we characterize the effect of light intensity and the temporal dynamics of light-induced recombination. These tools expand the microbial optogenetic toolbox, offering the potential for precise control of DNA excision with light-inducible recombinases in bacteria.

2.3. Introduction

Optogenetic tools enable novel applications for synthetic biology.[6,10,77–79] These tools typically use light to control expression of genes, often relying on light-dependent changes in protein state to control protein-protein interactions,[29,39] promoter systems,[20,24] and ion channels.[80] Optogenetic systems offer many advantages over traditional chemical approaches for controlling gene expression due to the direct and programmable nature of light as an input. Using light instead of small molecules can give precise spatiotemporal control over regulation, and can circumvent the need to change media or otherwise disrupt the system to add or remove a chemical inducer. As light is easily programmable using electronics, optogenetic tools can also interface with dynamic computer-based control and feedback.[81,82]

Microbial optogenetic approaches have revealed a myriad of new applications that take advantage of the precise, programmable nature of light. As examples, light has been used to control expression of enzymes involved in biofuel synthesis[83,84] and to regulate bacterial growth via metabolic control.[53,85] In addition, it has been used to enable light-activated drug release from hydrogels[86] and patterning of *Escherichia coli* onto multiple materials,[87] indicative of the wide ranging potential of optogenetic approaches. At present, the current bacterial optogenetic toolset primarily includes one or two-component systems[20–22,88,89] and split proteins.[29,90,91]

Recombinases are proteins that recognize specific 30-50 base pair (bp) sequences of DNA, and excise the “target” DNA between the sites along with one of the recognition sites. Their ability to manipulate DNA makes them particularly useful for complex

cellular logic circuits and engineering gene circuits with memory.[36,92,93] Light-inducible recombinases have been notably useful in mammalian systems[39,94–98] and yeast.[44] Having recombinases that are inducible at the protein-level can allow specific cells within a population to be targeted for recombination in response to spatial patterning of light, and there is no need to change media or wait for a chemical inducer to diffuse. Recombinase enzymes can be made light sensitive by splitting the gene into N-terminal and C-terminal fragments, and linking a sequence for a light-sensitive photodimer to each fragment. Upon light induction, the photodimer undergoes a conformational change that allows it to dimerize, bringing the two fragments together. This split-protein approach has been shown to work for both chemogenetic and optogenetic split-recombinases in eukaryotic systems.[39,95] However, although split-recombinases for prokaryotes do exist, inducibility has not been characterized and they can be slow, for example, requiring 24 hours for DNA excision.[99]

Here, we develop and optimize an optogenetic recombinase for *E. coli*. We focus primarily on split Cre linked to Vivid (Vvd) photodimers. Cre is a commonly used tyrosine recombinase from the P1 bacteriophage that excises DNA flanked by *loxP* sites.[100] Vvd is derived from the fungus *Neurospora crassa*, and homodimerizes under blue light and separates in the dark.[101,102] In developing our light-inducible recombinase we also explored Flp recombinase and Magnet photodimers,[103] as well as multiple protein split sites within each recombinase. Here, we introduce an optimized design, which we denote OptoCreVvd, which excises target DNA completely in 2 hours. We also characterize sensitivity to ambient light exposure, the impact of light intensity, and the

response time of the system.

2.4. Results

2.4.1. Structure of a light-inducible recombinase

To make Cre light sensitive, we split it into N-terminal (nCre) and C-terminal (cCre) fragments, with Vvd photodimers attached to the internal end of each fragment (Figure 2-1a). When exposed to blue light, Vvd changes conformation to allow dimerization, bringing the Cre fragments together.

Cre excises DNA fragments between *loxP* sites that are oriented in the same direction. We used this to develop a reporter for the efficiency of our recombinase constructs. We placed a transcription terminator flanked by *loxP* sites between the gene for red fluorescent protein (*rfp*) and a constitutive promoter. In the absence of Cre, the terminator prevents transcription of *rfp*. Functional Cre excises the terminator, leading to RFP production (Figure 2-1a). To perform these tests, we used a light plate apparatus (LPA).[104] We exposed samples to 465 nm blue light using LEDs for one hour and then took samples for polymerase chain reaction (PCR) immediately following light exposure. To verify that the recombinase was excising the target DNA properly, we first used PCR to check the length of the plasmid region containing the *loxP*-flanked terminator with and without exposure to light. We used a forward primer upstream of the promoter, and a reverse primer in the *rfp* gene to amplify the region, which is approximately 500 bp if the terminator and both *loxP* sites are intact, and 300 bp when the terminator is removed by recombination (Figure 2-1b). As a negative control, we used cells with the reporter but no recombinase. As a positive control, we used a strain containing recombinase and the

reporter plasmid with the terminator excised. In addition, using microscopy we confirmed that after exposure to blue light, cultures showed a clear increase in RFP (Figure 2-1c). For the microscopy experiments we refreshed cultures overnight to allow full RFP expression and maturation after recombination.

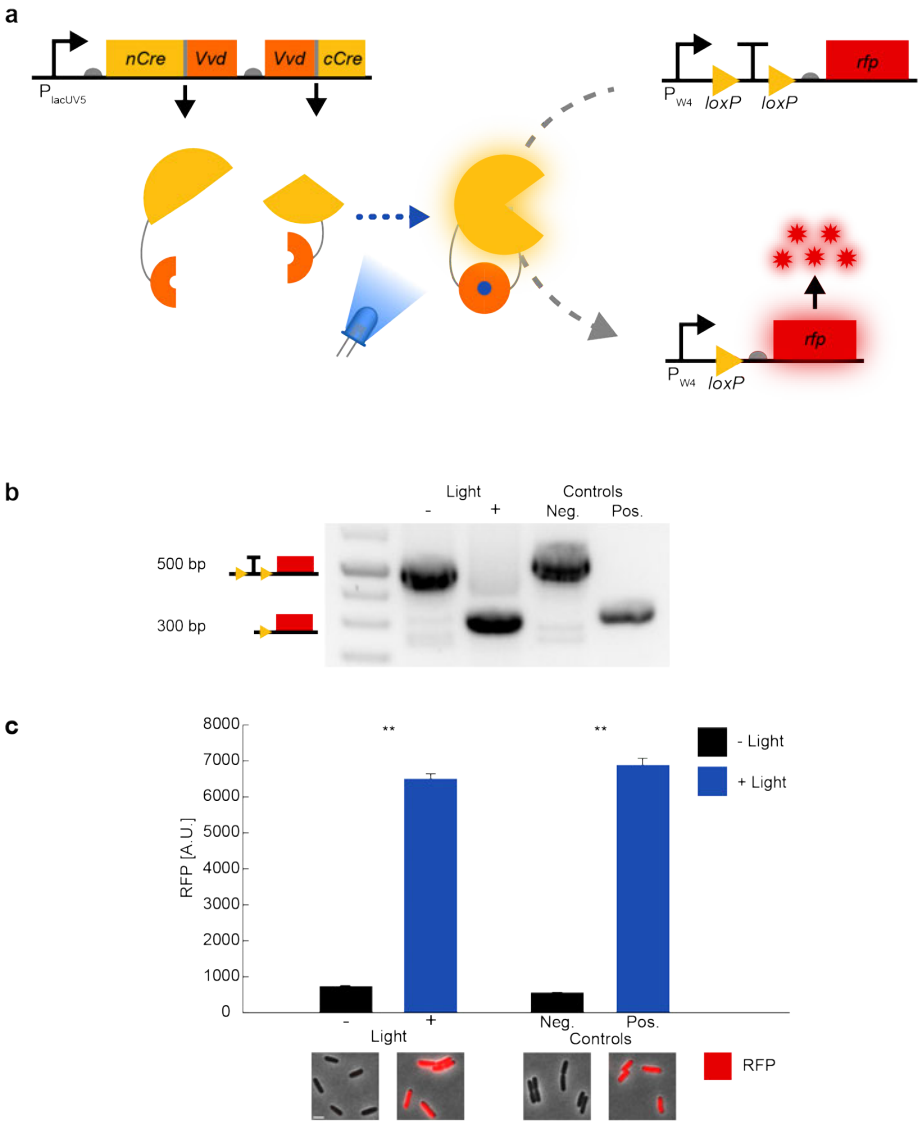

Figure 2-1. Light-inducible recombination in *E. coli*.

(a) Split Cre fragments are linked to Vvd photodimers and expressed under the control of an IPTG-inducible promoter (P_{lacUV5}). When exposed to blue light, Vvd dimerizes, forming functional Cre protein. Cre can then act on the reporter plasmid, excising the *loxP*-flanked

transcription terminator and allowing expression of RFP. RFP is under the control of a constitutive promoter (P_{W4}). **(b)** Gel electrophoresis images showing DNA excision. PCR of the reporter region containing *loxP*-flanked terminator shows a 500 bp band when full terminator is intact, and 300 bp band after recombination. Negative control contains cells with the reporter plasmid alone (terminator upstream of *rfp*); positive control contains cells with recombinase and a pre-cut reporter plasmid (no terminator upstream of *rfp*). **(c)** Single-cell fluorescence microscopy showing RFP expression for cells with and without light exposure. Insets below show representative cell images (scale bar = 2 μm). Error bars show standard error around the mean (n ≈ 300 cells per sample). In addition, we tested for statistical significance between conditions with and without light exposure using a two-tailed Welch's *t*-test by using individual microscopy images as replicates, $^{**}P < 0.005$.

2.4.2. Recombinase, photodimer, and split site variants

When developing the photoactivatable split recombinase, we considered several variants on the design, including different recombinase enzymes, alternative photodimers, and multiple protein split site locations. First, we tested two widely-used recombinases, Cre and Flp (Figure 2-2a). Flp is a tyrosine recombinase originally native to *Saccharomyces cerevisiae*,[105] and like Cre has been used as a split photo-activatable recombinase in mammalian systems.[94,95] We tested each recombinase using previously established split sites (Cre 43,[39] Flp 374[95]) with two photodimer options, Vvd and Magnets. In contrast to the blue light-sensitive homodimer Vvd, Magnets are engineered heterodimer Vvd variants with separate positively-charged and negatively-charged dimer interfaces.[103] We worked with these photodimers due to their efficiency in mammalian split-recombinases,[39,94,95,106] and established function in other bacterial split-protein systems.[29,90] We found that Cre, especially when paired with Vvd, showed substantially improved activation relative to Flp when exposed to blue light (Figure 2-2a).

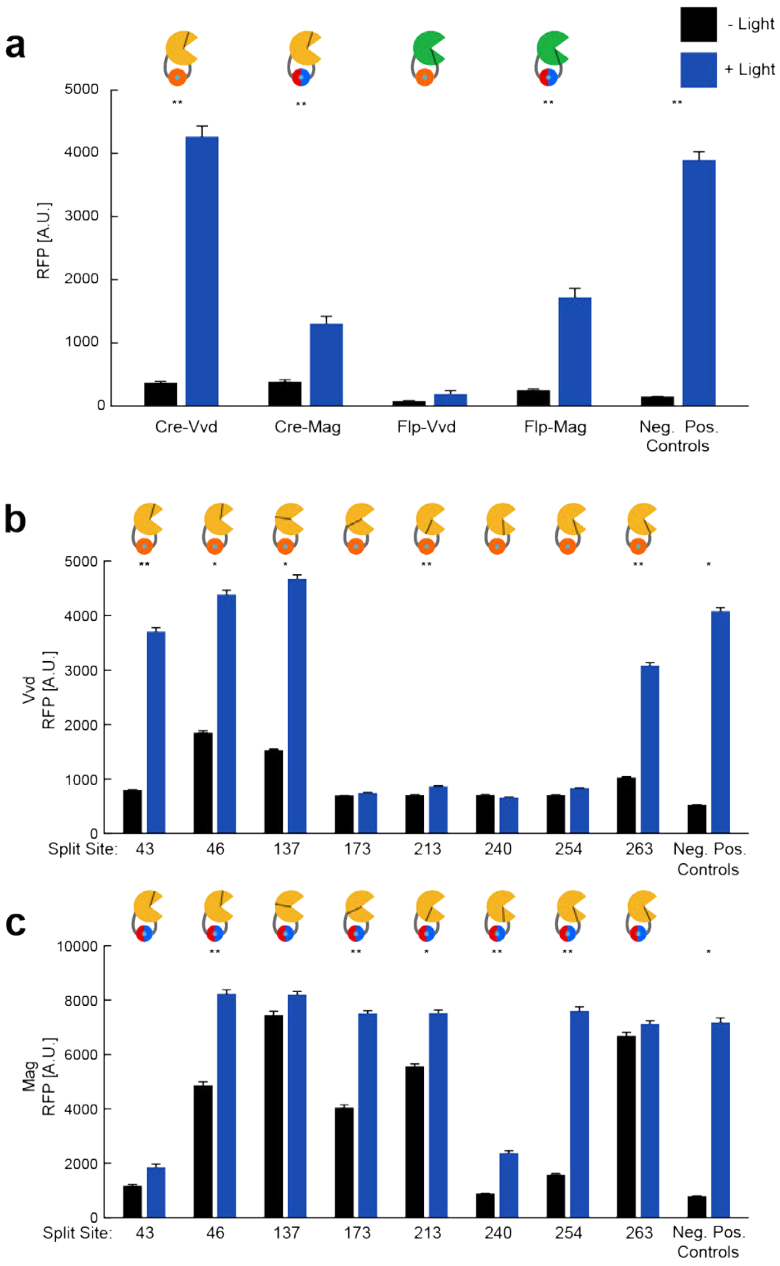

Figure 2-2. Comparison of optogenetic recombinase protein variants.

(a) RFP reporter output with and without light exposure for Cre and Flp recombinases, each with Vvd and Magnet photodimers. Split sites used are Cre with nCre length of 43 AA, Flp with nFlp length of 374 AA. **(b)** Assay of split sites tested for Cre-Vvd and **(c)** Cre-Mag. Numbers shown for split sites on the x-axis are the length of nCre. All figure data obtained using fluorescence microscopy. In all cases, 100 μM IPTG was used for induction and samples were exposed to one hour of light at 120 $\mu W/cm^2$. Error bars show standard error around the mean ($n \approx 750$ cells per sample). Statistical significance comparing conditions with and without light use a two-tailed Welch's *t*-test using microscopy images as replicates. $*P < 0.05$, $**P < 0.005$.

Focusing on Cre recombinase with the Vvd photodimer, we next tested several variants where the protein was split at different locations (Figure 2-2b). We considered sites reported in the literature, structurally-predicted sites, and algorithmically-derived sites (Table 2-1). Literature derived sites included Cre 43,[39] and Cre 213, 240, 254.[95] We also used the SPELL algorithm to determine novel potential split sites.[107] We ran SPELL on the Cre structure PDB 3MGV,[108] which led to predictions for Cre 46 and Cre 137. We also found structurally-informed sites for Cre by analyzing the PDB structure 3MGV in PyMol.[109] Using this crystal-derived structure, we assessed B-factor to select flexible regions within the protein,[110] and chose split sites between flexible amino acids such as glycine and serine.[111] This method led us to Cre 173 and 263.

nCre Length (AAs)	Amino Acids	Source
43	NN	Kawano 2016[39]/Weinberg 2019[95]
46	KW	SPELL
137	DR	SPELL
173	DG	PyMOL
213	GV	Weinberg 2019[95]
240	LS	Weinberg 2019[95]
254	RL	Weinberg 2019[95]
263	SG	PyMOL

Table 2-1. Split sites tested for Cre recombinase.

Cre recombinase split sites used in this study, given as lengths of the nCre fragment (from methionine at position 1 to the split site), the amino acids on either side of the split, and the source of the split. Note that we use truncated Cre from Kawano *et al.*,[39] which starts at AA 18 of native Cre.

We observed split site-dependent variation in both the level of activation with light and in recombination in the absence of light. Some sites showed almost no activation with light (173, 213, 240, 254). Others sites showed high activation with light exposure, but also increased activation in the absence of light (46, 137). From this screen,

we found Cre-Vvd 43 to be our best candidate, as it showed a good fold change in RFP expression in response to light and minimal activation without light. We also tested each split site using the Magnet photodimers (Figure 2-2c), and observed varied activation at different split sites. Of these, Cre-Mag 254 was the most promising candidate, however it showed a growth defect compared to Cre-Vvd 43, so we focused our efforts on Cre-Vvd 43 (Figure AI-1). Although there were commonalities, not all split sites behaved consistently with both types of photodimers. Overall, we found that Magnets were more likely to strongly activate, but also had much higher activation without light than Vvd. This may be due in part to Vvd's ability to form homodimers, as "incorrect" dimer pairs containing two nCre or two cCre fragments could help to lower formation of Cre in the absence of light. It is also notable that the dark-state expression seen here is higher than in the original mammalian PA-Cre.[39] Tests of five literature-derived split sites for Flp-Mag showed similar split site-dependent results, but were ultimately inferior to the Cre variants (Figure AI-2). Due to its significant activation and high fold change we chose to use Cre-Vvd 43, which we denote OptoCreVvd, for further characterization.

2.4.3. Effect of light intensity and duration on OptoCreVvd

An important practical experimental consideration for light-inducible recombinases is their sensitivity to ambient light. Therefore, we next tested how OptoCreVvd performed with 5 minutes of ambient light exposure. We chose this duration to mirror conditions that might be experienced in a setting where plates are temporarily removed from darkness, such as would be necessary to transfer cultures from growth conditions to flow cytometry or microscopy assays. We found that OptoCreVvd showed

minimal sensitivity to short duration exposure to ambient light (Figure 2-3a).

Next, we tested experimental parameters for OptoCreVvd, including the light intensity used for induction, the timing of light exposure, and concentration of IPTG for recombinase induction. When optimizing split sites and photodimer variants, we used a blue light intensity that corresponded to the maximum value accessible with the LEDs used in the LPA (120 $\mu W/cm^2$) to minimize excision times (Figure 2-3b). Using microscopy, we observed no discernable differences in cell morphology with and without light exposure in these conditions, suggesting that phototoxicity effects were minimal with this exposure level (Figure AI-1a). We also confirmed that our constructs and IPTG induction levels did not have adverse effects on cell growth in bulk cultures (Figure AI-1b). Overall, we found that even at much lower light intensities, we observed complete excision when samples were exposed to blue light for a longer time (Figure 2-3b). Cultures exposed to lower intensities of light showed partial excision after 1 hour, while cultures exposed to high intensity light showed near-complete excision. When we exposed cultures to constant blue light for 4 hours, we found that all intensities of light yielded comparable, high levels of excision (Figure 2-3b). In addition, we found OptoCreVvd to have consistent, low basal levels of activation without light between experiments conducted on different days (Figure AI-3).

In our design, the split Cre fragments are under the control of a lacUV5 promoter to prevent excision of the target DNA prior to induction and subsequent light exposure. We found that inducing with IPTG concentrations above 50 μM for two hours prior to light exposure was sufficient to induce Cre for light activation (Figure 2-3c). We used

100 µM IPTG as a standard value, which remains solidly above the induction threshold for our experiments.

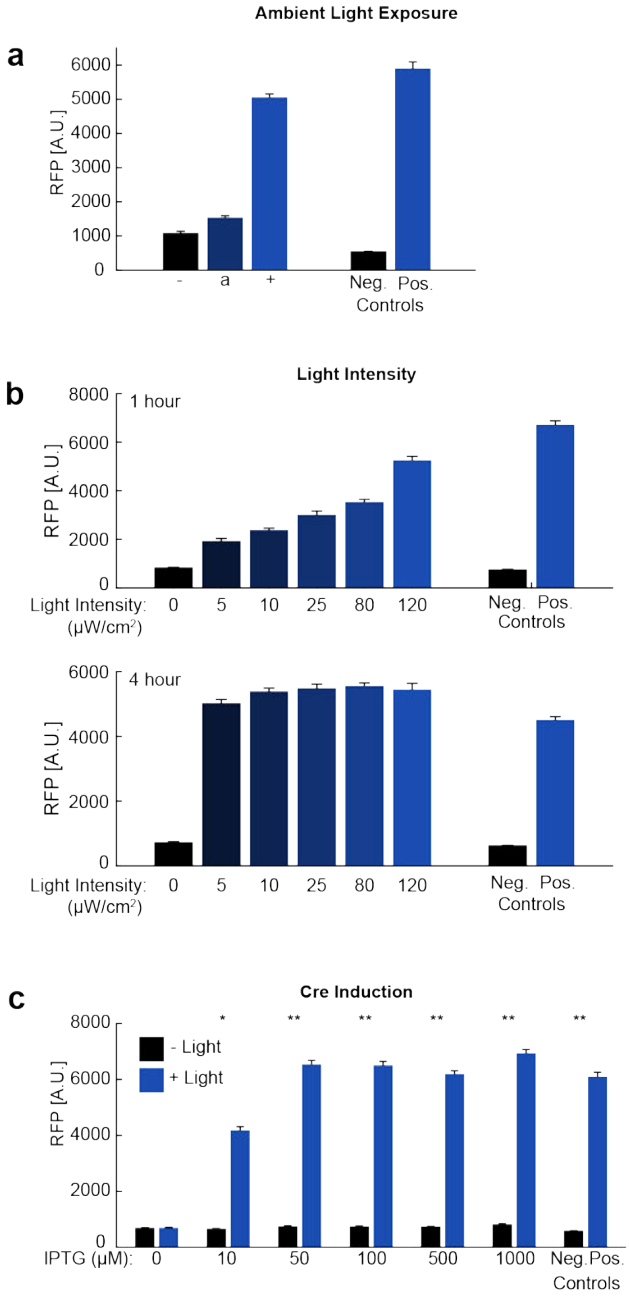

Figure 2-3. Characterization of OptoCreVvd.

(a) RFP reporter output for OptoCreVvd without light (-), with a 5 minute exposure to ambient light (a), and with full exposure to blue light (+). **(b)** Effect of blue light intensity on OptoCreVvd

activation when exposed for 1 or 4 hours. **(c)** Effect of IPTG induction levels for OptoCreVvd. Statistical significance comparing conditions with and without light use a two-tailed Welch's *t*-test using microscopy images as replicates. **P* < 0.05, ***P* < 0.005. In all cases, error bars show standard error around the mean from microscopy data (n ≈ 350 cells per sample).

2.4.4. Temporal dynamics of OptoCreVvd

We were also interested in exploring the duration of light exposure that cells need to induce full RFP expression (Figure 2-4). To test this, we exposed separate cultures to light for 5 minutes, 30 minutes, 1 hour, 2 hours, 4 hours, or 8 hours. Cultures exposed to light for less than 8 hours were kept in the dark following light exposure for the remainder of the time. At the end of the 8 hour period, we refreshed all cultures and grew them for two hours without light to allow for protein maturation and then assessed transcription terminator excision both genotypically and phenotypically. Genotypic excision was assessed by PCR and gel electrophoresis (Figure 2-4a). Phenotypic results were assessed by microscopy (Figure 2-4b,c) and spotting on agar (Figure 2-4d). We observed general agreement between all characterization methods. OptoCreVvd shows substantial RFP expression with 1 hour of blue light exposure, and RFP values comparable to the positive control, indicative of near-complete activation, by 2 hours. Live time course results, which include the time for protein maturation, indicate RFP expression within 2 hours after exposure to blue light, and expression comparable to the positive control by 4 hours post-exposure (Figure 2-4e).

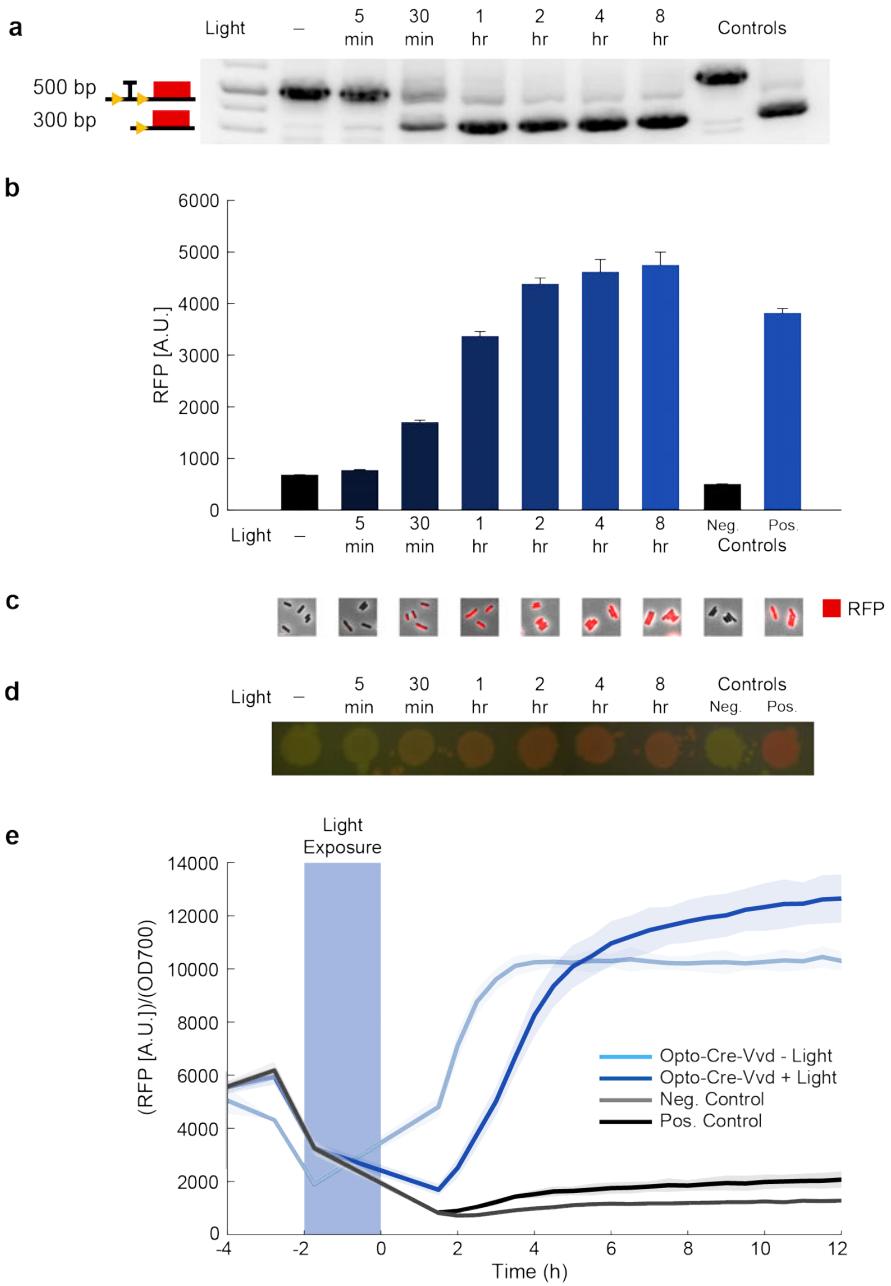

Figure 2-4. Temporal dynamics of OptoCreVvd.

(a) DNA gel image showing reporter bands with and without transcription terminator excision, **(b)** single-cell fluorescence microscopy averages of RFP values, **(c)** representative microscopy images (scale bar = 2 μm), and **(d)** samples of culture spotted on agar plates of OptoCreVvd exposed to different durations of blue light. Error bars show standard error around the mean (n ≈ 750 cells per sample). **(e)** OptoCreVvd activation in real-time, with the blue bar indicating light exposure. Shaded error bars represent standard deviation around the mean from plate reader data (n = 3 wells).

2.4.5. Development of OptoCreVvd2

After publication of the original manuscript, a reader alerted us to a mistake in the sequence of the OptoCreVvd construct, where we had erroneously placed a stop codon between the Vvd photodimer and the cCre sequence. Although, in principle, the design should not work with the stop codon in place, in practice the construct does function well, as described above. Our hypothesis is that in the original construct, even minimal stop codon read-through between Vvd and cCre produces sufficient Vvd-cCre to allow for recombination. In the original design, we had OptoCreVvd on a high copy number plasmid (ColE1 origin).

We removed the stop codon from between Vvd and cCre and transferred the system to a low copy number plasmid (SC101). We denote this new design OptoCreVvd2. We have repeated all the key results from the original manuscript with OptoCreVvd2, including light-induction time courses for DNA excision and *rfp* expression at the single-cell and population levels (Fig. 2-5). In all cases, the performance of OptoCreVvd2 is nearly identical to the OptoCreVvd results described in the original manuscript.

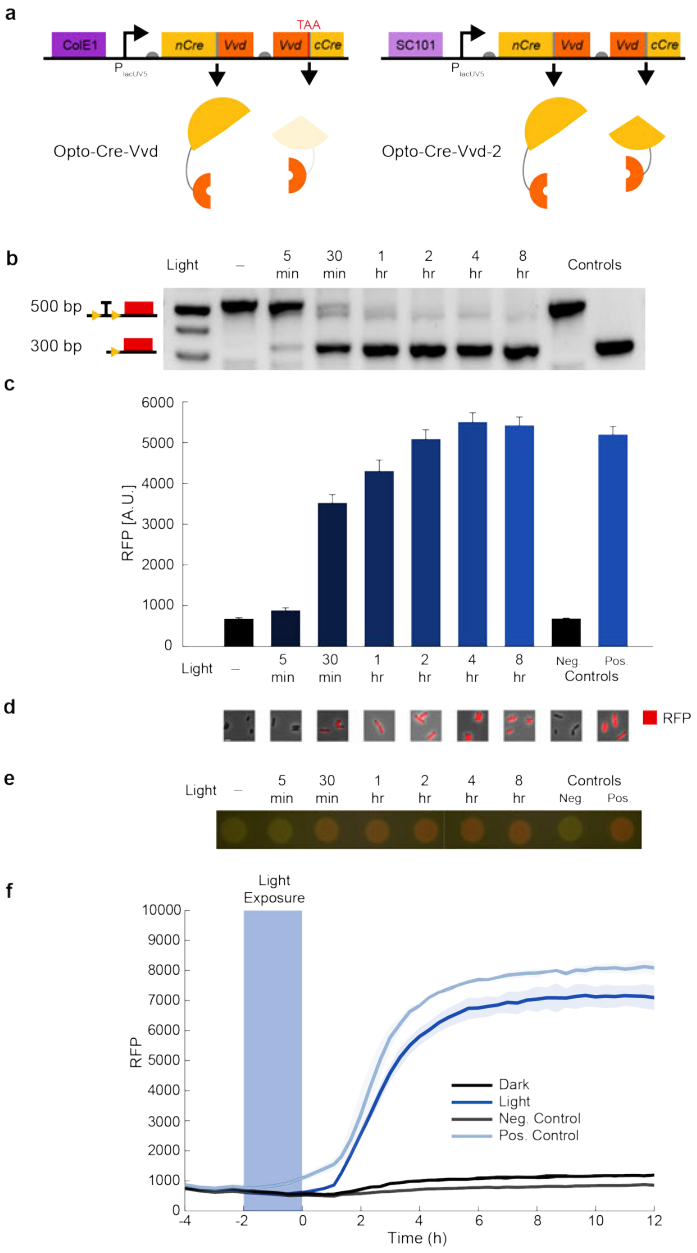

Figure 2-5. OptoCreVvd2 performance with blue light induction.

(a) OptoCreVvd has a stop codon between Vvd and cCre and is on a high copy number plasmid (ColE1). OptoCreVvd2 does not have the stop codon and is on a low copy number plasmid (SC101). **(b)** DNA gel image showing reporter bands with and without transcription terminator excision. **(c)** Single-cell fluorescence microscopy averages of RFP values. Error bars show standard error around the mean (n ≈ 100 cells per sample). **(d)** Representative microscopy images (scale bar = 2 μm). **(e)** Samples of culture spotted on agar plates of OptoCreVvd2 exposed to different durations of blue light. **(f)** OptoCreVvd2 activation in real-time, with the blue bar indicating light exposure. Shaded error bars represent standard deviation around the mean from plate reader data (n = 3 wells).

We note that we also tested the construct with the stop codon between Vvd and cCre removed on a high copy number plasmid (ColE1 origin). This variant does exhibit blue light-inducible recombination but has impaired growth and recombination relative to the OptoCreVvd and OptoCreVvd2 designs (Fig. 2-6a,b). Another variant with cCre removed entirely showed no recombination (Fig. 2-6c).

The original OptoCreVvd system works as described in the manuscript and can continue to be used as is, however moving forward we suggest users consider working with OptoCreVvd2 as an alternative.

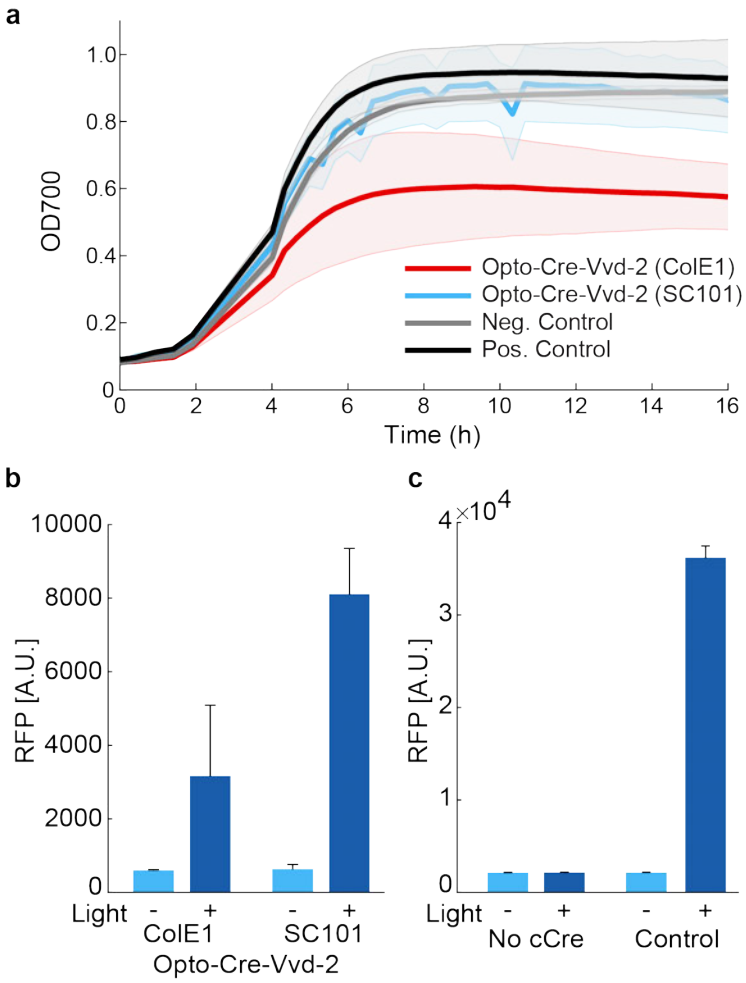

Figure 2-6. OptoCreVvd2 shows improved function on a low-copy plasmid.

(a) Growth curve data for cultures with reporter and OptoCreVvd2 for the ColE1 or SC101 origin of replication, the reporter plasmid only, or no plasmid. Shaded error bars show standard deviation around the mean from plate reader data (n = 3 wells). **(b)** RFP values of OptoCreVvd2 on the ColE1 or SC101 origin plasmids grown overnight after a 2 hour light exposure. **(c)** RFP values for the OptoCreVvd construct without cCre grown overnight after a 2 hour light exposure. Error bars show standard deviation around the mean from plate reader data (n = 3 wells).

2.5. Discussion

We have developed, optimized, and characterized a light-inducible recombinase for *E. coli*. We found that both Cre and Flp associated with either Vvd or Magnet photodimers have the potential for photo-activatable recombination. However, split site location and the recombinase-photodimer pairing impact efficacy. Our most promising candidate, OptoCreVvd, exhibits blue light-dependent excision and low sensitivity to ambient light. We also found that OptoCreVvd shows activation at both low and high light intensities, but at different timescales. The construct can cut completely within 2 hours, which is comparable to the timeframe observed for mammalian photoactivatable Cre[39] and existing Magnet-based split proteins in *E. coli*.[29]

A well-characterized recombinase tailored to *E. coli* is a powerful new tool for bacterial optogenetics. Moving forward, this offers expanded potential for interfacing engineered cells with computational control via light. Applications include the ability to target sub-populations of cells, real-time genetic modifications, or experiments where small molecule inducers are impractical due to crosstalk. For example, this could enable studies on population dynamics through controlled spatial development of subpopulations, establishing interfaces between neighboring cells. A future version of this system may also be useful for changing genetic state during biomolecule production, such as in metabolic engineering applications, as light is an inexpensive inducer. Cre

could also be used to activate or inactivate multiple genes using constructs similar to a dual-fluorescent assay.[99] Along these lines, future extensions to this system may involve development of orthogonal light-inducible recombinases for bacteria. Alternate photodimer systems that are sensitive to other wavelengths of light could also be used to multiplex the approach.[11] It would also be interesting to develop an in-depth understanding of the differences between Cre and Flp, to perform detailed characterization at the molecular level, or to engineer variants with alternative optogenetic tools such as CRY2/CIB[96,97] or iLID.[112] As an immediate application, OptoCreVvd can be used as-is to perform gene knock outs in real time and is compatible with plate-based or microscopy platforms. These light-inducible recombinases expand the optogenetic methods available for bacteria and have great potential for the design of novel synthetic circuits.

2.6. Methods

Strains and plasmids

Expression studies use *E. coli* strain MG1655. All recombinase constructs use a plasmid with a high-copy ColE1 origin and an ampicillin resistance cassette where the recombinase genes are under the control of an IPTG-inducible lacUV5 promoter to prevent activation from light exposure prior to experiments. The construct is derived from the pBbE5a BioBrick plasmid.[113] All reporter constructs use a medium-copy p15A origin plasmid with a kanamycin resistance cassette and the gene for red fluorescent protein (mRFP1)[114] under the control of a constitutive, medium-strength promoter (denoted P_{W4}), which is modified from the phage T7 A1 promoter:

TTATCAAAAAGAGTATTGCATTAAAGTCTAACCTATAGGAATCTTACAGCCAT CGAGAGGGACACGGCGAA (underline indicates mutations from original T7 A1 promoter).[115] Plasmids were constructed using the Gibson assembly method.[116] Primer data can be found in Table AI-1.

Original Cre and Magnet heterodimer plasmids are from Weinberg (2019).[95] The original Flp gene sequence was derived from the pCP20 plasmid from Datsenko & Wanner (2000).[117] We obtained the Vivid homodimers from AddGene plasmid #58689 (mV-NcVV-LOV_231) deposited by Harald Janovjak.[102] We express Cre split with a photodimer pair as an operon (Fig 1a). The N-terminal fragment of Cre (nCre) is followed by a 10 AA glycine-serine linker and a photodimer. A separate RBS is used to express the second photodimer linked by a 10 AA glycine-serine linker to the C-terminal fragment of Cre (cCre). Plasmids from this study and their sequences are available on AddGene (https://www.addgene.org/Mary_Dunlop/). We thank Elliot Tague and John Ngo for their input on split site selection; Ben Weinberg, Armin Baumschlager, and Mustafa Khammash for helpful discussions on experimental design; and Nathan Tague for early work on light-inducible Flp.

Cre split site selection

Split sites for Cre were selected using three methods: chosen from the literature, using the first two optimal choices from the SPELL algorithm (https://dokhlab.med.psu.edu/spell/)[107] based on the PDB structure 3MGV[108], or by using PyMOL (https://pymol.org/2/) on 3MGV and selecting two sites around glycine and

serine AAs in regions with high B-factor values. Further information and source of each split site for Cre can be found in Table 2-1. Primers used to make each split are listed in Table AI-1. Split Cre variants were made by amplifying from plasmids containing Cre without a photodimer from the location of the split site with overhangs for the linker sites. In parallel, we amplified the photodimer and linker inserts and combined via Gibson assembly.[116] Split sites for Flp were chosen from the literature and cloned in a similar fashion; their information can be found in Table AI-2.

Light exposure assays

Strains were grown overnight from a single colony in LB medium containing 100 μg/mL carbenicillin and 30 μg/mL kanamycin for plasmid maintenance. The next day, cultures were refreshed 1:100 in selective LB and induced for 2 hours with 100 μM IPTG unless otherwise noted. Blue light exposure was performed using a LPA,[104] with two 465 nm wavelength LEDs per well (ThorLabs LED465E), outputting a total of 120 μW/cm^2. Unless otherwise noted, cultures were exposed to blue light for 1 hour. After exposure, samples were prepared for analysis by PCR to check for target excision by gel electrophoresis, and refreshed in selective LB medium without IPTG overnight. In light intensity experiments, cultures were exposed to light for 4 hours total, with intermediate samples taken at 1 hour for characterization.

All liquid cultures through the experiment were grown at 37^{o}C with 220 rpm shaking. Note that agar plates with the Flp recombinase and reporter were also kept at 37^{o}C at all times, as we observed substantial activation even without light when stored at

4ºC. After transformation, all cultures were kept in the dark throughout the entire experiment with the exception of blue or ambient light exposure periods. For ambient light exposure, samples were exposed to lab lighting in a shaking incubator for 5 minutes after induction, and then kept in the dark for the remainder of the experiment.

Recombinase efficiency characterization

Target DNA excision via the recombinase was measured genetically by amplifying the promoter region of the reporter using PCR. We used a forward primer ~200bp upstream of the first *loxP* site (ATCTTCCCCATCGGTGATGTCG) and a reverse primer ~100bp downstream of the second *loxP* site (GACGACCTTCACCTTCACCTT) to check for differences in band length before and after recombination.

Plate reader data were collected on a BioTek Synergy H1 with OD absorbance read at 700 nm to avoid overlap with the RFP spectra, and fluorescence read with excitation at 584 nm and emission at 610 nm.

In addition to the PCR-based measurements, efficiency was also measured visually by imaging plated samples with a mobile phone camera using standard settings (Samsung Galaxy Note 8) on a Blue LED transilluminator through the attached orange filter (IO Rodeo).

Microscopy and image analysis

Post light-exposure samples were refreshed overnight in LB medium with 100

μg/mL carbenicillin and 30 μg/mL kanamycin for plasmid maintenance to allow full RFP expression and maturation. Before imaging, samples were refreshed for 2 hours in 1:100 in MGC medium (M9 salts supplemented with 2 mM $MgSO_4$, 0.2% glycerol, 0.01% casamino acids, 0.15 μg/ml biotin, and 1.5 μM thiamine). Samples were then placed on 1.5% low melting agarose pads made with MGC medium. Cells were imaged at 100x using a Nikon Ti-E microscope. Images were segmented and analyzed using the SuperSegger software[118] and custom MATLAB analysis scripts. Statistical significance (*P* value) was assessed using a two-tailed Welch's *t*-test, treating each microscopy image as a sample.

CHAPTER 3. An optogenetic toolkit for light-inducible antibiotic resistance

3.1. Disclosure & Copyright Statement

This chapter is a modified version of "An optogenetic toolkit for light-inducible antibiotic resistance" by Michael B. Sheets, Nathan Tague, and Mary J. Dunlop, 2023. Reprinted from *Nature Communications* 14, 1034.

3.2. Abstract

Antibiotics are a key control mechanism for synthetic biology and microbiology. Resistance genes are used to select desired cells and regulate bacterial populations, however their use to-date has been largely static. Precise spatiotemporal control of antibiotic resistance could enable a wide variety of applications that require dynamic control of susceptibility and survival. Here, we use light-inducible Cre recombinase to activate expression of drug resistance genes in *Escherichia coli*. We demonstrate light-activated resistance to four antibiotics: carbenicillin, kanamycin, chloramphenicol, and tetracycline. Cells exposed to blue light survive in the presence of lethal antibiotic concentrations, while those kept in the dark do not. To optimize resistance induction, we

vary promoter, ribosome binding site, and enzyme variant strength using chromosome and plasmid-based constructs. We then link inducible resistance to expression of a heterologous fatty acid enzyme to increase production of octanoic acid. These optogenetic resistance tools pave the way for spatiotemporal control of cell survival.

3.3. Introduction

Antibiotic resistance genes are widely used in synthetic biology. They are included in genetic constructs to ensure plasmid propagation. Resistance genes also play an important role in cloning methods. Examples include chromosomal insertions, where expression of resistance genes can be used as a selective marker for successful integration,[117] or in the creation of transposon libraries, where drug resistance is used as an intermediate selection mechanism before being swapped for an alternative sequence.[119,120]

Although antibiotic resistance genes are a staple of synthetic biology and microbial biotechnology research, there are few methods for dynamic control of their expression. The ability to control drug resistance spatially and temporally could open new avenues for synthetic biology research. As an analogy, when Sheth *et al.*[59] developed an inducible origin of replication—another ubiquitous feature within synthetic biology constructs—it sparked new areas of research including biological data storage[60] and whole-cell riboswitch diagnostics.[61] Spatiotemporal control over drug resistance could enable spatial patterning in living biomaterials,[121] selection of single cells from microfluidic systems,[122,123] and improved understanding of the role dynamics play in

clinical antibiotic resistance.[124] For example, resistance is often spread through horizontal gene transfer events,[125,126] which are difficult to monitor and control at the single-cell level. New systems for control offer the potential for future studies quantifying how different spatiotemporal arrangements of cells acquiring resistance can lead to population-level proliferation or collapse.

Optogenetic methods are a powerful and widely used tool for controlling gene expression.[12] The delivery of light to cells can be regulated in space and time, and can be integrated directly into computational workflows.[19,127] Optogenetic systems in bacteria have been used to control gene expression for a variety of applications,[11,12] including to drive metabolic flux,[128] regulate the gut microbiome,[31] control cell morphology,[23] and regulate co-culture dynamics.[55] Using light to control cell survival has been a focus of microbial engineering across species. For example, optogenetic regulation has been used to control nourseothricin resistance in *Saccharomyces cerevisiae*[129] and bleomycin resistance in *Yarrowia lipolytica.*[130] In *Escherichia coli*, light has been used to control antibiotic resistance via individually designed photo-caged antibiotics[131] or by leveraging the natural photosensitivity of tetracycline.[132] However, because these methods require careful protein engineering or exploit properties specific to a single drug, they do not easily generalize across different resistance mechanisms. An alternative approach used a light-inducible promoter to reversibly control chloramphenicol resistance.[22,55] Such a method could generalize to other resistance genes, however experiments were limited to control of the chloramphenicol acetyltransferase enzyme. The ideal platform for light-inducible resistance would be both generalizable for different antibiotic resistance genes

and tunable across antibiotic concentrations to flexibly enable diverse studies in synthetic biology and microbiology.

To address these needs, we used the blue light-inducible Cre recombinase OptoCreVvd2 to activate antibiotic resistance genes.[133] Using this system, we excise a *loxP*-flanked transcription terminator between a gene and promoter, allowing for increased gene expression after exposure to 465 nm blue light (Fig 3-1a). Recombinase technology has been used successfully for a variety of applications that require robust and inducible control of gene expression, including gene logic circuits and cell lineage tracking.[40,92,134] We selected this system for its relatively short activation time, flexibility in construct design (requiring only the addition of *loxP* sites), and minimal basal expression in uninduced cells.[133] In addition, the permanent OFF-ON switch caused by Cre allows for selection of resistant cells at any point after light exposure, allowing for cellular memory after the light input has been removed. Although this irreversibility does not allow for complex temporal dynamics, one-time induction provides benefits that may be advantageous in certain applications such as allowing irreversible activation before a culture becomes too dense for light penetration, or minimizing exposure in light-sensitive strains.

Here, we used Cre to induce expression of four antibiotic resistance genes, which we selected for their ubiquity in synthetic biology applications as well as their range of mechanisms of action (Table 3-1). Specifically, we chose the carbenicillin/ampicillin resistance gene beta-lactamase (*bla*), which is both clinically relevant and widely used in synthetic biology. Beta-lactam antibiotics inhibit cell wall biosynthesis, and are

enzymatically degraded by the beta-lactamase enzyme.[126,135,136] We also included kanamycin nucleotidyltransferase (*knt*), which provides enzymatic resistance against kanamycin, an antibiotic that causes mistranslation by the 30S ribosomal subunit.[137] Chloramphenicol acetyltransferase (*cat*) provides enzymatic resistance against chloramphenicol, which interferes with the 50S ribosomal subunit to cause protein synthesis to stall.[138] Lastly, we included the tetracycline efflux pump A (*tetA*) as a non-enzymatic, efflux-based resistance mechanism.[139] Tetracycline binds the 30S ribosomal subunit to inhibit protein synthesis.[140] These four antibiotics include both bactericidal (carbenicillin/ampicillin and kanamycin) and bacteriostatic (chloramphenicol and tetracycline) drugs. This selection of resistance mechanisms shows both the broad variety of mechanisms that can be controlled using this system and introduces multiple options for synthetic tools that can be incorporated into existing bacterial systems.

Antibiotic	Effect	Target	Resistance	Mechanism
Carbenicillin/Ampicillin	Bactericidal	Cell wall	bla	Enzymatic
Kanamycin	Bactericidal	Ribosome (30S)	knt	Enzymatic
Chloramphenicol	Bacteriostatic	Ribosome (50S)	cat	Enzymatic
Tetracycline	Bacteriostatic	Ribosome (30S)	tetA	Efflux pump

Table 3-1. Antibiotics and resistance genes used in this work.

When controlling expression of antibiotic resistance genes, key performance metrics include the uninduced and induced expression levels. For example, when using potent enzymes like beta-lactamases, even a small amount of basal expression can allow bacterial growth in the presence of an antibiotic. Moreover, expression in the induced

state should also be sufficient to provide resistance at drug concentrations comparable to typical working ranges for the antibiotic, which could further vary between use cases. To optimize these two features in our platform, we varied the gene copy number, promoter, ribosome binding site (RBS), and coding sequence to tune the minimum inhibitory concentration (MIC) of antibiotic at which cells survive after exposure to blue light, while maintaining basal expression levels that are low enough to avoid erroneously triggering survival. We further demonstrated live activation of resistance genes and characterized cellular responses using single-cell time-lapse microscopy.

Finally, we demonstrated the utility of light-inducible resistance in a biotechnology application by co-expressing resistance genes with the heterologous thioesterase *Cp*FatB1 to increase production of octanoic acid, a medium-chain fatty acid. Medium-chain fatty acids are high-value biochemicals used in fuels, polymer production, flavorings, and fragrances, making them key metabolic engineering targets.[141,142] However, induction of *Cp*FatB1 is metabolically taxing, a common issue with expression of heterologous enzymes for bioproduction applications. This challenge has prompted researchers to develop systems where pathway expression timing can be precisely tuned to balance the tradeoff between growth and production.[143,144] For example, light induction has been used to increase production of other chemicals in *E. coli*, such as mevalonate and isobutanol.[52] In our system with OptoCreVvd2, light induction of *Cp*FatB1 coupled with antibiotic selection for high expression of the heterologous enzyme significantly increased fatty acid production over light induction of *Cp*FatB1 alone.

This toolkit of light inducible resistance genes supports and extends the long use

of antibiotics as cellular control mechanisms in synthetic biology, adding a spatial and temporal control mechanism to existing systems and setting the stage for future applications where light is used in combination with antibiotics to enable flexible control of cell behavior and survival.

3.4. Results

3.4.1. Light induction of beta-lactamase resistance

For optogenetic control of resistance genes, we used the blue light-inducible split Cre recombinase OptoCreVvd2.[133] This system allows for excision of genetic elements placed between *loxP* sites when cells are exposed to blue light. Excision can be completed in approximately two hours, which is comparable to or faster than many existing bacterial optogenetic systems.[21–24] We used OptoCreVvd2 to excise a transcription terminator placed inside *loxP* sites between a promoter and an antibiotic resistance gene, allowing for expression of the resistance gene only after exposure to blue light.

We first used this system to control transcription of the beta-lactamase (*bla*) resistance gene (which we denote 'OptoCre-*bla'*, Figure 3-1a). Beta-lactam antibiotics, including ampicillin and carbenicillin, inhibit peptidoglycan layer biosynthesis in the bacterial cell wall. Beta-lactamase enzymes can inactivate beta-lactam antibiotics by hydrolyzing the beta-lactam ring on the antibiotic.[145] For these studies, we used the TEM-116 beta-lactamase, which is commonly used in antibiotic resistance cassettes for plasmid selection.[58] We integrated this genetic construct after *nupG* in the *E. coli* MG1655 chromosome.

To measure light-induced antibiotic resistance, we exposed cultures of OptoCre-*bla* to blue light for two hours, then grew them overnight in the presence of carbenicillin and compared growth to cultures kept in the dark. We observed blue light-dependent differences in cell proliferation, where the MIC necessary to prevent growth was 300 μg/mL for cultures kept in the dark and 1200 μg/mL for cultures exposed to blue light (Figure 3-1b). Negative control (- Control) cells with only the reporter and no Cre recombinase had comparable survival to cells with the full construct grown in the dark, indicating low expression of *bla* in the uninduced state. Positive control (+ Control) cells with constitutive expression of *bla* from its native promoter and RBS grew in all concentrations of carbenicillin tested, including at levels above the light-inducible strain, as expected for a fully resistant strain expressing the resistance gene in its native context. We further included *E. coli* MG1655 as a wild-type negative control, which did not grow in any concentration of carbenicillin used here.

To confirm that blue light-induced cells grow at rates comparable to the positive control strain, we collected time-series data demonstrating normal growth rates under a broad range of carbenicillin concentrations for cells grown in blue light, while cells without light induction failed to grow (Figure 3-1c). We further validated the optical density-based MIC data by using colony forming unit (CFU) counts after antibiotic exposure (Figure 3-1d). Although MIC data is an accurate assessment of cell growth in the presence of antibiotic, beta-lactam antibiotics also cause cell filamentation, which can increase optical density (OD) readings even when cells are not dividing, making *bla* resistance specifically important to confirm by CFU measurement.[146] However, our

results using CFU counts confirm that the optical density measurements also translate to a clear difference in cell survival.[147] Overall, we found that OptoCreVvd2 can be used to induce beta-lactamase resistance and we identified concentrations of carbenicillin with robust differences between dark and blue light-activated expression of the *bla* resistance gene construct (Figure 3-1e, Table 3-2).

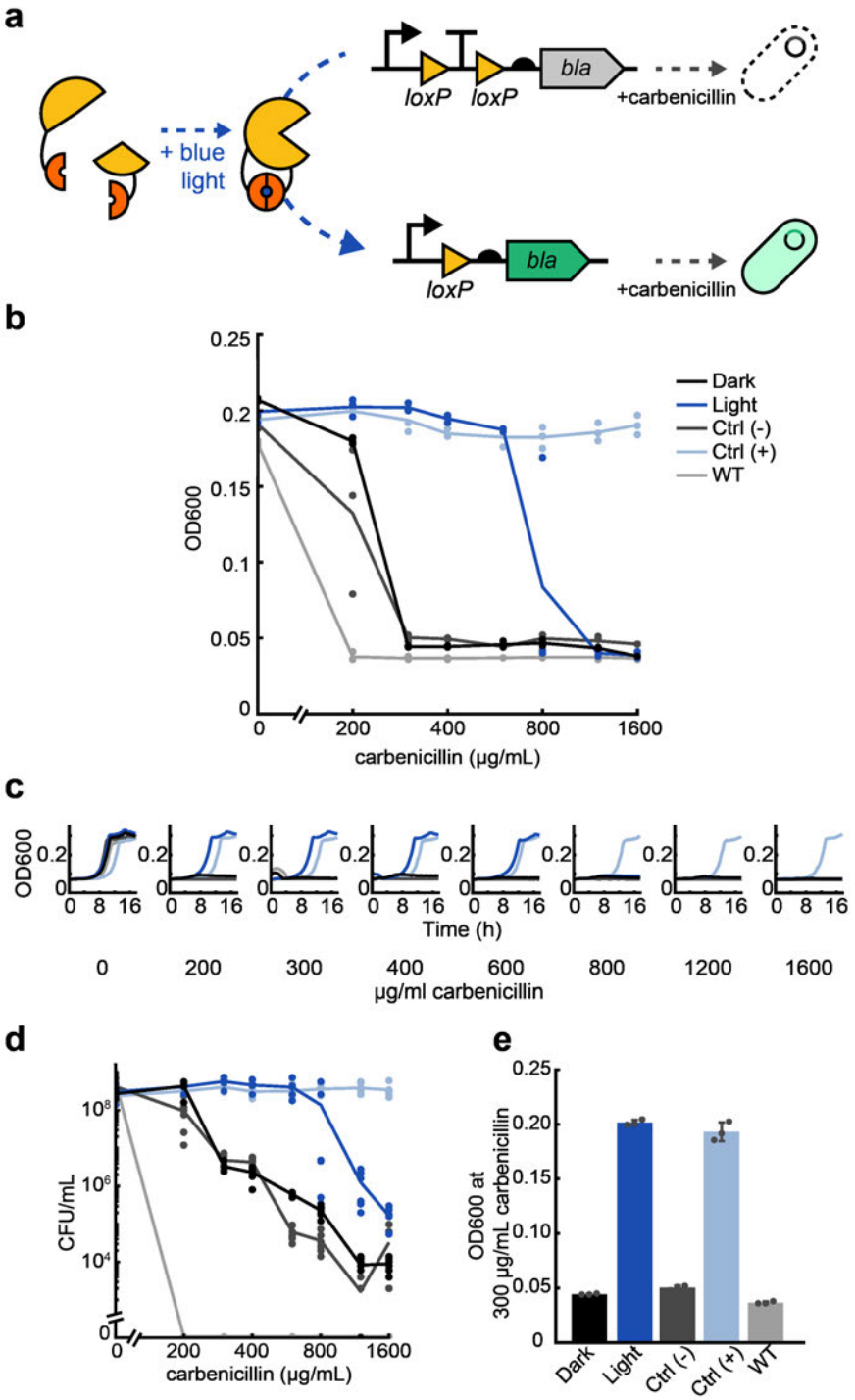

Figure 3-1. Optogenetic activation of antibiotic resistance from beta-lactamase.

(a) Split Cre recombinase fragments are linked to blue light-inducible Vvd photodimer domains. When exposed to blue light, Cre becomes active and can excise a transcription terminator between two *loxP* domains, allowing increased expression of beta-lactamase (*bla*). The expression of OptoCre-*bla* then allows cells to survive in the presence of the antibiotic

carbenicillin. **(b)** Minimum inhibitory concentration (MIC) curves of chromosomally-integrated OptoCre-*bla* constructs grown in carbenicillin for 18 hours. Light-induced samples were exposed to blue light for two hours immediately before exposure to carbenicillin. Growth measured by OD600 (n = 3). The strains in both the dark and light conditions contain the resistance induction construct and OptoCreVvd2. Control (-) cells contain the resistance activation construct but no Cre recombinase. Control (+) cells contain a constitutively expressed *bla* gene. Wild-type (WT) cells are MG1655 without modification or plasmids. **(c)** Time-course growth of OptoCre-*bla* resistance activation constructs across different concentrations of carbenicillin. **(d)** Colony forming unit (CFU) counts of cultures from MIC data (n = 6). After growth in carbenicillin for 18 hours, samples were spotted on agar plates and colonies were counted the next day. **(e)** Optimal OptoCre-*bla* activation conditions. Resistance activation constructs grow in 300 µg/mL carbenicillin after exposure to blue light for 2 hours, but not when kept in the dark. Growth is quantified by OD600 after 18 hours. Error bars show standard deviation around the mean (n = 3 biological replicates).

3.4.2. Genetic-level optimization of kanamycin resistance

We next sought to generalize this system to other antibiotic resistance genes. While the excision of a terminator can easily couple light to the expression of an antibiotic resistance gene, this is not the same as light-inducible survival. Control of survival requires no or low expression of the antibiotic resistance gene in the dark, such that cells remain susceptible to antibiotics. The design also requires that induction of the resistance gene is sufficient to confer resistance. The thresholds for these two features can vary dramatically with different antibiotic resistance mechanisms, which have different rates of antibiotic degradation and export. Thus, while previous work in our lab has shown that OptoCreVvd2 can control expression of a fluorescent protein with low basal expression and a 10-fold change with light,[133] naively replacing the fluorescence gene with an antibiotic resistance gene may not produce the desired behavior. Therefore, we defined a general process for adapting the OptoCreVvd2 system to different antibiotic resistance genes (*bla, knt, cat,* and *tetA*) and were able to show survival at customized ranges of antibiotic concentration.

To generalize our system to other antibiotics, we began by exchanging *bla* for *kanamycin nucleotidyltransferase* (*knt*) in our induction construct to make OptoCre-*knt* (Figure 3-2a). The antibiotic kanamycin causes mistranslation by binding to the 30S subunit of the bacterial ribosome. The *knt* enzyme catalyzes transfer of a nucleotide to kanamycin, inactivating the antibiotic.[137] Although our initial design of OptoCre-*knt* did show resistance activation using light, the kanamycin concentration required to see this difference was very high — over 1000 μg/mL (Figure 3-2b), compared to 25-50 μg/mL commonly used for plasmid propagation.[58,132] Although matching common working concentrations of antibiotics is not essential, using concentrations in the vicinity of these ranges provides benefits including the ability to study community effects at physiological concentrations and limiting overall antibiotic needs.

Thus, we set out to tune gene expression through optimization of the genetic architecture surrounding the gene. To lower basal expression, we weakened the promoter or RBS driving *knt* expression. By changing the promoter and RBS of OptoCre-*knt,* we were able to shift the expression of the resistance gene to allow survival at antibiotic concentrations much closer to the MIC of wild-type MG1655 (Figure 3-2b). We tested a range of promoter and RBS combinations to show how these alterations impact survival at varying antibiotic concentrations. We used constitutive promoters of varying strength all based on the T7A1 viral promoter, ranging from medium, P, to medium-low, P*, to low, P**, transcriptional strength. We also used the RBS of gene 10 in the T7 phage,[148] which we denote R, and a RBS that we computationally designed to be weaker,[149] which we denote R* (Figure 3-2a). Changing P to P* decreased the MIC for the dark state to

200 μg/mL kanamycin, while P** further reduced it to 150 μg/mL (Figure 3-2b). The MIC for the light state was also reduced, as expected, but still maintained a wide range of kanamycin concentrations resulting in survival. With P*, kanamycin levels between 200 and 800 μg/mL resulted in light-induced survival, while for P** the range was from 150 to 500 μg/mL. Using R* in combination with P caused a dramatic decrease in both the dark state MIC and the effective concentrations for light-induced survival, resulting in a narrow range between 4 and 6 μg/mL kanamycin.

Although the chromosomally integrated constructs used so far have the advantages of low background expression and do not require a selection marker, plasmids offer their own advantages for light-inducible resistance systems. Many resistance genes are naturally found on plasmids, and a plasmid origin allows for convenient transfer of systems between different strains. We further characterized our constructs on plasmids containing the p15A origin of replication, which has approximately ten copies per cell (Figure 3-2c).[150] Changing from chromosomal integration to a p15A plasmid increased the range of antibiotic concentrations at which cells containing OptoCre-*knt* selectively survive by over 5-fold. Despite this increase, we found that strategies such as lowering promoter or RBS strength can have a counterbalancing effect. We also characterized a p15A plasmid-based OptoCre-*bla*, however its basal resistance was too high to be considered functional (Figure AII-1a). Overall, the plasmid-based system with OptoCre-*knt* removes the need for the chromosomal insertion process, increasing the ease at which these constructs can be used in different strains or contexts.

The flexibility afforded by these different designs led us to develop multiple

constructs, and the optimal construct is likely to be application-specific. For example, the lower concentrations shown here are near the wild-type MIC, which is optimal for studies looking to characterize resistance acquisition using phenotypically-relevant antibiotic concentrations. In contrast, the higher concentrations allow more stringent cell selection for studies where only the activated cells should survive. Through this optimization process, we found constructs that allow a greater kanamycin MIC fold change between dark and light-exposed cultures compared to our original construct, notably P* and R driving OptoCre-*knt* expression on the chromosome is an ideal example of our optimized design (Figure 3-2d, Table 3-2).

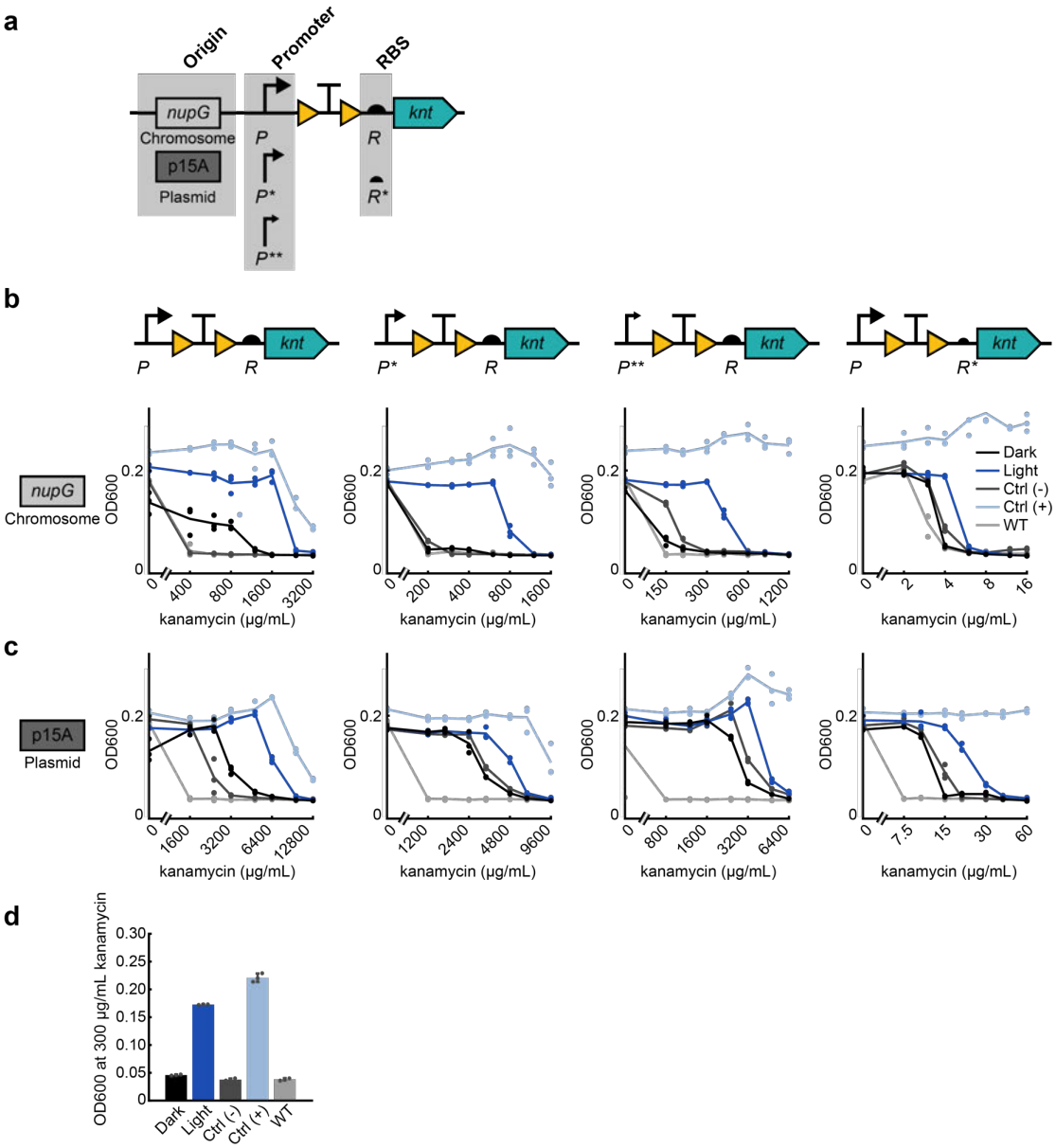

Figure 3-2. Promoter and RBS optimization of kanamycin resistance.

(a) Expression levels of the kanamycin resistance gene *knt* can be tuned by changing the strength of the promoter and ribosome binding site, as well as the origin of replication. Promoter strength ranges from P (medium) to P* (medium-low) to P** (low). Ribosome binding site strength ranges from R (strong) to R* (weak). **(b)** MIC curves of OptoCre-*knt* activation cassettes on the chromosome, with promoter P, P*, or P** and RBS R or R* (n = 3). **(c)** MIC curves of OptoCre-*knt* activation cassettes on a plasmid with the p15A origin of replication (n = 3). **(d)** Optimal OptoCre-*knt* activation conditions, using P* and R on the chromosome at 300 μg/mL kanamycin. Growth is quantified by OD600 after 18 hours. Error bars show standard deviation around the mean (n = 3 biological replicates).

3.4.3. Protein-level optimization of chloramphenicol resistance

Light-induced survival requires a tight OFF-state where cells are susceptible to antibiotic. As we have demonstrated, this can be achieved with low basal expression of the resistance gene. However, the uninduced state can also be minimized if the resistance enzyme itself is weaker. Thus, when activating the chloramphenicol acetyltransferase (*cat*) enzyme, we took advantage of a known mutation to decrease the strength of the enzyme itself. Chloramphenicol prevents protein synthesis by binding to the 50S ribosomal subunit, where it inhibits peptide bond formation. The *cat* enzyme prevents chloramphenicol from binding to the ribosome by attaching an acetyl group from acetyl-CoA to the antibiotic.[151] By using the weaker cat_{T172A} variant,[152,153] we lowered the concentration of antibiotic at which cells survive (Figure 3-3a). In the OptoCre-*cat* design, we used the promoter P and RBS R, and compared light-induced survival by *cat* and cat_{T172A}. Here we observed a sharper decrease in dark OFF-state resistance with cat_{T172A} compared to *cat*, lowering basal resistance to that of the wild-type strain on a chromosomally integrated construct (Figure 3-3b). We also observed a decrease in MIC values for *cat* and cat_{T172A} on a p15A plasmid origin (Figure 3-3c). This enzyme mutant approach to optimization may be particularly helpful when working with enzymes that show resistance to high concentrations of antibiotic even with minimal basal gene expression, or if using this system on a plasmid with a high copy number where it is hard to limit basal expression. This approach creates another point at which resistance levels can be fine-tuned, and the light-induced growth difference shown by cat_{T172A} on a p15A plasmid origin is a particularly versatile optimized design (Figure 3-3d, Table 3-2).

We wondered whether it would be possible to tune resistance levels by adjusting light exposure properties. To test this, we further characterized the OptoCre-*cat* design by modifying light exposure duration and intensity (Figure AII-2). We found that resistance levels were tunable, and depended on a combination of both duration of light exposure and the intensity of the blue light.

A common issue with many of our designs is that basal expression results in resistance levels that, although low, still exceed those observed in the wild-type strain. In principle, this leakiness could be the result of several different issues including spontaneous recombination events, mutations in the terminator, or readthrough of the terminator. We sequenced the *loxP* and terminator region of the (-) Control strain without Cre from both 0 μg/mL chloramphenicol and 75 μg/mL chloramphenicol conditions, where the latter represents the highest antibiotic concentration condition that showed any growth. Sequencing results from both conditions matched the original sequence of the plasmid, confirming that leaky expression is not the result of spontaneous recombination or terminator mutations. These results are in line with characterizations of the original OptoCreVvd2 design, which showed consistent low basal expression of a fluorophore with no evidence of spontaneous recombination.[133] To mitigate the potential for terminator readthrough we then attempted to lower basal expression by swapping the strong BBa_B0015 terminator from our original design to the synthetic terminator L3S2P21, which was the strongest terminator identified in an extensive set characterized in Chen *et al*.[154] However, this did not show further improvement over the terminator used in our initial design (Figure AII-3), so we did not pursue this avenue further. For

applications where minimal basal expression is critical, alternative designs could test other terminators[154,155] or different circuit design approaches.[156–158]

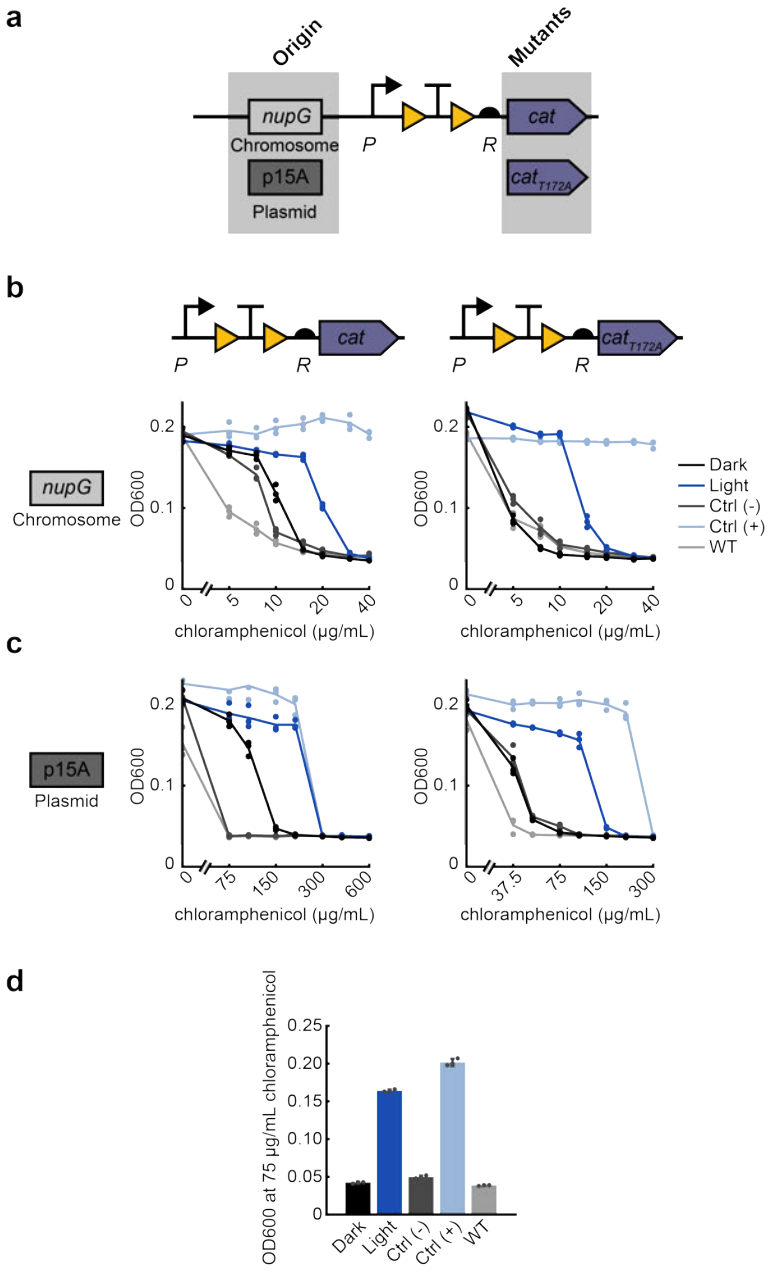

Figure 3-3. Enzymatic activity tuning of chloramphenicol resistance.

(a) Resistance given by the chloramphenicol resistance gene *cat* can be lowered by using the cat_{T172A} variant on a chromosomal or plasmid origin. **(b)** MIC curves of OptoCre-*cat* activation

cassette with the native enzyme *cat* or weakened enzyme cat_{T172A} on the chromosome (n = 3). **(c)** MIC curves of the *cat* and cat_{T172A} activation cassettes on a plasmid with the p15A origin (n = 3). **(d)** Optimal activation conditions, using cat_{T172A} with promoter P and RBS R on a plasmid origin at 75 µg/mL chloramphenicol. Growth is quantified by OD600 after 18 hours. Error bars show standard deviation around the mean (n = 3 biological replicates).

3.4.4. Efflux pump enabled tetracycline resistance

Light induction can also be applied to non-enzymatic antibiotic resistance mechanisms, such as the *tetA* efflux pump. The antibiotic tetracycline reversibly binds to the 30S ribosomal subunit, inhibiting protein synthesis. The *tetA* efflux pump localizes to the inner membrane and exports magnesium-tetracycline chelate complexes by importing a proton.[140] In sharp contrast to *bla*, *knt*, and *cat* where the native resistance levels were high and our engineering efforts aimed at reducing potency, we found that our initial design for inducible *tetA* did not show resistance over wild-type MG1655 when expressed with promoter P and RBS R on a p15A origin plasmid (Figure AII-1b), conditions which produced the highest levels of resistance in the constructs we tested previously. To compensate for this, we opted to use the strong native promoter P_{tet} with its corresponding RBS R_{tet} to allow full expression of the *tetA* gene[159] to create OptoCre-*tetA* (Figure 3-4a). Using this native architecture, OptoCre-*tetA* showed some activation when chromosomally integrated (Figure 3-4b), and exhibited strong activation on the p15A plasmid origin (Figure 3-4c). Notably, the dark-state basal resistance over wild-type MG1655 was minimal, allowing for activation of OptoCre-*tetA* at low tetracycline concentrations. Thus, we found that the p15A plasmid-based version is an ideal construct for tetracycline resistance (Figure 3-4d, Table 3-2).

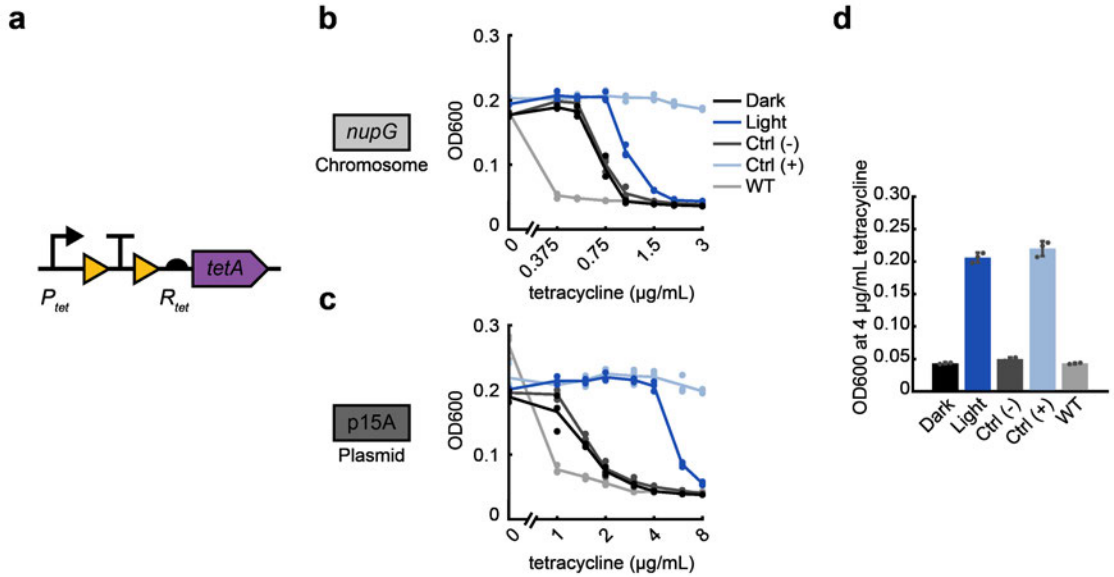

Figure 3-4. Optogenetic activation of efflux-based tetracycline resistance.

(a) Tetracycline resistance gene *tetA* is expressed using the native promoter P_{tet} and native RBS R_{tet}, to allow maximal expression of the gene. **(b)** MIC curves of OptoCre-*tetA* on the chromosome and **(c)** p15A plasmid origin (n = 3). **(d)** Optimal OptoCre-*tetA* activation conditions, using the p15A plasmid origin at 4 µg/mL tetracycline. Growth is quantified by OD600 after 18 hours. Error bars show standard deviation around the mean (n = 3 biological replicates).

3.4.5. Single-cell microscopy showing resistance activation

The spatial and temporal precision enabled by optogenetics allows these constructs to be used for a variety of applications, including single-cell studies of bacterial antibiotic resistance. How resistance acquisition leads to bacterial survival at the single-cell level is of particular interest in the context of horizontal gene transfer. Existing single-cell horizontal gene transfer studies have previously characterized gene transfer rates and shown important connections to quorum sensing.[160,161] However, natural instances of horizontal gene transfer are infrequent and difficult to control in space and time, especially relative to antibiotic exposure. Previous studies have also shown that stochastic acquisition of resistance in single cells is not always enough to cause the

proliferation of phenotypically resistant cells.[162] To study when horizontal gene transfer events lead to the spread of resistance in populations, it would be interesting to model a single cell's acquisition of resistance with optogenetic control of antibiotic susceptibility. This could be used to characterize when and how resistance acquisition in single cells leads to antibiotic evasion, and how specific antibiotic dosing schedules and concentrations impact evasion frequency.

Here we show a proof-of-concept for the first steps in this class of studies by inducing cell growth using blue light for cells on agarose pads. Using time-lapse microscopy, we placed cells containing light-activatable antibiotic resistance on agarose pads containing antibiotics and compared the growth of cells that were kept in the dark to those exposed to blue light. For these studies we elected to focus on a subset of resistance genes, selecting kanamycin and chloramphenicol as examples of bactericidal and bacteriostatic antibiotics, respectively. We characterized resistance activation for chromosomally integrated OptoCre-*knt* resistance to kanamycin (Figure 3-5a, Supplementary Movie 1 from Sheets *et al.* 2023[163]), and plasmid-based OptoCre-*cat* resistance to chloramphenicol (Figure 3-5b, Supplementary Movie 2 from Sheets *et al.* 2023[163]). We found that cells with light-induced resistance showed a short lag before growth compared to their constitutively resistant positive controls, which likely corresponds to the time needed to excise the transcription terminator and allow expression of the resistance gene. In contrast, when cells were kept in the dark, growth was inhibited and we observed examples of loss of membrane integrity (Supplementary Movies 1 and 2 from Sheets *et al.* 2023[163]). To quantify recovery of resistance-induced

cells, we calculated the percentage of cells in the initial frame that recovered over the course of the movie (Figure AII-4). We defined the time of recovery as the point at which a cell first divides, and found 70% recovery for OptoCre-*knt* and 42% recovery for OptoCre-*cat* with light exposure (compared to 13% and 4% for cells in the dark, though notably cells in the dark rarely experienced more than one division event, Supplementary Movies 1 and 2 from Sheets *et al.* 2023[163]). Although these data show clear differences between light and dark exposure, the incomplete rates of recovery under light exposure may be due to simultaneous exposure to antibiotic and light, likely rendering some cells nonviable before they can be induced. In the future, microfluidic experiments could help to assess recovery rates as a function of relative light induction and antibiotic addition timing.

Looking towards future applications that require the control of subpopulations of cells, we also used a digital micromirror device (DMD)[16] to activate resistance in a subset of cells. The DMD allows for programmed illumination of specific areas within a field of view. We illuminated half of the field of view and saw preferential activation of cells in the blue light illuminated region (Figure AII-5). We did observe some growth in a subset of the cells in the dark half of the field of view, albeit at reduced levels relative to the illuminated half. This may be due to diffusion of light from the DMD, as we do not see this activation until after DMD illumination starts. Compared to the longer, lower intensity exposures we used in liquid culture experiments, the DMD is designed to deliver intense periods of light. These differences suggest that DMD activation protocols and setups could be optimized for improved activation timing in the future.

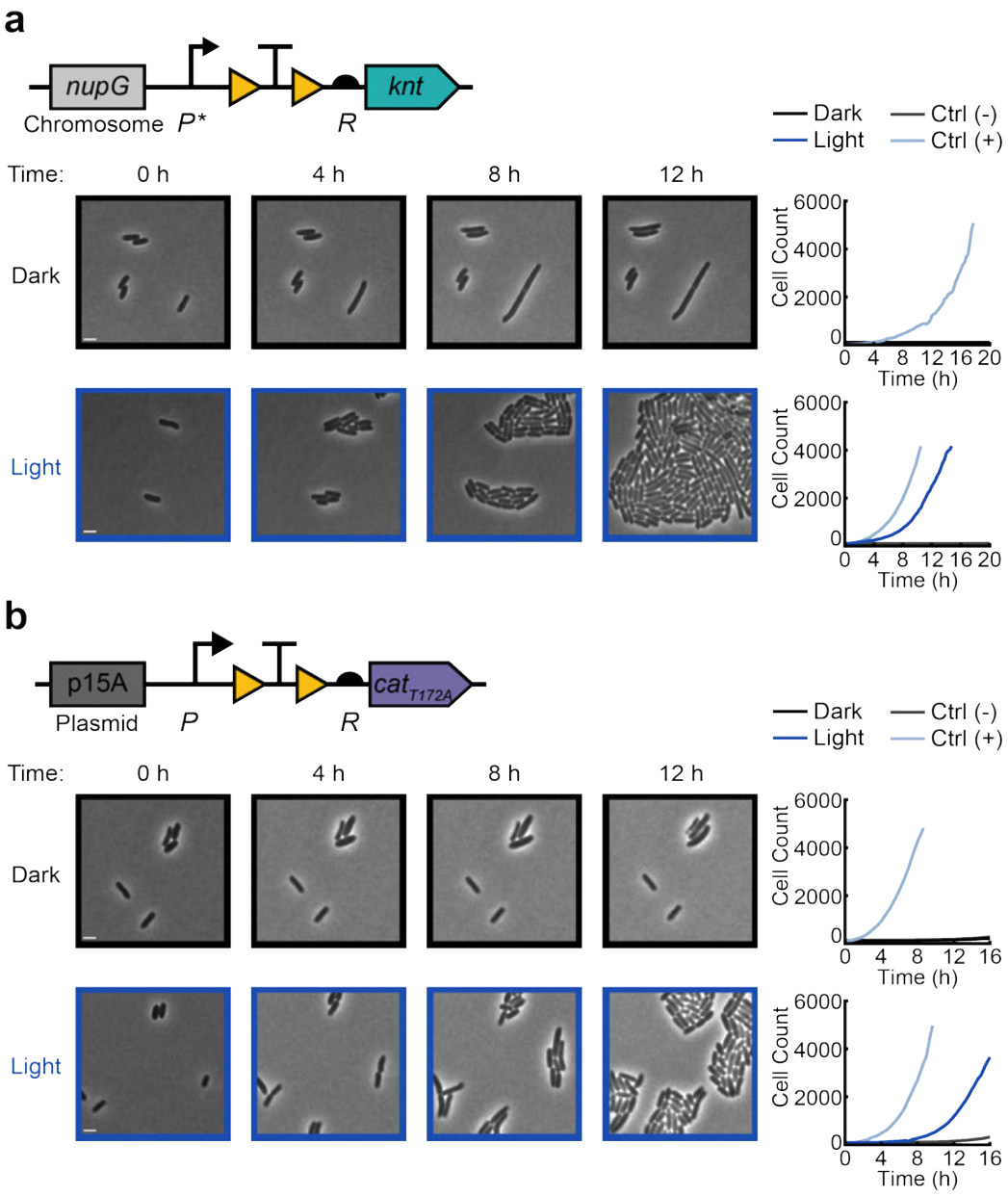

Figure 3-5. Single-cell time-lapse microscopy of light-induced resistance.

Activation of **(a)** the chromosomal OptoCre-*knt* resistance construct with promoter P* and RBS R on agarose pads containing 400 µg/mL kanamycin, and **(b)** the p15A plasmid-based OptoCre-*cat* resistance construct using cat_{T172A} with promoter P and RBS R on agarose pads containing 60 µg/mL chloramphenicol. Microscopy images show representative samples of the resistance activation strains in the dark or with blue light (scale bar = 2 µm). Cell counts over time are cumulative across multiple imaging positions for each condition, with each plot containing the OptoCre resistance strain along with negative and positive controls (n = 3 biological replicates).

3.4.6. Improving octanoic acid production using antibiotic selection

To demonstrate the utility of the system for biotechnology applications, we next focused on increasing yield of octanoic acid through co-expression of *cat* or *tetA* with the thioesterase *Cp*FatB1 (Figure 3-6a,b). *Cp*FatB1 is derived from the plant species *Cuphea palustris* and has been optimized for expression in *E. coli.*[164] *Cp*FatB1 expression is taxing on cells, therefore directly coupling its induced expression with antibiotic resistance can allow for selective growth of cells actively producing both enzymes, thereby preventing the growth of non-expressing cells (Figure 3-6c). We used OptoCre-*cat* with the cat_{T172A} mutant and OptoCre-*tetA* for selection due to their wide induction ranges and minimal basal resistances on the p15A plasmid origin. For fatty acid production, we used the highly active variant *Cp*FatB1.2-M4-287 which has been previously shown to boost octanoic acid production.[164] To optimize expression of the *Cp*FatB1 gene without disrupting the resistance activation architecture, we placed it immediately downstream of the resistance gene under expression of a strong computationally-designed RBS denoted R'. Consistent with the protocol for inducing antibiotic resistance alone, we performed induction by exposing cells to blue light for two hours early in the growth phase. From a bioproduction perspective, an advantage of the OptoCreVvd system is its irreversibility, which enables permanent activation of *Cp*FatB1 without the need for continuous illumination. This circumvents issues with dynamic light induction systems, where light penetration can become a concern for dense cell cultures in metabolic engineering contexts.[52,83] We found that light induction alone leads to a significant increase in octanoic acid production for both the *cat* and *tetA* systems. We

next asked whether introducing antibiotic selection could further improve yields. We found that with OptoCre-*cat*, adding 150 µg/mL chloramphenicol significantly improved production, increasing it by 29% over the light induction-only condition, with higher chloramphenicol concentrations resulting in similar performance (Figure 3-6d). Light induction alone or with antibiotic also showed a substantial improvement in yield over a constitutively expressed version of *Cp*FatB1 with identical genetic architecture and constitutive Cre recombinase expression (Figure 3-6d). With OptoCre-*tetA*, octanoic acid production increased 150% over light induction alone when it was supplemented with 1.5 µg/mL tetracycline (Figure 3-6e). Higher tetracycline concentrations improved yield further, reaching a 300% increase over light alone when 6 µg/mL tetracycline was added. These concentrations are on the upper range of the resistance levels we see in our MIC experiments for the respective strains, possibly due to the higher OD (OD600 ≈ 0.6) at the time antibiotics are added in our bioproduction protocol. The induction system with OptoCre-*tetA* did not boost production over constitutive expression of *Cp*FatB1, though the addition of antibiotic did greatly improve yield over light alone (Figure 3-6e). Importantly, the constitutively expressed versions of both the *cat* and *tetA* constructs showed poor growth profiles compared to the light-inducible versions (Figure AII-6). This growth deficit in the constitutive constructs is problematic, as it may lead to escape mutants and reduce the stability of production strains. Thus, coupling octanoic acid production with resistance selection leads to higher yields of octanoic acid than light induction alone, without the taxing growth deficit associated with continuous production.

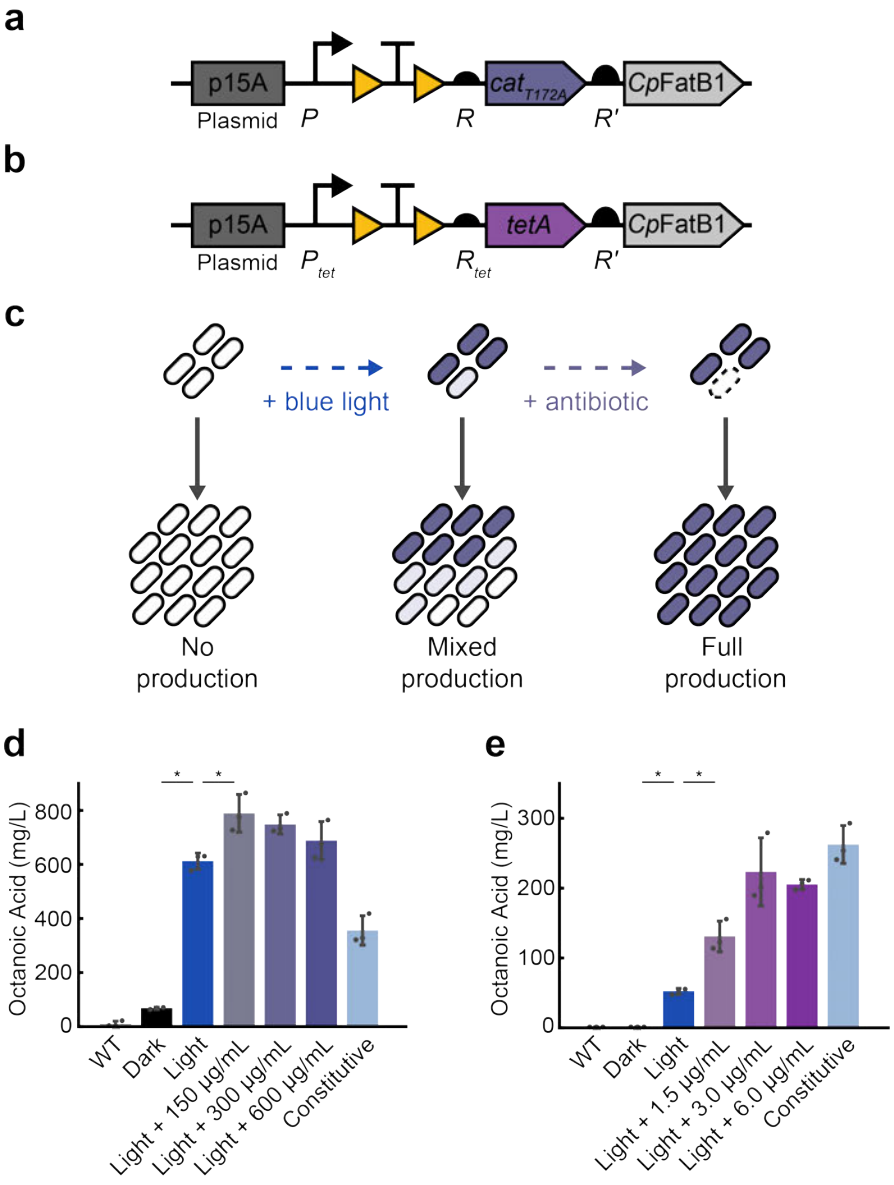

Figure 3-6. Light-inducible production of octanoic acid.

(a) Activation of OptoCre-*cat* using cat_{T172A} or **(b)** OptoCre-*tetA* is coupled with *Cp*FatB1 by introducing the gene downstream of the drug resistance marker under the strong RBS R'. **(c)** Blue light induces expression of the resistance gene and *Cp*FatB1, but does not guarantee all individuals within a community are expressing the genes. Non-producers have a growth advantage due to the burden of *Cp*FatB1. Addition of chloramphenicol prevents growth of any individuals not producing the resistance gene and consequently *Cp*FatB1. **(d)** Octanoic acid production coupled with OptoCre-*cat* measured by GC-MS. **(e)** Octanoic acid production coupled with OptoCre-*tetA* measured by GC-MS. Significance was determined using a two-tailed Welch's t-test: *, $P < 0.05$; n.s. not significant. Error bars show standard deviation around the mean (n = 3 biological replicates).

Comparing the OptoCre-*cat* and OptoCre-*tetA* constructs, we found that while OptoCre-*cat* showed higher production overall, OptoCre-*tetA* showed a greater increase in production with increasing antibiotic concentrations over the range tested. This could be due to the difference between resistance types (enzymatic vs. efflux) and their impact on population dynamics, or the different promoters of the constructs (P vs. P_{tet}), suggesting that these constructs and their induction could likely be optimized further to increase production. This work shows the potential of using light to control antibiotic resistance for metabolic engineering and bioproduction applications.

3.5. Discussion

We have developed and optimized optogenetically controlled systems for four antibiotic resistance genes. Using a blue light-inducible Cre recombinase, we have shown activation of *bla*, *knt, cat*, and *tetA* to induce resistance over a range of antibiotic concentrations. These resistance genes span multiple mechanisms and represent antibiotics and resistance genes commonly used in synthetic biology and microbiology labs. A crucial aspect of designing inducible resistance is the level of expression in the uninduced and induced states, and optimal levels vary dramatically with the strength of the resistance gene. Therefore, we tested promoters, RBSs, and enzyme mutants of varying strength to find constructs that show optimal basal expression and fold changes of resistance activation. To control copy number at the DNA level, we also compared constructs chromosomally-integrated in the *nupG* region and on a p15A medium copy plasmid, which improved flexibility in experimental design. We found that optimizing

resistance induction constructs at the promoter, RBS, enzyme, and copy number levels can be used as a generalizable approach, providing multiple options for altering expression to allow for flexibility in construct design to meet experimental constraints. For example, studies which require a native promoter, specific plasmid origin, or particular resistance protein to be compatible with other elements of the strain design, can be accommodated as this system is adapted to different use cases or other resistance genes. This system also allows for the expansion of resistance genes beyond the ones shown here, using the optimization approaches mentioned above. Future experiments characterizing expression directly could also be an effective route for further optimizing designs. Using techniques like qPCR or Western blots could enable relative measurement of transcription and translation levels, or protein fusions with a fluorophore could enable measurement in cases where the fusion is known not to impact function.

We selected the four antibiotic resistance mechanisms here to be broadly applicable for both synthetic biology and microbiology uses. These antibiotics and resistance genes are often used as plasmid selection markers and in synthetic biology control systems.[58,132] As an example of an application, these constructs have the potential to be applied to single-cell selection in microfluidic systems. Selection of single cells of interest from a microfluidic device is a challenge, and current methods require complex optical traps and valve-based microfluidic devices.[123] Combining light-inducible resistance with a DMD[16] for precise targeting of light would allow for antibiotic selection of a cell line of interest from device outflow, without any chip modification or additional hardware requirements beyond light exposure. Using light also allows integration into

computational workflows, potentially facilitating automated screening and selection for phenotypes of interest. The permanent switch would ensure that the selection signal is not lost, allowing progeny of selected bacteria to be harvested for characterization at any point after activation. Additionally, given the prevalence of recombinases in cellular logic,[40] this system could be modularly integrated with larger recombinase circuits as a logic output controlling cell survival. For instance, recombinase-controlled resistance genes could be broadly used to regulate cell survival only if certain environmental conditions (e.g. small molecule, light, or temperature) are met.[40] In these cases, it may be worth using a constitutive version of OptoCreVvd2, rather than the IPTG-inducible version used here, to simplify the workflow and minimize chemical induction requirements. As both recombinases and the selected resistance genes are commonly used in synthetic biology, this allows for optogenetic control to be straightforwardly incorporated into existing genetic systems.

Further, we envision these light-inducible antibiotic resistance genes being useful as a synthetic system for studying horizontal gene transfer. These systems are well-suited to examine how single-cell resistance gene acquisition events lead to population expansion or decline. Being able to permanently activate resistance gene “acquisition” using light removes the need to rely on observations of infrequent and stochastic natural horizontal gene transfer events. Notably, *bla* is particularly problematic in clinical settings,[136] and known to be transferred extensively when the gut is exposed to ampicillin.[126] Recent studies looking at single-cell instances of horizontal gene transfer have also shown that quorum sensing and biofilm structures can be important in initiating

transfer events,[160,161] however experiments thus far have been limited to the study of infrequent horizontal transfer events. Critically, because not all resistance acquisition events lead to the proliferation of resistant populations,[162] synthetic control of resistance acquisition could reveal when and how cells acquiring resistance proliferate. In the future, this system could also be modified to enable resistance to be turned off or controlled reversibly, allowing for both resistance acquisition and loss studies. Using light as an inducer also enables studies with spatial dynamics, beyond what could be achieved using chemical induction. However, light penetration may become an issue for complex 3D spatial geometries. Overall, the spatial and temporal control afforded by these optogenetic systems could allow researchers to determine what cellular arrangements and antibiotic treatment schedules lead to expansion or collapse of microbial communities consisting of resistant cells and their susceptible neighbors.[162,165]

This system also provides novel benefits to synthetic bioproduction systems, which we demonstrated in a pilot study using *Cp*FatB1 to increase production of octanoic acid. Although efficient, the expression and enzymatic activity of *Cp*FatB1 are taxing at high levels, resulting in a growth advantage for non-producers and potentially giving rise to cheaters.[164,166] By coupling expression of a resistance gene with the bioproduction enzyme, we can limit growth to only cells expressing *Cp*FatB1, further increasing yield over the equivalent system with light induction alone. This work can be expanded to other bioproduction enzymes of interest, or co-expressed with multiple genes to require expression of several enzymes in a pathway for growth.

Antibiotic resistance genes are ubiquitous and fundamental tools of synthetic

biology. However, there are few current methods that allow dynamic regulation of their expression. The ability to activate resistance using light expands this core tool, improving spatiotemporal control and enabling new applications in cellular selection and the study of antibiotic resistance acquisition.

Resistance	Site	Promoter	RBS	Dark MIC (μg/mL)	Light MIC (μg/mL)
OptoCre-*bla*					
	chromosomal (*nupG*)	P	R	300	1200
	plasmid (p15A origin)	P	R	10000	10000
OptoCre-*knt*					
	chromosomal (*nupG*)	P	R	1600	2400
	chromosomal (*nupG*)	P*	R	200	1200
	chromosomal (*nupG*)	P**	R	200	600
	chromosomal (*nupG*)	P	R*	4	6
	plasmid (p15A origin)	P	R	6400	9600
	plasmid (p15A origin)	P*	R	4800	6400
	plasmid (p15A origin)	P**	R	4800	6400
	plasmid (p15A origin)	P	R*	15	40
OptoCre-*cat*					
	chromosomal (*nupG*) cat	P	R	15	30
	chromosomal (*nupG*) cat_{T172A}	P	R	10	30
	plasmid (p15A origin) cat	P	R	150	300
	plasmid (p15A origin) cat_{T172A}	P	R	75	200
OptoCre-*tetA*					
	chromosomal (*nupG*)	P	R	1.5	1.5
	chromosomal (*nupG*)	P_{tet}	R_{tet}	1	2
	plasmid (p15A origin)	P	R	1.5	1.5
	plasmid (p15A origin)	P_{tet}	R_{tet}	4	8

Table 3-2. Dark and light state MICs of all resistance activation constructs.

Optimal constructs for each antibiotic are highlighted in gray, where this selection considers both fold change and total numerical difference in MIC on light exposure.

3.6. Methods

Strains and plasmids

All antibiotic resistance assays use *E. coli* strain MG1655. We constructed plasmids using the Gibson assembly method,[116] or using Golden Gate assembly[167] in cases where the constructs contained fragments under 100 base pairs in length (Table AII-1). Chromosomally integrated constructs were inserted using the Lambda Red recombinase system[117] downstream of *nupG* (forward homology site: GGTTCTGGCCTTCGCGTTCATGGCGATGTTCAAATATAAACACGT, reverse: GGCGTGAAACGGTTGTACGGTTATGTGTTGAAGTAAGAATAA). Antibiotic resistance cassettes flanked with FRT sites were used to select successful integrations (we used *knt* for *bla* and *cat* activation constructs, *cat* for *knt* and *tetA* activation constructs); these cassettes were then cured using a plasmid-based Flp recombinase on a temperature sensitive origin following the protocol from Datsenko and Wanner.[117] Finally, we cured the temperature sensitive plasmid before subsequent experiments.

The plasmids used for OptoCreVvd2 expression were derived from Sheets *et al*.[133] For *bla* activation studies, we changed the plasmid selection cassette from *bla* to *cat*, using the gene from the BglBrick plasmids[58] and primers listed in Table AII-1. The antibiotic resistance activation plasmids were made by changing the respective promoter, RBS, and reporter gene of pBbAk-W4-loxTTlox-mRFP1 from Sheets *et al*.[133] Plasmid origins of replication and sequences for *bla*, *knt*, and *cat* were taken from the BglBrick plasmid series.[58] The cat_{T172A} mutation was taken from Ciechonska *et al.*[152] We thank Caroline Blassick for creating the cat_{T172A} mutant and Mark Isalan for pointing us to this

variant. The sequence for *tetA* was obtained from AddGene plasmid #74110 (pRGD-TcR) deposited by Hans-Martin Fischer.[168] The sequence for *Cp*FatB1.2-M4-287 was obtained from Hernández Lozada *et al.* and synthetized using Twist Bioscience.[164] Constitutive *Cp*FatB1.2-M4-287 expression strains were created by co-transforming the same reporters used for the light expression experiments with pBbE5a-Cre, which acts constitutively. All plasmid-based resistance constructs contain the p15A origin. Plasmid-based constructs for *knt* activation contain *cat* as a selection marker, and constructs for *bla, cat,* and *tetA* activation contain *knt* as a plasmid selection marker. Positive controls for *bla* and *tetA* contain the respective gene with its native promoter and RBS on a plasmid with the p15A origin. Positive controls for *knt* and *cat* contain the respective gene with its native promoter and RBS on a plasmid with the p15A origin for studies using a plasmid-based reporter, or integrated into the *nupG* region for studies using chromosomally integrated reporters. Promoters used were medium, medium-low, and low-strength variants of T7 A1,[115] denoted P (TTATCAAAAAGAGTA *TTG***CA***T* TAAAGTCTAACCTATAG *GA***AT***CT* TACAGCC**A**TCGAGAGGGACACGGCGAA), P* (TTATCAAAAAGAGTA *TTG***T***CT* TAAAGTCTAACCTATAG *GAT***T***CT* TACAGCC**A**TCGAGAGGGACACGGCGAA), and P** (TTATCAAAAAGAGTA *TTG***TAA** TAAAGTCTAACCTATAG *GAT***TT***T* TACAGCC**A**TCGAGAGGGACACGGCGAA). Underlines indicate mutations from the original T7 A1 promoter. Ribosome binding site R is the RBS of gene 10 in the T7 phage (TTTAAGAAGGAGATATACAT).[148] R* (ATCACTCTACGGCCAGCTGCAAAC) was computationally designed using De Novo DNA version 2.1 to have a 10x weaker

translation strength (14.8 A.U.) compared to R (148 A.U.), and R' (TTTGTTTAATTACTAAGCGGGAGGTTAT) was designed for increased translation strength (100,000 A.U.).[149,169] The rrnB terminator BBa_B0015, used in the original pBbAk-W4-loxTTlox-mRFP1 from Sheets *et al*.,[133] was used as the *loxP*-flanked terminator in all constructs unless otherwise noted. The strong synthetic terminator L3S2P21[154] was synthesized by IDT and cloned into an *mCherry* variant of the original fluorescent reporter plasmid. Primers used to change each of these elements are included in Table AII-1. Plasmids and strains from this study and their sequences are available on AddGene (https://www.addgene.org/Mary_Dunlop/).

Blue light exposure

Strains were grown overnight from a single colony in selective LB media containing 100 μg/mL carbenicillin, 30 μg/mL kanamycin, or 25 μg/mL chloramphenicol as required for plasmid maintenance. Cultures were refreshed 1:100 in selective M9 minimal media (M9 salts supplemented with 2 mM $MgSO_4$, 0.1 mM $CaCl_2$, and 0.1% glucose) for two hours with 100 μM IPTG for induction of OptoCreVvd2 split recombinase production. Cultures were then either exposed to blue light or kept in the dark for two hours. Light exposure was performed using a 24-well light plate apparatus (LPA)[104] using 1 mL cultures with two 465 nm wavelength LEDs per well (ThorLabs LED465E), with a total output of 120 μW/cm^2 per well. For the light intensity variation experiment, the LPA was used to deliver 5, 60, or 120 μW/cm^2 for 0.5, 1, or 2 hours following the same protocol.

Minimum inhibitory concentration measurement

Minimum inhibitory concentrations (MICs) were measured based on the protocol outlined in Wiegand *et al*.[170] Antibiotic stocks were made by dissolving the antibiotic in sterile distilled water (carbenicillin, kanamycin, tetracycline) or 99% ethanol (chloramphenicol), with concentrations normalized for potency based on CLSI standards.[171] Assay plates for measuring the MIC were prepared by performing serial dilutions of antibiotic in 100 μL M9 minimal media in 96-well plates. Low glucose media was used to reduce growth variability by creating carbon-limiting, rather than nutrient-limiting, growth conditions.[146] Antibiotic concentrations were selected to include values that spanned the MIC levels for the dark and light state cultures in each experiment. Immediately following light exposure, cultures were normalized by dilution to the lowest optical density (OD) of each experiment. Normalized cultures were then diluted 1/25 into 96-well plates in triplicate and grown overnight for 18 hours at 37°C. The OD absorbance reading of each well was then measured at 600 nm (OD600) using a BioTek Synergy H1 plate reader. Post-sample sequencing for OptoCre-*cat* reporter strain alone was done on liquid culture from the 0 μg/mL and 75 μg/mL (just below MIC) growth conditions, at the end of the 18-hour growth period for samples shown in Figure AII-2. Samples were amplified using Phusion polymerase by forward (AAGCCATCCAGTTTACTTTG) and reverse (CCAGCTGAACGGTCTGGTTATAGG) primers to encompass the terminator region.

Colony forming unit measurement

Colony forming units (CFU) were measured following the micro-spotting protocol outlined in Sieuwerts *et al*.[172] After MIC plates were grown overnight for 18 hours, cultures were serially diluted 1:10 in 1x M9 salts in a 96-well plate. Dilutions from 10^{-1} to 10^{-6} were spot-plated, with 5 µL on LB-agar plates in duplicate for each well (n = 6 for each condition). Plates were grown overnight at 37°C and colonies were counted by hand the next day for the lowest dilution with countable colonies for each sample. CFU counts per mL were then calculated by multiplying dilution level by the average number of colonies counted by per condition, normalizing for the 5 µL volume plated.

Microscopy and image analysis

Strains were grown overnight from a single colony in selective LB media. Cultures were refreshed 1:100 in selective M9 minimal media for two hours with 100 µM IPTG for induction of OptoCreVvd2. Samples were then placed on 1.5% low melting agarose pads made with M9 minimal media containing 100 µM IPTG and 400 µg/mL kanamycin (*knt* activation) or 60 µg/mL chloramphenicol (*cat* activation). Samples were grown at 30°C to prevent pads from drying out, and imaged every 15 minutes (*knt* activation) or 20 minutes (cat_{T172A} activation) for 18 hours. For whole-frame illumination experiments, cells were imaged at 100x using a Nikon Ti-E microscope. Blue light exposure was provided by a LED ring (Adafruit NeoPixel 1586), which was fixed above the microscope stage and controlled by an Arduino with a custom MATLAB script for a total output of 330 µW/cm^2. Images were segmented and analyzed using the DeLTA 2.0

software.[173] Cell divisions were annotated by hand. For digital micromirror device (DMD) experiments illuminating half of the field of view, cells were imaged at 100x using a Nikon Ti-2 microscope. Light exposure was provided by a DMD (Mightex Polygon400) connected to the illumination light path of the Nikon Ti-2 chassis. Light from the DMD was passed through a 10% neutral density filter (Chroma UVND 1.0) for a total of 1.2% power, or 160 mW/cm^2, for 4 out of 5 minutes for each imaging cycle. An Arduino Uno microcontroller was used to synchronize the camera, the illumination source, and the DMD for image acquisition.[174]

Fatty acid production and measurement

Strains were grown overnight from a single colony in selective LB media. Cultures were refreshed 1:50 in selective M9 minimal media containing 2% glucose[175] and 100 μM IPTG for strains with OptoCreVvd2. Cultures were grown to an OD600 ≈ 0.2. Induced cultures containing OptoCreVvd2 were then exposed to blue light for two hours. Immediately following light exposure, 150, 300, or 600 μg/mL chloramphenicol or 1.5, 3, or 6 μg/mL tetracycline was added to OptoCreVvd2 induced cells. Following 20 hours of growth post light induction, 400 μL of the cultures were taken and prepared for gas chromatography-mass spectrometry (GC-MS) quantification. Constitutively expressed *Cp*FatB1 strains were grown in identical conditions but did not receive light or antibiotic. Fatty acid extraction and derivatization into fatty acid methyl esters was completed as described by Sarria *et al*.[176] An internal standard of nonanoic acid (C9) was added to the sample at a final concentration of 88.8 mg/L and vortexed prior to

extraction. The samples were analyzed with an Agilent 6890N/Agilent 5973 MS detector using a DB-5MS column. The inlet temperature was set to 300°C with flow at 4 mL/min. The oven heating program was initially set to 70°C for 1 min, followed by a ramp to 290°C at 30°C/min, and a final hold at 290°C for 1 min. The nonanoic internal standard was used for quantification of octanoic acid titer.

Statistical analysis

OD600 values in MIC curves and bar plots are reported as the mean of three samples ± the standard deviation. Colony count values for CFU measurements are reported as the mean of six samples consisting of two dilutions and platings for each MIC data point. Fatty acid production measured using GC-MS is reported as the mean of three biological replicates for each condition ± the standard deviation. Statistical significance (P value) for fatty acid production was assessed using a two-tailed Welch's t-test.

CHAPTER 4. Efforts toward understanding the impact of resistance activation timing

4.1. Introduction

Understanding how bacteria gain resistance to antibiotics is vital to dealing with antibiotic resistance as a public health issue. Horizontal gene transfer (HGT), where bacteria acquire a resistance gene from the environment or another bacterium, is a major mechanism of resistance spread.[69] The impacts of HGT are seen at many scales: the single-cell event of DNA uptake and resistance gene expression, spread of single resistant cells to a population or problematic infection, and the broader spread of resistance genes and bacteria between people or in the environment. Many of the molecular mechanisms of gene acquisition at the molecular level are well understood, and important to developing novel antibiotics.[70,71] Similarly, the human population and global spread of resistance is highly studied, leading to knowledge that can impact public health policies and medical practices.[72,73] Recently, there has been increasing interest at bridging these two scales.

Characterizing when individual gene acquisition events lead to the spread of a resistant population is vital to understanding how to prevent problematic resistant infections. Due to various environmental factors, not all resistance acquisition events lead to the spread of a resistant population.[75,162] Studies documenting the spatiotemporal dynamics of the initial acquisition of the resistance can inform which treatment plans could best prevent different types of resistant infections in a clinical setting. Recent work in this area has shown promising results, revealing that tetracycline resistance, even when

attained after tetracycline exposure, can lead to survival in *E. coli*.[74] This is not true for all antibiotics however, as a recent study showed that kanamycin resistance events after kanamycin exposure do not lead to survival and proliferation in a multispecies context.[75] Within this class of studies, it is not clear how the nature of the antibiotic (bacteriostatic vs. bactericidal) and type of resistance (efflux-based vs. enzymatic) impact cell survival.

The OptoCreVvd-based antibiotic resistance induction system can serve as a model for horizontal gene transfer, where a resistance gene is suddenly switched "on" in a similar manner to horizontal acquisition. The standardization the system provides can create more direct comparisons between antibiotic classes and resistance types, giving a clear understanding of how these factors lead to resistant population survival or collapse at the single cell level. This chapter makes the first steps towards studies characterizing the environmental factors that lead to cell survival or death after antibiotic resistance activation.

When understanding the temporal dynamics of resistance acquisition, having a clear idea of when resistance genes are activated by OptoCreVvd will be important to understanding how resistance acquisition relative to antibiotic dose timing impacts cell survival. As an orthogonal output, we couple the resistance constructs developed in Chapter 3 with fluorophores. By visualizing fluorescence over time, we can get a closer understanding of when single cells and populations begin to produce resistant proteins, and how this leads to survival or death events. Ultimately, we hope to characterize the impact of resistance acquisition timing on cell survival at the single-cell and population level for all four antibiotics used here.

To aid future resistance construct development and optimization, we also develop a two-fluorophore Cre "stoplight" reporter and a red light-inducible Cre recombinase. The stoplight reporter can be used to test alternate terminators and activation architectures, with a clearer ratiometric output showing when bulk cultures and single cells are in pre- or post-recombination states. The red light-inducible CreREDMAP could be used in conjunction with blue or green light-inducible tools for multi-level control of gene expression.

4.2. Simultaneous activation of resistance and fluorescence

Coupling resistance and fluorescence activation allows us to precisely understand when and how strongly cells begin expressing resistance genes activated by OptoCreVvd. Two straightforward ways to couple gene expression is through transcriptional fusions, where the genes are placed under the same promoter (and here, after the same *lox*-flanked terminator) but with separate ribosome binding sites, or translational fusions, where the genes are expressed under the same ribosome binding site and connected physically by a short flexible protein linker. Both have approaches advantages and drawbacks. Transcriptional fusions can enable different expression levels of each protein, and are less likely to interfere with protein function. However, the two proteins may not fold at the same rate, and these different expression levels make comparison slightly more qualitative. Additionally, all spatial information about the protein of interest is lost. As an inverse, translational fusions can give more quantitative and spatial information about the protein of interest, but may interfere with protein function or localization. We attempt both approaches here to varying success.

We first set out to develop a resistance co-expression system with the p15A-based OptoCre-*cat*$_{T172A}$-P-R, due to its large antibiotic resistance induction window on a plasmid backbone. For a fluorophore we chose *mCherry*, because its fluorescence absorption and emission spectra are orthogonal to the blue light used to activate OptoCreVvd and will minimize the chance of basal activation. We initially found that a similar RBS strength to the one used for the resistance genes did not give readable fluorescence when placed after *cat*. To increase fluorescence to readable levels, we then tested multiple stronger RBSs (Figure 4-1a). RBS sequences were created using the De Novo DNA "RBS Control" program to have strengths of 10^3, 10^4, 10^5, and the maximum possible strength of 2.4 million.[149] For reference, the RBS used for *cat* and initially tested for *mCherry* was predicted to have a strength of 150 (Table 4-1). Fluorescence activation was clear with $R_{100,000}$ and R_{2M}, and the addition of a strongly expressed fluorophore did not have a substantial impact on resistance activation.

In addition to the successful transcriptional fusion, we also tested translational fusions with an eight amino acid flexible GS linker (GGGSGGGS) to *mCherry* or *sfgfp* (Figure 4-1b). The green fluorescent *superfolder gfp* was chosen due to its bright fluorescence and rapid maturation time of around 15 minutes, comparable to *mCherry*.[177,178] These fusions also did not appear to dramatically impact resistance induction, and both gave readable fluorescence levels. However, *sfgfp* fluorescence gave a much clearer signal, suggesting that despite its absorption spectra overlap with the spectra of OptoCreVvd, it may be a better candidate for translational fusion. Moving forward, brighter red fluorescent proteins could also be promising fusion candidates.[179]

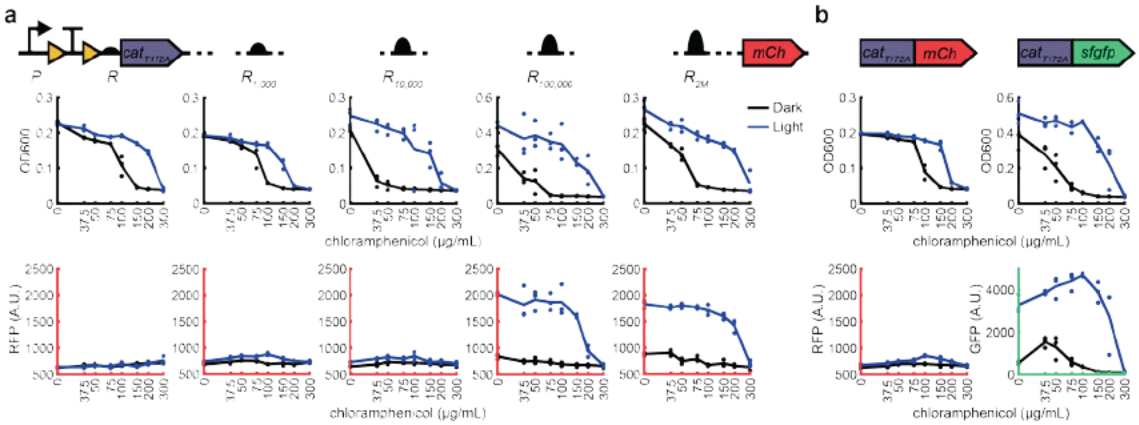

Figure 4-1. Impact of RBS on chloramphenicol co-fluorescence.

(a) Growth and fluorescence data across antibiotic concentrations for transcriptional fusions of cat_{T172A} and *mCherry*. The first construct shows cat_{T172A} alone, followed by RBS strengths 1,000, 10,000, 100,000, and 2,000,000 for *mCherry*. **(b)** Growth and fluorescence data across antibiotic concentrations for transcriptional fusions of cat_{T172A} and *mCherry* or *sfgfp*.

RBS	Strength	Sequence	Origin
R**	10	CAACTAAACTCATCGCTGAGTA	De Novo DNA
R*	15	ATCACTCTACGGCCAGCTGCAAAC	De Novo DNA
R_{B0034}	75	AAAGAGGAGAAATACTAG	BBa_B0034[180]
R	150	TTTAAGAAGGAGATATACAT	T7 phage[148]
R_{tet}	200	TTTAAGAAGCGTGT	TetA operon[168]
$R_{1,000}$	1,000	TAATAATTAAGACTATCAGGAATT	De Novo DNA
$R_{10,000}$	10,000	TCTTAAATAAAGAAATAAAGGATAGC	De Novo DNA
$R_{100,000}$	100,000	TTTGTTTAATTACTAAGCGGGAGGTTAT	De Novo DNA
R_{2M}	2,400,000	CAGAGAAACTGATAAGGAGGTATTTT	De Novo DNA

Table 4-1. Ribosome binding sites and calculated strengths.

RBS strengths are as predicted by De Novo DNA.[149,169] Sequences with an origin of De Novo DNA were created using the RBS Control feature.

Following the successful co-activation of *cat* and *mCherry*, we turned to the development of a *bla* and *mCherry* expression system. However, as our best performing *bla* activation candidate was chromosomally integrated, our previous approach using a strong RBS following the resistance gene did not give readable fluorescence when placed on the chromosome (Figure 4-2a). However, given the strength of the *bla* enzyme as

discussed in Chapter 3 and the weaker expression of the second position gene found when developing *cat-mCherry*, a potential approach to increase fluorescence readout and decrease basal *bla* expression was to place *bla* after *mCherry*. We tested chromosomal reporters with R-*bla* and R*-*bla* after *mCherry*, and inversely found that positioning after *mCherry* increased *bla* expression with RBS R (Figure 4-2b). Resistance levels were raised from 300 µg/mL carbenicillin in the dark and 1200 µg/mL in the light with *bla* alone, to resistance levels over 6400 µg/mL. This may be due to changes in the sequence before the *bla* RBS strengthening its ribosomal affinity, or cryptic RBS or promoter sequences in *mCherry*. Replacing R with R* before *bla* lowered the carbenicillin resistance range, but also decreased fluorescence below readable levels, even though the RBS before *mCherry* was unchanged.

We then tested both R and R* versions on the p15A plasmid (Figure 4-2c), and as expected found resistance and fluorescence levels to be higher. A construct with *mCherry-R*-bla* showed both readable fluorescence and resistance activation, however the induction window between light and dark states was at much higher concentrations than the original OptoCre-*bla*, now ranging from 800 µg/mL carbenicillin in the dark to 3200 µg/mL in the light (Figure 4-2c). In an attempt to lower resistance while keeping visible fluorescence, we again used De Novo DNA to design a weaker RBS with a strength of 10, RBS**.[149] We found that this lowered the resistance activation concentration somewhat, but kept a readable fluorescence level (Figure 4-2d). We are unsure why changing the RBS after *mCherry* changes fluorophore expression, but may have to do with spatial ribosome allocation, unintended changes to transcription, or other

unknown factors.

For *bla* and *mCherry* co-expression, we also tested a translational fusion with *mCherry* fused to the N-terminal of *bla* with the same flexible GS linker used previously. We found that this fusion showed high levels of resistance at all concentrations tested, but clear fluorescence (Figure 4-2e). Optimization of other translational variants using *sfgfp* or brighter red fluorophores with a weaker RBS or promoter may lead to inducible resistance and fluorescence. However, as *bla* is known to be exported in extracellular vesicles,[181,182] translational fusions may risk changing the community-level impacts of *bla* unless fully characterized.

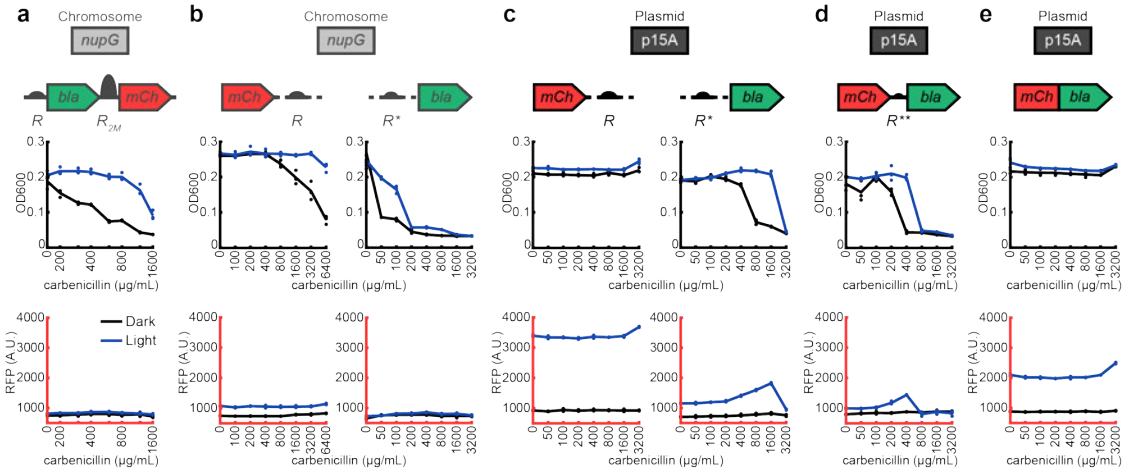

Figure 4-2. Impact of gene order on carbenicillin resistance and fluorescence.

(a) Growth and fluorescence data across antibiotic concentrations for chromosomally-integrated transcriptional fusions of R *bla* and R_{2M} *mCherry*, and **(b)** R *mCherry* and R or R* *bla*. **(c)** Growth and fluorescence data across antibiotic concentrations for p15A plasmid-based transcriptional fusions of R *mCherry* and R or R* *bla*, and **(d)** R *mCherry* and R** *bla*. **(e)** Growth and fluorescence data across antibiotic concentrations for p15A plasmid-based translational fusions of R *mCherry* and *bla*.

With the understanding gained from *cat* and *bla* fluorescence co-activation experiments, we developed similar constructs for *knt* and *tetA*. Given the potent

resistance activity of the *knt* enzyme, we used a similar approach as with *bla* and placed R*-*knt* after *mCherry*. This did raise the expression levels of *knt* above those seen when placed directly after the *lox* sites (from 15–40 µg/mL to 200–800 µg/mL kanamycin), but showed clearly readable fluorescence.

Given the strong promoter needed for phenotypic resistance with *tetA*, placing a fluorescent reporter after the gene showed a clearly readable fluorescence, even with a medium-strength promoter before the fluorophore. This did not substantially change the resistance activation window of *tetA*.

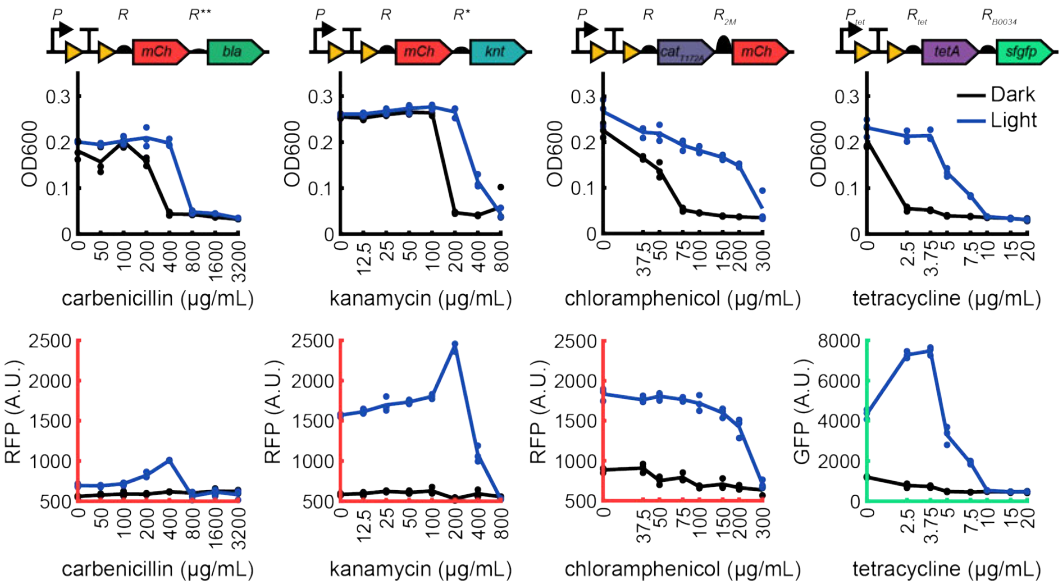

Figure 4-3. Resistance and fluorescence activation constructs.

Growth and fluorescence data across antibiotic conditions for *mCherry-R**-bla*, *mCherry-R*-knt*, cat_{T172A}-R_{2M}-*mCherry*, and *tetA*-R_{B0034}-*sfgfp*.

With these, we have developed four inducible resistance constructs which co-activate with fluorescence. Future optimization could be done to improve resistance activation windows, particularly for *bla* and *knt*, while still showing clear fluorescence. In

particular, use of brighter fluorophores may enable fluorophore genes to be placed after resistance genes, so constructs do not need to be optimized separately with and without fluorescence. Brighter red fluorophores may be especially useful,[179] so fluorescence readout does not interfere with OptoCreVvd activation. Alternate protein co-expression systems could be considered, such as self-cleaving peptides[183] to more directly couple resistance and fluorescence expression without compromising resistant protein function. Ultimately, these co-expression systems will allow us to precisely understand the impact of resistance activation timing on single-cell and population-level survival by visualizing when and how strongly resistance genes are expressed after activation.

4.3. Resistance timing activation

With co-expression of resistance and fluorescence established, future experiments can characterize the impact of resistance acquisition timing on bacterial survival. This can be done at two levels: in bulk populations and in single cells. The impact of timing on population survival can tell us how groups of cells expressing resistance at different times can survive or collapse. We hypothesize this population-level survival will be impacted most by antibiotic resistance mechanism. It is known that some resistance types have a protective effect on nearby susceptible cells, such as beta-lactamases which are secreted in outer membrane vesicles of resistant *E. coli* and allow nearby susceptible cells to survive in the presence of ampicillin.[181] Alternately, efflux pumps like *tetA* are likely to have a negative effect on the growth of nearby susceptible cells by increasing the local concentration of antibiotic, as has been shown with *acrAB*.[184] However, it is not immediately apparent how these different resistance mechanisms will impact the survival

of entire mixed populations of susceptible and resistant cells, and whether the timing of resistance acquisition compared to antibiotic exposure will impact these dynamics. Additionally, the different cellular impacts of bactericidal and bacteriostatic antibiotics may further affect how gene acquisition timing impacts antibiotic survival. Here, we hypothesize that resistance genes will need to be activated substantially before the introduction of antibiotic to confer a survival advantage for bactericidal antibiotics, but not for bacteriostatic antibiotics.[74,75]

Similarly, single-cell data may illuminate how these changes in resistance and antibiotic type impact the temporal dynamics of bacterial survival when acquiring resistance. Future work may use microfluidic devices like the "mother machine," which enables long-term tracking of individual cell linages.[185,186] Microfluidic single-cell tracking has enabled discoveries including efflux pump partitioning[187] and the mechanisms of cell-size control and homeostasis.[188,189] Here, we can use the mother machine to track individual cells over the course of resistance activation and antibiotic survival, and examine the impact of single-cell resistance activation times and intensities to differences in survival. This research could be expanded with devices like the family machine, which has already been used to characterize the impact of quorum sensing on horizontal gene transfer.[161,190] Here, long-term tracking of microbial populations can be used to map the impacts of individual resistant cells on the individual susceptible cells around them. This level of understanding can bridge the gap between single-cell and bulk population data, allowing us to understand how single-cell resistance behaviors over time impact the survival of the population as a whole for different resistance and antibiotic

types. This data can be used to distinguish how these behaviors lead to patient- or ecosystem-scale proliferation of antibiotic resistance in a clinical setting, and what cellular-level interventions can best prevent the spread of resistance.

4.4. Dual-fluorescence Cre stoplight reporter

Although the current resistance activation reporters are functional, further optimization focused on improving the *lox*-terminator architecture may be fruitful. A more generic optimization of the activation construct would be helpful across resistance genes to decrease basal expression and increase fold change, and could broadly apply to the activation of other genes of interest. To this end, we constructed the dual reporter "Cre stoplight" system,[191] where a red fluorescence gene is excised and a green fluorescence gene is activated (Figure 4-4a). This system enables direct reporting of pre- and post-recombination states, and would be useful for testing future recombinase or reporter variants. We found that this system behaved similarly to the original reporter, with a clear change in each fluorophore after light exposure. We characterized the system activation through bulk culture measurements (Figure 4-4b,c), as well as single-cell microscopy (Figure 4-4d,e,f). Overall, this system can be applied generally for testing future recombinases and reporters by enabling a clearer output of both pre- and post-recombination states through a ratiometric comparison of fluorophores. For instance, it could be used to test a wider variety of terminators in this reporter, in a similar manner to the terminator characterization in Chen *et al*.[154] It could also be useful for dual-sorting cells in pooled screenings for novel recombinase constructs. This also points to the potential for more complex levels of gene control using OptoCreVvd2, through activation

and deactivation of multiple genes simultaneously.

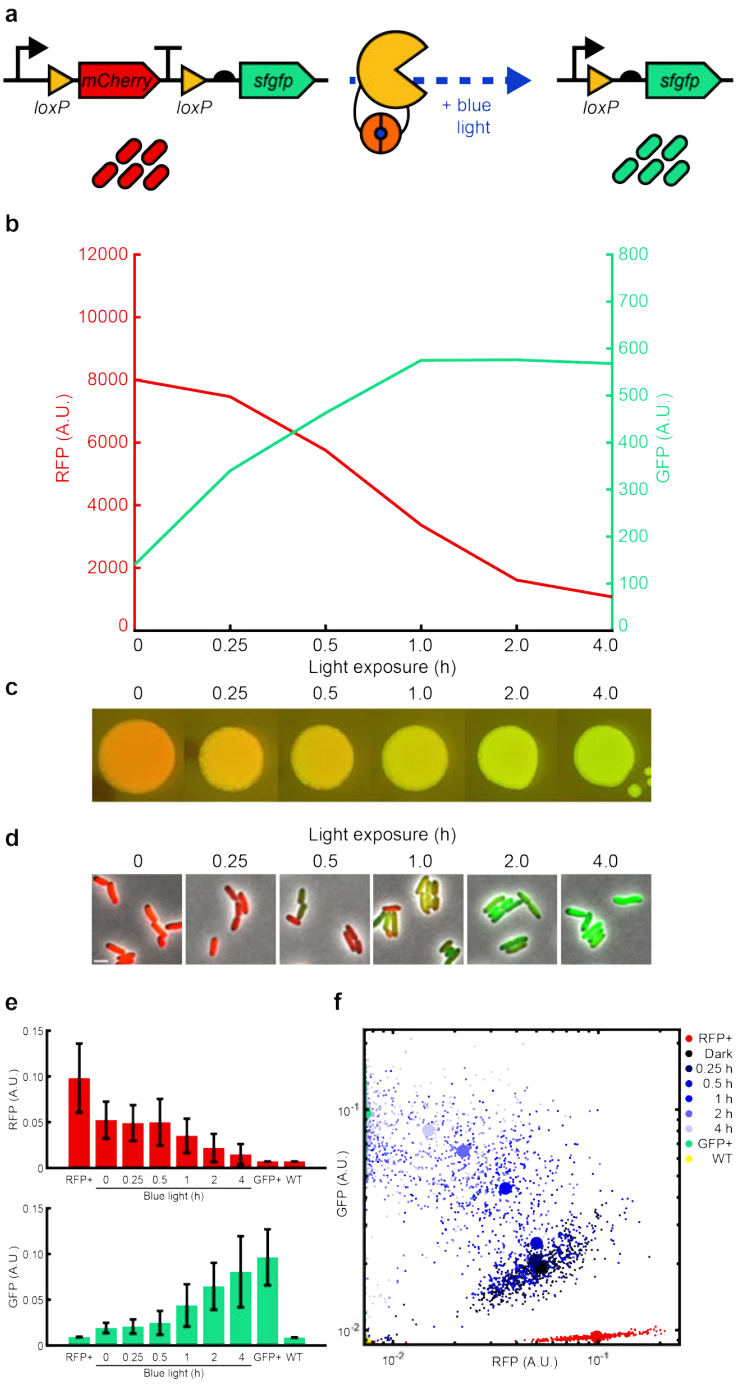

Figure 4-4. Cre stoplight reporter.

(a) Recombination of the stoplight reporter excises *mCherry* and a transcription terminator before *sfgfp*, allowing *sfgfp* expression after recombination. **(b)** Light activation dynamics of the

stoplight in liquid culture. **(c)** Cultures of the stoplight reporter with varying light exposure spotted onto an agar plate. **(d)** Single-cell images of the stoplight reporter with varying light exposure (scale bar = 2 μm). **(e)** Single-cell microscopy fluorescence averages of the stoplight reporter with varying light exposure. Error bars show standard deviation around the mean (n = ~100). **(f)** Single-cell red and green fluorescence data for the stoplight reporter with varying light exposure. The large dot for each color represents the mean.

4.5. Red light-inducible Cre recombination

A red light-inducible Cre recombinase can enable new uses and applications than a blue-light inducible system. Red light induction can be multiplexed with other blue light-activated systems,[21,23,29] or even the Flp-Mag construct developed in Chapter 2. Red light penetrates deeper into tissue than blue light,[192] and has been shown to work on optogenetic activation of *Caenorhabditis elegans* gut microbiota.[31] In this way, a red light-activated recombinase may be a more functional tool for studying activation of antibiotic resistance in the gut. Similar to Vvd or Magnets, the REDMAP system consists of miniaturized PhyA and FHY1 dimers from *Arabidopsis thaliana*, which instead dimerize with red (660 nm) and dissociate with far-red (730 nm) light.[193] A promising red light-induction strategy is to use the red light-inducible REDMAP dimers, which were previously shown to work for kinase and CRISPR/Cas control in mammalian systems.[193] Here, we use the REDMAP dimers in *E. coli* to create a red light-inducible Cre recombinase.

We constructed REDMAP-split systems using Cre, Flp, and FlpO,[194,195] a mammalian-optimized but less temperature-sensitive version of Flp (Figure 4-5a). We split Cre recombinase at the site used in OptoCreVvd2, N43/N44. We split Flp at L374/K375, one of the most optimal split sites found to work with Magnet photodimers

in Chapter 2. Additionally, REDMAP dimers require phycocyanobilin (PCB) as a cofactor to sense red light, which is not natively produced in *E. coli*. We co-transformed recombinase and reporter plasmids with pNO286-3 from the CcaSR system, which contains the heme oxygenase-1 (*ho1*) and phycocyanobilin:ferredoxin oxidoreductase (*pcyA*) genes required for PCB synthesis.[25]

We conducted an initial tested exposing each system to 12 hours of red or blue light at 37°C, and included OptoCreVvd2 as a control (Figure 4-5b). We found CreREDMAP showed substantial recombination under red light, and some basal recombination in the dark or under blue light. Both FlpREDMAP and FlpOREDMAP showed no recombination. We then characterized the responsiveness of CreREDMAP to varying amounts of red light, and OptoCreVvd with or without the genes for PCB production to varying amounts of blue light (Figure 4-5c). This was to ensure that the PCB production genes did not affect the performance of OptoCreVvd or the *lox* reporter. We saw that although CreREDMAP began activating fluorescence at similar levels to OptoCreVvd after 0.25 hours of light exposure, CreREDMAP appeared to cap at lower fluorescence levels than OptoCreVvd. This could be because of a lack of activity, or other intracellular factors impacting CreREDMAP expressing cells. REDMAP is fairly large compared to Vvd, where even the miniaturized PhyA and FHY1 used are 617 AA and 202 AA respectively, while Vvd is only 153 AA. Additionally, the red light intensity in the optoWELL device used in this system is almost four times weaker than the blue light intensity, leaving plenty of room for protocol optimization. Overall though, CreREDMAP shows very promising initial performance.

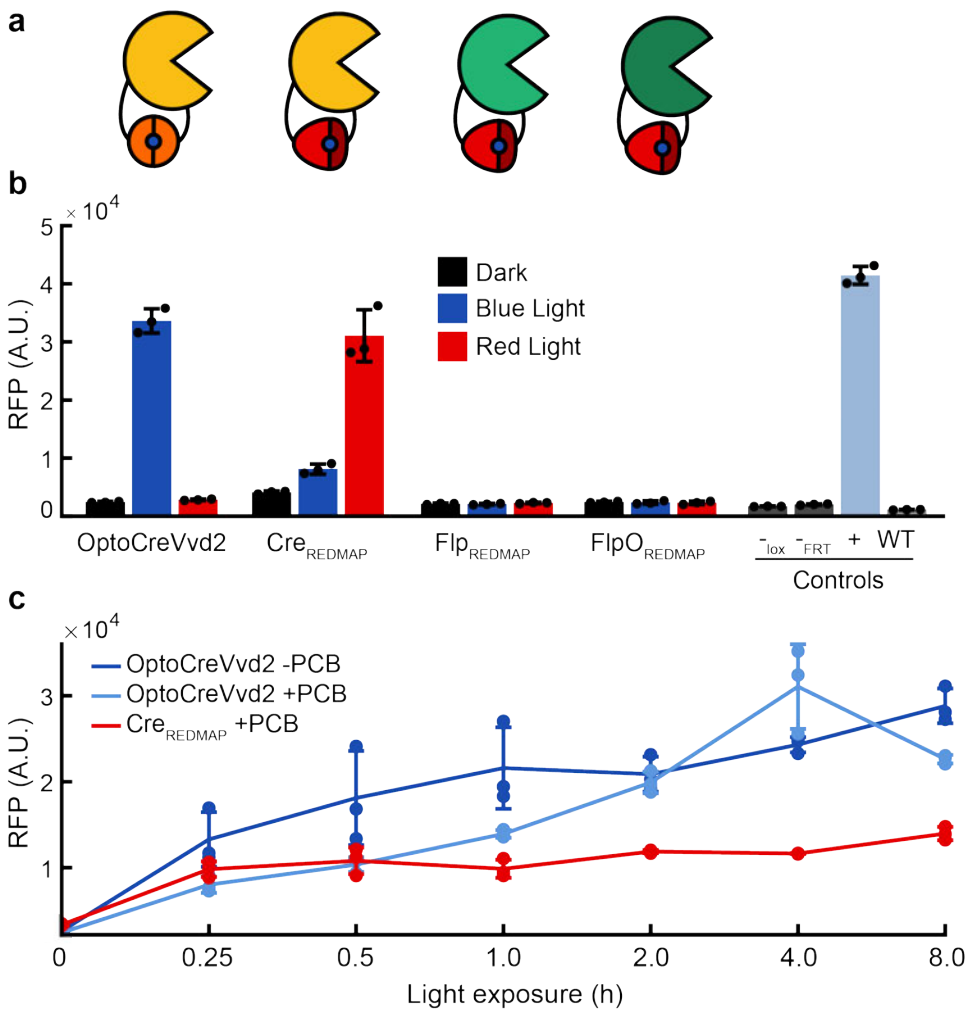

Figure 4-5. Red light-inducible recombination using REDMAP.

(a) Light-inducible recombinases using Cre-Vvd, Cre-REDMAP, Flp-REDMAP, and FlpO-REDMAP. **(b)** Induction of REDMAP systems kept in the dark, blue light, or red light for twelve hours. **(c)** Induction of OptoCreVvd2 with or without PCB production genes with 0 to 8 hours of blue light exposure, and of Cre-REDMAP with PCB production genes with 0 to 8 hours of red light exposure after overnight refresh. Error bars show standard deviation around the mean (n = 3).

Due to the temperature sensitivity of Flp recombinase found in Chapter 2, we also tested FlpREDMAP constructs with 12 hours of red or blue light at 30°C (Figure 4-6). We found minimal but clear activation of FlpOREDMAP under these conditions. Notably, FlpOREDMAP shows similar performance to PA-Flp using the same

L374/K375 split site. This indicates that the two could potentially be further optimized in parallel at the protein and protocol levels similar to OptoCreVvd, leading to blue-inducible Cre and red-inducible Flp or the inverse. It is also interesting that FlpOREDMAP shows induction only at 30°C where FlpREDMAP does not, as FlpO is optimized for improved function at higher temperatures compared to Flp,[194] which may point to further protocol optimization strategies by further lowering the temperature and ensuring that optoWELL is not heating samples beyond incubator temperatures. Overall, FlpOREDMAP shows additional promise for multi-color multi-recombinase gene control.

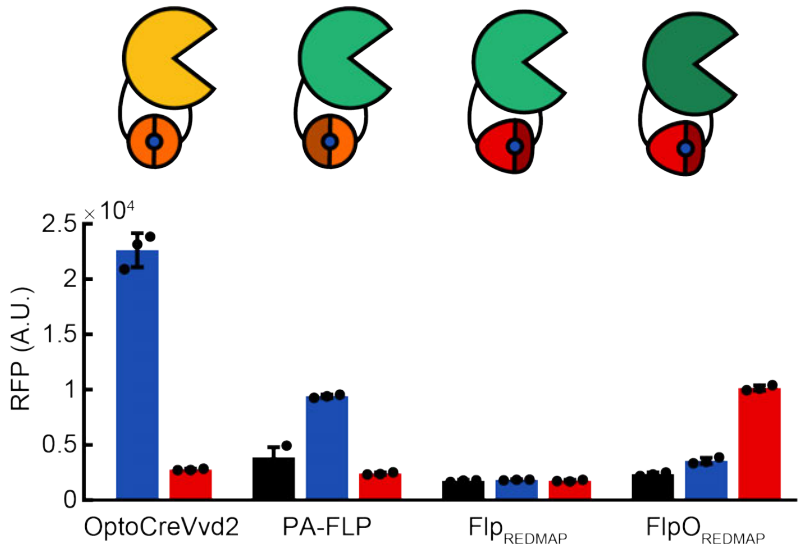

Figure 4-6. Induction of Flp-REDMAP constructs at 30°C.

Induction of Flp-Mag and Flp-REDMAP systems kept in the dark, blue light, or red light for twelve hours at 30°C.

A red light-inducible recombinase opens possibilities for multiple interesting applications, including control of engineered cells within the gut microbiota[31] or multiplexed gene control with other blue light-activated systems. In particular, future

efforts to functionalize a red light-inducible Flp recombinase may be valuable. It is likely that red light-inducible Flp could be developed using similar optimization techniques to those used for OptoCreVvd and the blue light-inducible Flp-Mag in Chapter 2. Specifically, a red light-inducible Flp could be a powerful tool for multiplexed recombinase-based control with OptoCreVvd. In future experiments, we could test alternate photodimers such as PhyB/PIF[196] or RedMag,[197] as well as different split sites, protein linker lengths, or light exposure timing. In tandem, multi-color control of recombinases could enable more dynamic gene regulation, multi-gene regulation, or genetic circuit design. With a red light-inducible Flp complete, we could then turn genes on with blue light and off with red (or vice versa), control different genes with different wavelengths, or create separate light-sensing systems within the same cell. Overall, the development of CreREDMAP here shows that REDMAP can function in the bacterial chassis *E. coli*, and opens the possibility for a variety of other bacterial red light-inducible split proteins.

4.6. Discussion

The tools developed here will enable further research into how the timing of antibiotic resistance acquisition impacts bacterial survival at the population and single-cell level. By co-activating resistance and fluorescence, we can characterize precisely when cells begin to express resistance genes, and compare single-cell or population-level variances to understand what conditions allow resistant bacteria to proliferate. The dual-color stoplight reporter will assist with future optimization of Cre-activated resistance cassettes, with new designs that may further reduce basal expression levels or increase

total expression for a next generation of inducible resistance genes. Finally, red light-inducible recombination shows the potential to be multiplexed with existing blue light-inducible systems and be applied to control engineered cells in the gut.

In particular, the optogenetic nature of these systems can allow for novel studies exploring the spatial impacts of antibiotic resistance on nearby susceptible cells. It is known that beta-lactamases have a protective effect on susceptible neighbors,[181] and likely that the tetracycline efflux pump will harm nearby cells by increasing local antibiotic concentrations.[184] Through spatial patterning with a digital micromirror device, we can create cell geometries that let us explore more precisely how different resistance and antibiotic types shape interactions between resistant cells and susceptible neighbors. The inducible nature of our system also allows us to explore how populations change when these impacts first emerge, as would be seen with horizontal gene transfer or the initial acquisition of a resistant pathogen in the gut. It is our hope that this preliminary work will act as a precursor to a wide variety of experiments examining what environmental and cellular factors in single cell resistance acquisition lead to bacterial population-scale survival, and help inform future treatment strategies to prevent the further spread of antibiotic resistance.

4.7. Methods

Strains and plasmids

All experiments use *E. coli* strain MG1655. We constructed plasmids using the Gibson assembly method,[116] or using Golden Gate assembly[167] in cases where the constructs contained fragments under 100 base pairs in length. Chromosomally integrated

constructs were inserted using the Lambda Red recombinase system[117] downstream of *nupG* (forward homology site: GGTTCTGGCCTTCGCGTTCATGGCGATGTTCAAATATAAACACGT, reverse: GGCGTGAAACGGTTGTACGGTTATGTGTTGAAGTAAGAATAA). Antibiotic resistance cassettes flanked with FRT sites were used to select successful integrations (we used *knt* for *bla* and *cat* activation constructs, *cat* for *knt* and *tetA* activation constructs). The plasmids used for OptoCreVvd2 expression were derived from Sheets *et al.*[133,163] All plasmid-based resistance constructs contain the p15A origin. We thank Cristina Tous and Wilson Wong for the donation of plasmids containing the REDMAP dimers from Zhou *et al.*,[193] and Loran Gliford for her contributions in designing REDMAP constructs. We thank Jeffery Tabor for depositing pNO286-3 (Addgene Plasmid #107746) from Ong *et al.*[25]

Light exposure

Strains were grown overnight from a single colony in selective LB media containing 100 μg/mL carbenicillin, 30 μg/mL kanamycin, 25 μg/mL chloramphenicol, and 50 μg/mL spectinomycin as required for plasmid maintenance. Selective M9 minimal media (M9 salts supplemented with 2 mM $MgSO_4$, 0.1 mM $CaCl_2$, and 0.1% glucose) was used for resistance activation studies, and LB was used for Cre stoplight and REDMAP studies. Cultures were refreshed 1:100 for two hours with 100 μM IPTG for induction of split recombinase production. Cultures were then either exposed to blue light or kept in the dark for two hours unless otherwise noted. Light exposure was performed

using a 24-well light plate apparatus (LPA)[104] using 1 mL cultures with two 465 nm wavelength LEDs per well (ThorLabs LED465E), with a total output of 120 μW/cm^2 per well.

For REDMAP induction studies, light exposure was performed using 24-well optoWELL device (OptoBiolabs). optoWELL blue light exposure was at 460 nm wavelength and 2.58 mW/cm^2, and red light exposure was at 660 nm wavelength and 0.69 mW/cm^2. All REDMAP constructs were co-transformed with pNO286-3, which contains the genes for PCB production. Although pNO286-3 shares the same p15A origin as the *lox* and FRT reporters, it has a unique selective resistance to spectinomycin and did not impact the performance of OptoCreVvd transformed with the *lox* reporter and pNO286-3. Additionally, all samples were used within one refresh after transformation before any selective plasmid is likely to be lost.[198]

Immediately after light exposure, resistance activation samples were taken for minimum inhibitory concentration experiments, otherwise samples were refreshed in LB overnight to allow full *mCherry* and *sfgfp* expression and maturation. Samples were measured after ~18 hours for OD absorbance at 600 nm (OD600), red fluorescence (excitation 584 nm; emission 610 nm), and green fluorescence (excitation 485 nm; emission 515 nm) using a BioTek Synergy H1 plate reader.

Minimum inhibitory concentration measurement

Minimum inhibitory concentrations (MICs) were measured based on the protocol outlined in Wiegand *et al*.[170] Antibiotic stocks were made by dissolving the antibiotic in

sterile distilled water (carbenicillin, kanamycin, tetracycline) or 99% ethanol (chloramphenicol), with concentrations normalized for potency based on CLSI standards.[171] Assay plates for measuring the MIC were prepared by performing serial dilutions of antibiotic in 100 μL M9 minimal media in 96-well plates. Low glucose media was used to reduce growth variability by creating carbon-limiting, rather than nutrient-limiting, growth conditions.[146] Antibiotic concentrations were selected to include values that spanned the MIC levels for the dark and light state cultures in each experiment. Immediately following light exposure, cultures were normalized by dilution to the lowest optical density (OD) of each experiment. Normalized cultures were then diluted 1/25 into 96-well plates in triplicate and grown overnight for 18 hours at 37°C. Each well was then measured for OD absorbance at 600 nm (OD600), red fluorescence (excitation 584 nm; emission 610 nm), and green fluorescence (excitation 485 nm; emission 515 nm) using a BioTek Synergy H1 plate reader.

Microscopy and image analysis

Post light-exposure samples were refreshed overnight in LB medium with 100 μg/mL carbenicillin and 30 μg/mL kanamycin for plasmid maintenance to allow full *mCherry* and *sfgfp* expression and maturation. Before imaging, samples were refreshed for 1 hour in 1:100 in selective M9 minimal media. Samples were then placed on 1.5% low melting agarose pads made with MGC medium. Cells were imaged at 100x using a Nikon Ti-E microscope. Images were segmented and analyzed using the DeLTA 2.0 software.[173]

CHAPTER 5. Alternate optogenetic system designs

Over the course of this thesis, we developed and tested multiple gene control constructs which did not function or performed suboptimally compared to existing systems. We present those here.

When developing tools for genetic control, important metrics are the basal-state expression, speed of induction, and total activation level. These were all key factors when developing OptoCreVvd in Chapter 2, and applying it to control antibiotic resistance in Chapter 3. Although OptoCreVvd performed well on these metrics, we were particularly interested in improving the induction speed through changes to the recombinase itself, and decreasing basal-state expression through modifying the *loxP* reporter. We also discuss efforts to create a directly light-inducible beta-lactamase, as a way to reversibly control antibiotic resistance at the protein level. The recombinase, reporter, and split protein variants cataloged here did not outperform the original OptoCreVvd and reporters discussed in Chapters 2 and 3. Despite this, the systems here can form a useful starting point for future optimization and development of novel optogenetic systems. Many of these systems show the potential for optimization in a similar manner to OptoCreVvd, or highlight pitfalls in light-inducible system development.

5.1. Alternate light-inducible recombinases

Through photodimer, split site, and recombinase optimization, we developed blue light-inducible recombinase OptoCreVvd2. Although this construct worked well, one downside was that it requires one or more hours of blue light for full reporter activation. In an effort to improve the speed and efficiency of OptoCreVvd2, we continued to test

alternate optogenetic constructs. Although these constructs do not work well as-is, their current efficiency and mechanisms of failure may provide insights for the design of a more efficient light-inducible recombinase in the future.

5.1.1. Vivid photodimer variants

One variant was a modified version to the original Vvd photodimers, with improved binding (Vvd**) or slower dissociation (Vvd**^{slow}) kinetics (Figure 5-1a). These are based the version of Vvd used to make a light-inducible AraC[23] and the intermediates between Vvd and Magnets,[103] with key mutations to increase binding or prevent dissociation while bound (Figure 5-1b). When working with Vvd and Magnets in developing OptoCreVvd (Chapter 2), generally Vvd-based constructs were more likely to stay off in the dark state but less likely to activate in the light state, while the more enhanced Magnet-based constructs often had leaky dark-state expression and strong light-state expression. Our hope here was that in using an intermediate between Vvd and Magnets, we could find a construct that stayed off in the dark state but had improved or faster activation in blue light. All versions of Vvd used, including the one used in OptoCreVvd, include a 36-AA truncation of the N-terminal, which creates a more stable protein without changing the photocycle or light responsiveness.[101] The Vvd** variant has three single amino acid changes which are known to enhance the stability of the Vvd dimer under blue light (W50Y,[199] N56K,[200] C71V[199]), while Vvd**^{slow} has these as well as two amino acid changes which have been found decelerate dimer dissociation by lengthening the Vvd photocycle (M135I and M165I).[201] Additionally, Vvd** and Vvd**^{slow} gene sequences are based on the Vvd used in Romano *et al*., which has been

codon optimized differently than the Vvd used in OptoCreVvd.[23]

We tested this system with either ten or sixty minutes of blue light to compare leaky activation and activation timing between variants (Figure 5-1c). OptoCreVvd with the standard Vvd variant showed little basal activation, and almost complete activation with one hour of blue light, consistent with previous characterization. The Vvd** variant showed faster activation, with only 10 minutes of light giving near complete activation, but also showed much higher levels of leaky basal activation. The Vvd**^{slow} variant showed complete activation from leaky expression in the dark. Overall, the high dark-state leak from Vvd** and Vvd**^{slow} make them poor candidates for an optogenetic recombinase tool, but the rapid activation of Vvd** indicates that other photodimers or Vvd variants may enable rapid activation without increasing basal expression. This work shows a potential avenue for future optimization of OptoCreVvd by screening multiple known or predicted Vvd mutants for further optimized optogenetic recombinases.

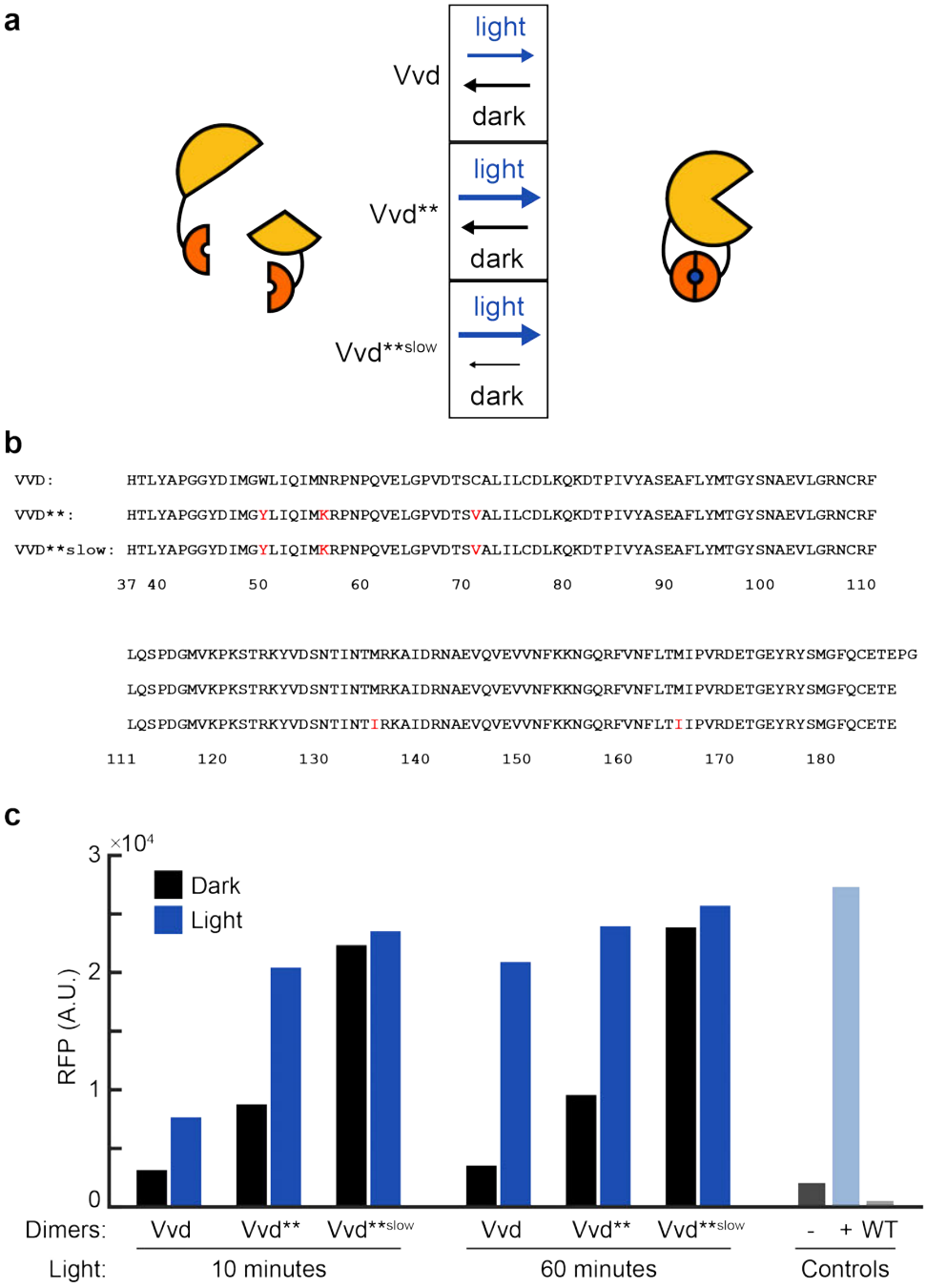

Figure 5-1. Variants of the Vvd photodimer tested with OptoCreVvd2.

(a) The Vvd** variant improves binding kinetics, and Vvd**^{slow} further decreases the rate at which Vvd dimers dissociate in the dark state. **(b)** Protein sequences of Vvd, Vvd**, and Vvd**^{slow}, with changes highlighted in red. **(c)** Light activation dynamics of Vvd variants after 10 or 60 minutes of darkness or blue light.

5.1.2. Single-chain LiCre

Another variant was the AsLOV2-based single-chain LiCre,[45] which had been shown to work in yeast and mammalian systems with rapid activation and minimal basal expression. Compared to most dimer-based split protein systems, LiCre uses the blue light-activated unfolding of the Jα helix of the AsLOV2 photoreceptor domain from *Avena sativa* to regulate Cre expression. In the dark, the tightly wound Jα helix deforms the N-terminal of a destabilized Cre recombinase, which is hypothesized to prevent Cre from tetramerizing and performing recombination.[45] Under blue light, the Jα helix relaxes, freeing the Cre N-terminal and allowing active recombination (Figure 5-2a).

We tested this system with the high-copy colE1 and low-copy SC101 origins in the same genetic context as OptoCreVvd2 with the SC101 origin, with two or four hours of light. Compared to OptoCreVvd2, we found no activation with the colE1 origin, and minimal activation with the SC101 origin (Figure 5-2b). Although the system did not show strong activation, it did show very minimal basal expression. This suggests that further optimization of LiCre could create a promising tool for bacterial optogenetics. In particular, developing a similar construct lacking some of the destabilizing mutants used in the initial study could help improve the light-activated recombination. Alternately, different LOV variants or different linkers between AsLOV2 and Cre could be tested to improve LiCre activation.

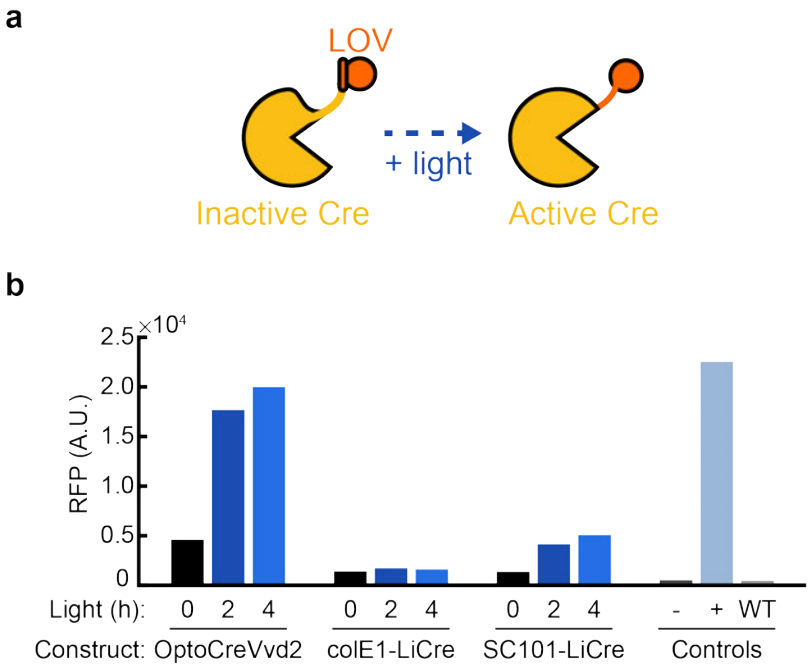

Figure 5-2. Single-chain, light-inducible Cre recombinase LiCre tested in *E. coli*.

(a) LiCre is made light sensitive through an asLOV2 domain fused to the N-terminal of Cre. In the dark, the tight caging of the Jα-helix of the LOV domain prevents Cre recombination. When the Jα-helix relaxes upon blue light exposure, Cre can perform recombination. **(b)** Light activation dynamics of LiCre on the colE1 and SC101 plasmid origins compared to OptoCreVvd2.

5.1.3. Discussion

Ultimately, none of these systems showed improved function over the original OptoCreVvd2 system. While Vvd** and Vvd**^{slow} showed greatly increased basal recombination, LiCre did not show substantial activation. As with OptoCreVvd itself, further optimization efforts may yield promising recombinases using these or other photodimers. Continuing to test novel photodimers and recombinase variants as they are developed could create a faster optogenetic recombinase or systems with other specific functions.

5.2. Alternate recombinase reporters

The recombinase reporter was another candidate for optimization. In Chapter 3, we discussed extensive tuning of reporter strength through copy number, promoter, and ribosome binding site strength. These led to a range of basal and maximal expression levels for the resistance genes they controlled. We also described an alternate transcription terminator we tested, which did not change basal expression levels of the reporter (Figure AII-3). In addition to these efforts, we developed and tested a variety of alternate reporter constructs to improve system performance by increasing the activation fold change, decrease basal expression, or improve speed.

5.2.1. Irreversible loxP *variants*

The *lox*71/*lox*66 mutants are variants of the *loxP* site which when recombined, create an inactive *lox* site. Each variant individually has one end of the *lox* sequence which has a slightly lower affinity for Cre. When recombined, they form one standard *loxP* sequence, and one double mutant sequence with a much lower affinity for Cre. This creates a system where recombination is likely to occur once in the forward direction, but unlikely to occur again.[202] We hypothesized that this variant may improve performance by removing the chance for re-insertion of the transcription terminator, or by preventing any potential transcription interference caused by Cre binding to the *loxP* site left after recombination. We tested the activation of this construct with OptoCreVvd2 (Figure 5-3). Overall, we did not find this *lox* variant had any impact on reporter output.

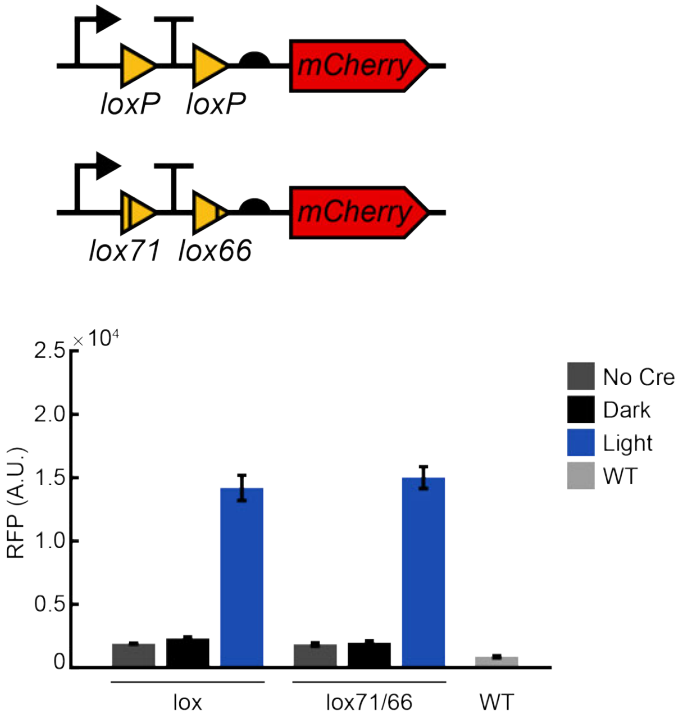

Figure 5-3. Optogenetic activation of irreversible *loxP* variants.

Error bars show standard deviation around the mean (n = 3).

5.2.2. Inversion loxP *reporters*

Inversion-based recombination is another common way to gate gene expression, by placing a gene inside *lox* sites facing each other, where a gene element is flipped into the correct direction by active Cre recombinase. Here, we placed the W4 promoter used in the reporter in a reverse position between *lox* sites facing each other. Our hope was that this construct may decrease basal expression, as transcription terminator readthrough would no longer be an issue with a reversed promoter (Figure 5-4a). However, this construct showed very high basal expression levels. We also tested a different inversion variant, where instead the RBS and *mCherry* were flipped into the correct position by Cre (Figure 5-4b). Although this variant showed a small fold-change when exposed to blue

light, it had both a higher basal expression level and lower total activation. The lower induced activation was expected, as the construct can reversibly flip and would equilibrate to 50% of reporters in the correct position. This could also be corrected with a FLEX switch design, where alternate *lox* variants are used to permanently stabilize the construct the active position after recombination.[203] However, due to the higher basal expression we did not pursue this strategy further. More complex designs may also enable improved reporters, such as flipping a promoter and terminator together to prevent activation in the off-state, or placing a reversed terminator after *mCherry* when flipping the gene itself.

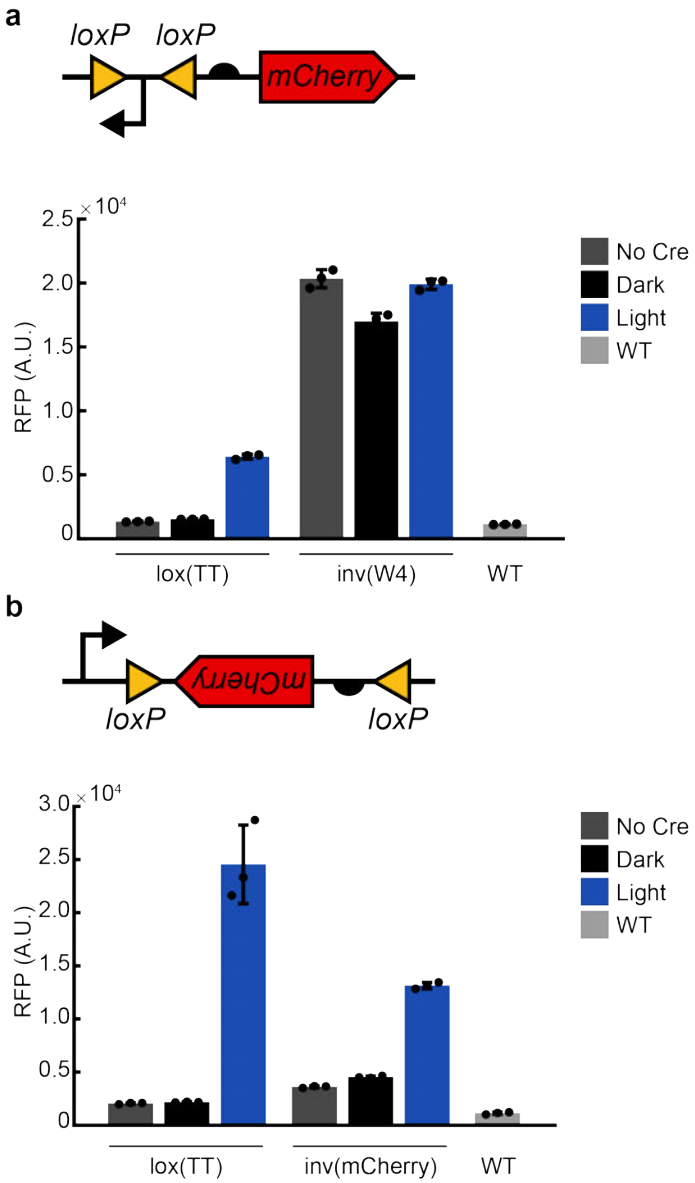

Figure 5-4. Inversion-based activation of *mCherry*.

(a) Light activation dynamics of a reporter with *lox* sites flanking a constitutive promoter. **(b)** Light activation dynamics of a reporter with *lox* sites flanking a RBS and *mCherry* gene. Error bars show standard deviation around the mean (n = 3).

5.2.3. RNA toehold repression

Toehold switches are powerful tools that regulate gene expression at the translational level.[204] Through RNA binding regions, they can be used in a variety of

ways to make a RBS or start codon inaccessible until certain conditions are met. Translational inhibition is an especially appealing optimization tactic for recombinase reporters, as basal expression can still be minimized even with some terminator readthrough. This approach could also give greater flexibility in the choice of promoter and other genetic components regulating the reporter. Here, we use a toehold switch designed into a *lox* excision reporter construct in an attempt to decrease basal expression of the reporter (Figure 5-5a). Using NUPACK,[205] we designed and tested multiple toehold switch variants. Concept Th1.123 and Th1.32 were designed for repression in the off state using a larger hairpin loop, and high activation after recombination. Design Th1.32 was a three-way junction, another form of RNA-based repression.[206] Concept Th2.1 and Th2.2 were designed for minimal interference with the existing reporter structure.

We then tested activation of toehold-based constructs with OptoCreVvd2 in the dark and when exposed to blue light (Figure 5-5b). Construct Th1.123 showed both increased basal expression and decreased maximal expression compared to the original reporter. Constructs Th1.32 and Th2.1 both showed similar performance to the original reporter. Construct Th2.2 showed no activation. Ultimately, none of this first set of reporters showed decreased basal activation while retaining their function. In the future, trying other variants of these constructs or novel RNA toehold design holds promise for decreasing basal expression of the off-state construct at the translational level, without limiting the total on-state expression.

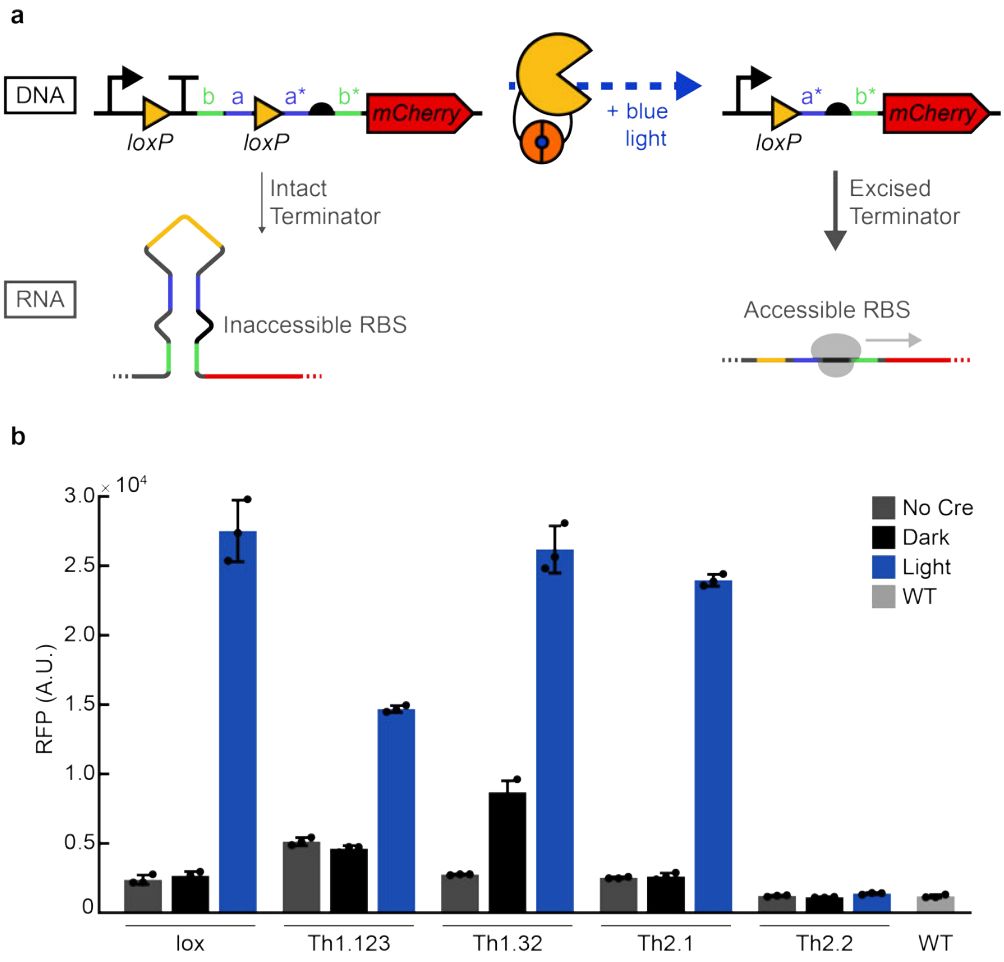

Figure 5-5. Toehold switch-based repression of inactive *loxP* reporters.

(a) At the DNA level, little transcription happens until the transcription terminator is removed by OptoCreVvd. At the RNA level, any transcripts created prior to recombination further repress *mCherry* expression through sequestering the RBS in a hairpin, preventing ribosome binding and translation initiation. After recombination, homology sites for the sequence around the RBS will no longer be present in the transcript, allowing ribosome binding and *mCherry* translation.
(b) Characterization of toehold constructs with and without light exposure. Error bars show standard deviation around the mean (n = 3).

5.2.4. Discussion

Although these reporters did not show substantial improvement over the original transcription terminator excision reporters, they each highlight potential avenues for further optimization. Use of variant *lox* sites and reporter architectures could be used to

create alternate outputs or tune for specific expression levels. Further optimization of toehold-switch based repression could enable control of gene expression at both the transcriptional and translational levels, allowing tight regulation while keeping strong on-state expression.

5.3. Split beta-lactamase

Transient control of antibiotic resistance has the potential for more complex temporal studies investigating single-cell resistance to antibiotics such as carbenicillin. Optogenetic control at the protein level also enables the potential for a faster temporal response than control at the genetic level. Using an established functional split site in the TEM beta-lactamase previously used for protein fragment complementation assays,[207] we designed and created a split beta-lactamase linked to Magnet or Vivid blue light-inducible photodimers (Figure 5-6a). From preliminary experiments, this split enzyme did not enable resistance to even low concentrations of carbenicillin with or without light exposure (Figure 5-6b,c).

5.3.1. Results

To develop the split beta-lactamase, we used Gibson Assembly to insert a pair of Magnet or Vivid photodimers into the TEM-116 beta-lactamase gene. Photodimers were connected by 10 AA flexible GS linkers to Gly196 and Leu198 respectively, based on the established split site from literature.[207] The split beta-lactamases were controlled by the native *bla* promoter and RBS, and created with p15A (medium copy) and pSC101 (low copy) origins to enable multiple expression levels with different plasmid copy numbers (Figure 5-6a).

When testing for resistance, light-induction samples were pre-induced with blue light for four hours to enable the best chance for survival upon antibiotic exposure. At the end of four hours, light and dark state samples were diluted 1/20 into a MIC assay (Figure 5-6c). Dark-state samples were kept in the dark for the entire process, and the light induction MIC plate was exposed to blue light continuously for 18 hours of growth. For positive and negative growth controls, constitutively resistant cells and wild type MG1655 cells with no plasmid were used respectively. We tested a range of carbenicillin concentrations, starting from just above the wild type MIC. No cells other than the positive controls showed growth in any concentration of carbenicillin tested.

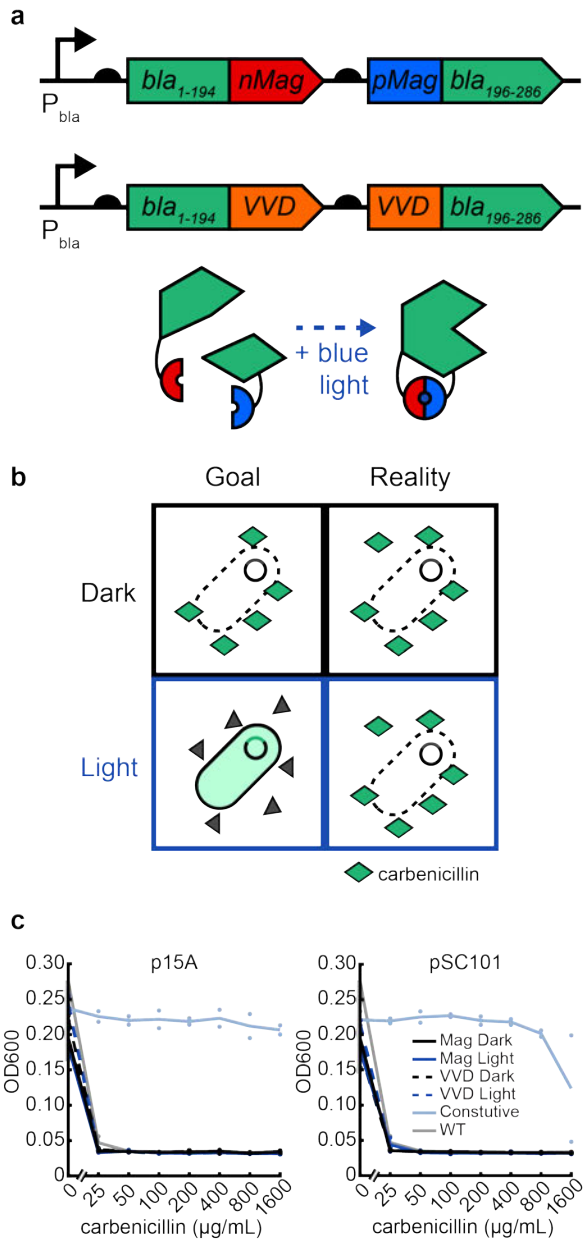

Figure 5-6. Design of an optogenetic split beta-lactamase.

(a) Split beta-lactamase fragments are linked to Magnet or Vvd photodimers and expressed under their native promoter and RBS. When exposed to blue light, Mag or Vvd dimerizes, theoretically forming an active beta-lactamase with the ability to degrade carbenicillin. **(b)** The system was designed so that beta-lactamase is activated by blue light, degrading carbenicillin and allowing cell survival. The system did not allow survival of carbenicillin upon exposure to blue light. **(c)** Minimum inhibitory concentration curves of split beta-lactamase constructs with the p15A and pSC101 origins. Light exposed samples were pre-treated with light for four hours then kept under blue light, and dark samples were kept in the dark for the entire experiment.

5.3.2. Discussion

Although our initial test did not develop a functional system for protein-level control of carbenicillin resistance, other approaches may enable this goal. Similarly to the development of OptoCreVvd, alternate split sites or photodimers may enable light-inducible carbenicillin resistance at the protein level. Other protein engineering tools, such as circular permutation,[208] site-directed mutagenesis,[209] or computational prediction of alternate split sites[107,210] may also create a functional induction system. Additionally, the *bla* gene used in the original study used TEM-1 without the periplasmic secretory signal sequence consisting of the first 23 amino acids.[207] This was due to the mammalian context in which it was used and seems unlikely to impact split function, but may be worth testing in future works. This previous work also only used *bla* to hydrolyze nitrocefin for a color change, rather than induce antibiotic resistance, so this split has not been tested to confirm efficiency at a level that would confer antibiotic resistance. With these factors in mind, future work could also consider using different antibiotic resistance genes, with computationally or structurally predicted split sites. These protein-level split resistances could enable faster response times to light and complex temporal dynamics.

5.4. Methods

Strains and plasmids

All experiments use *E. coli* strain MG1655. We constructed plasmids using the Gibson assembly method,[116] or using Golden Gate assembly[167] in cases where the constructs contained fragments under 100 base pairs in length. The plasmids used for OptoCreVvd2 expression were derived from Sheets *et al*.[133,163] All plasmid-based

resistance constructs contain the p15A origin. We thank Caroline Blassick for creating the Vvd** and Vvd**^{slow} variants proteins based on Romano *et al.*[23] and Kawano *et al.*[103] We thank Gaël Yvert for depositing pGY416/LiCre (Addgene Plasmid #166660) from Duplus-Bottin *et al.*[45] We thank Justin Letendre and Wilson Wong for donation of plasmids containing the *lox*71/*lox*66 sequences. We thank Chris Kuffner for creating the *mCherry* inversion reporter plasmid. We thank Alexander Green for refining the RNA toehold design, James Robson for designing the RNA toehold sequences in NUPACK,[205] and Hellen Huang for cloning the toehold constructs.

Blue light exposure

Strains were grown overnight from a single colony in selective LB media containing 100 μg/mL carbenicillin, 30 μg/mL kanamycin, and 25 μg/mL chloramphenicol as required for plasmid maintenance. Selective M9 minimal media (M9 salts supplemented with 2 mM $MgSO_4$, 0.1 mM $CaCl_2$, and 0.1% glucose) was used for resistance activation studies, and LB was used for all other studies. Cultures were refreshed 1:100 for two hours with 100 μM IPTG for induction of split recombinase production for recombinase experiments. Cultures were then either exposed to blue light or kept in the dark for two hours unless otherwise noted. Light exposure was performed using a 24-well light plate apparatus (LPA)[104] using 1 mL cultures with two 465 nm wavelength LEDs per well (ThorLabs LED465E), with a total output of 120 μW/cm^2 per well.

Immediately after light exposure, resistance activation samples were taken for

minimum inhibitory concentration experiments, and all other samples were refreshed in LB overnight to allow full *mCherry* expression and maturation. Fluorophore activation samples were measured after ~18 hours for OD absorbance at 600 nm (OD600), red fluorescence (excitation 584 nm; emission 610 nm) using a BioTek Synergy H1 plate reader.

Minimum inhibitory concentration measurement

Minimum inhibitory concentrations (MICs) were measured based on the protocol outlined in Wiegand *et al*.[170] Carbenicillin stocks were made by dissolving the antibiotic in sterile distilled water, with concentrations normalized for potency based on CLSI standards.[171] Assay plates for measuring the MIC were prepared by performing serial dilutions of antibiotic in 100 μL M9 minimal media in 96-well plates. Low glucose media was used to reduce growth variability by creating carbon-limiting, rather than nutrient-limiting, growth conditions.[146] Antibiotic concentrations were selected to include values that spanned the MIC levels for the dark and light state cultures in each experiment. Immediately following light exposure, cultures were normalized by dilution to the lowest optical density (OD) of each experiment. Normalized cultures were then diluted 1/25 into 96-well plates in triplicate and grown overnight for 18 hours at 37°C. Each well was then measured for OD absorbance at 600 nm (OD600) using a BioTek Synergy H1 plate reader.

CHAPTER 6. Conclusion

Antibiotics and resistance genes are both important tools across biology, medicine, and bioengineering. As scientists and clinicians have discovered, applied, and expanded these tools, we have fundamentally altered medicine and our ability to engineer organisms. In this work, we make a small step to enhance the control we have over antibiotic resistance and expand our understanding of how bacteria use resistance genes. Here, we developed an optogenetic recombinase for use in *Escherichia coli*, used this recombinase to control cell survival through antibiotic resistance, and applied these light-inducible resistance genes for metabolic engineering and bacterial resistance studies.

In **Chapter 2**, we develop a blue light-activated recombinase that functions in *E. coli* by splitting a recombinase protein into photodimer-linked halves. By testing Cre and Flp recombinases, Magnet and Vivid photodimers, and multiple recombinase split sites derived from literature, rational prediction, and computational models, we find an optimal variant with low basal activity and high fold change. We then characterize this variant, examining the impacts of light intensity and exposure length on bulk culture and single cells. Next, we expand the use of this split recombinase by optimizing antibiotic resistance induction cassettes in **Chapter 3**. We tune induction of bacterial survival through antibiotic resistance to four antibiotics: ampicillin/carbenicillin, kanamycin, chloramphenicol, and tetracycline. In this process we use various optimization approaches, varying gene copy number, promoter strength, ribosome binding site strength, and enzyme strength to enable control of bacterial survival across antibiotic concentrations. We then characterize a subset of these systems through single-cell

microscopy, and apply them to increase yields of octanoic acid by using resistance to select for cells actively expressing a bioproduction enzyme of interest.

Ultimately, we hope these systems will be used to study the activation dynamics of antibiotic resistance, and their impact on survival with clinical relevance. We make the first steps towards this class of studies in **Chapter 4** by coupling resistance and fluorescence activation, tuning fluorescence ribosome binding site strength and gene order to create dual-induction systems. Using fluorescence, we can know precisely when cells begin expressing resistance genes, and can characterize the impact of gene activation on survival relative to antibiotic exposure timing. This has relevance for horizontal gene transfer, and understanding what kind of antibiotic dosing schedules can best prevent the spread of resistance. Finally, we characterize a variety of notable but nonfunctional systems in **Chapter 5**. In the development of functional recombinase and resistance systems, we tested multiple light-inducible recombinase, gene induction cassette, and split protein alternatives that did not function as well as our existing systems. We include these here to inform future optogenetic system engineering efforts.

In summary, this thesis presents novel tools for the control of bacterial gene expression and survival, and shows initial applications for these tools. We hope that these light-inducible proteins and the engineering approaches used to build them set a path for even faster, more precise, and highly functional gene and resistance control platforms. As future applications, we hope that the approach taken to select high metabolic producers can be used to boost bioproduction for other compounds, and that improved control of antibiotic resistance can inform how resistance spreads from the single-cell to population

level, leading to clinical approaches to prevent antibiotic resistance and expanding our understanding of microbial community dynamics.

APPENDIX I: Supplementary Information for Chapter 2

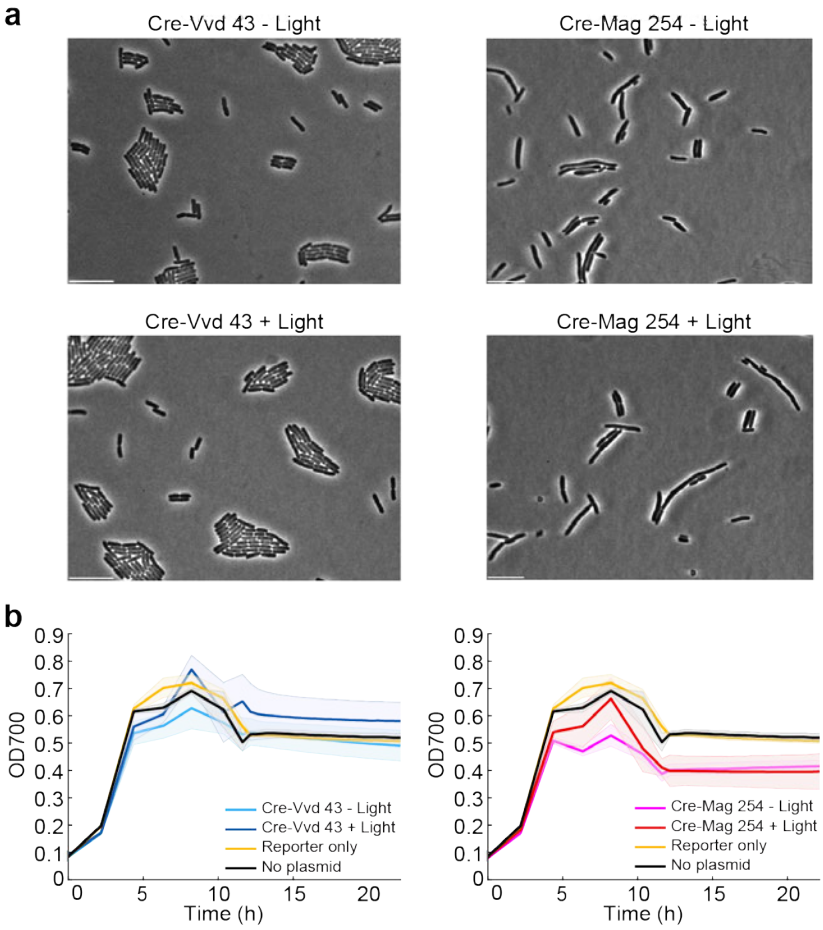

Figure AI-1. Growth defect in Cre-Mag 254 compared to Cre-Vvd 43.

(a) Single-cell phase contrast microscopy of fully induced Cre-Vvd 43 cells (left) or Cre-Mag 254 cells (right) without blue light exposure, and after 2 hours of 120 μW/cm^2 blue light exposure. Note the elongated cells visible in the Cre-Mag 254 case, which are independent of light exposure status. Scale bar = 10 μm. **(b)** Growth curve data for cultures with reporter and Cre-Vvd 43 (left) or Cre-Mag 254 (right) with and without light exposure (for hours 2 to 4), the reporter plasmid only, or no plasmid. Shaded error bars show standard deviation around the mean from plate reader data (n = 3 wells). Note that Cre-Vvd 43 is the construct we denote OptoCreVvd.

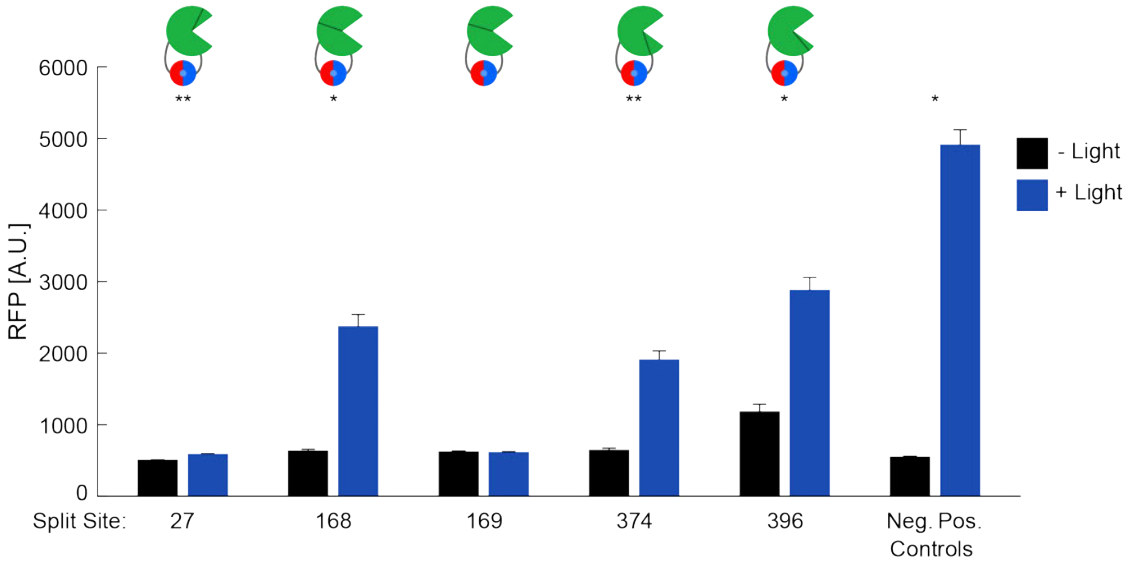

Figure AI-2. Split sites for Flp-Mag.

Numbers shown for split sites on the x-axis are the length of nFlp (AA). Error bars show standard error around the mean for microscopy data (average n ≈ 100 cells per sample). Statistical significance comparing conditions with and without light use a two-tailed Welch's *t*-test using microscopy images as replicates. *$P < 0.05$, **$P < 0.005$.

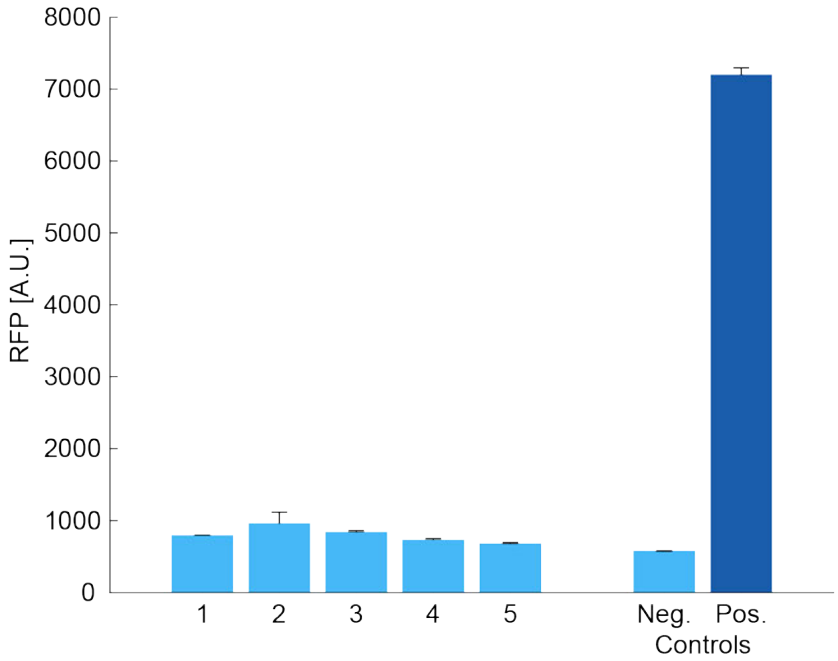

Figure AI-3. Consistent off-state of OptoCreVvd in the dark.

Replicate experiments from different days showing cell cultures of OptoCreVvd induced for 4 hours with 100 μM IPTG but not exposed to light, and refreshed overnight before microscopy. Cultures show a consistent low off state. Data taken from: 1, Fig 2-2b; 2, Fig 2-3a; 3, Fig 2-3b 1 hour; 4, Fig 2-3b 4 hours; 5, Fig 2-4a; Controls, Fig 2-2b. Error bars show standard error around the mean for microscopy data (average n ≈ 600 cells per sample).

Element	Primer
Mag/Vvd + Linkers Insert F	GGGTCTGGCTCCGGATC
Mag/Vvd + Linkers Insert R	CGGAGGTTCAGGAGGTTCA
Cre-43-F	ccggaggttcaggaggttcaAACAGGAAATGGTTCCCTGC
Cre-43-R	cttgatccggagccagacccGCCTGGTGCAAGCTGAAC
Cre-46-F	ccggaggttcaggaggttcaTGGTTCCCTGCTGAACCT
Cre-46-R	cttgatccggagccagacccTTTCCTGTTGTTCAGCTTGCA
Cre-137-F	ccggaggttcaggaggttcaAGATGCCAGGACATCAGGA
Cre-137-R	cttgatccggagccagacccGTCAGAGTTCTCCATCAGGGA
Cre-173-F	ccggaggttcaggaggttcaGGTGGGAGAATGCTGATCC
Cre-173-R	cttgatccggagccagacccATCGGTGCGGGAGATGT
Cre-213-F	ccggaggttcaggaggttcaGTGGCTGATGACCCCAAC
Cre-213-R	cttgatccggagccagacccACCAGACACAGAGATCCATCT
Cre-240-F	ccggaggttcaggaggttcaTCCACCCGGGCCCT
Cre-240-R	cttgatccggagccagacccCAGTTGGGAGGTGGCAGA
Cre-254-F	ccggaggttcaggaggttcaCTGATCTATGGTGCCAAGGATG
Cre-254-R	cttgatccggagccagacccGCGGTGGGTGGCCTC
Cre-263-F	ccggaggttcaggaggttcaGGGCAGAGATACCTGGCC
Cre-263-R	cttgatccggagccagacccTGGTGCCAAGGATGACTCT

Table AI-1. Primers used for plasmid assembly of split site constructs.

Overhang regions are shown in lowercase.

nFlp Length (AAs)	Amino Acids	Source
27	SG	Jung 2019[94]/Weinberg 2019[95]
168	TS	Weinberg 2019[95]
169	SR	Jung 2019[94]
374	LK	Weinberg 2019[95]
396	GS	Weinberg 2019[95]

Table AI-2. Flp recombinase split sites.

Split sites listed as lengths of the nFlp fragment (from methionine at position 1 to split site), the amino acids on either side of the split, and the source of the split.

APPENDIX II: Supplementary Information for Chapter 3

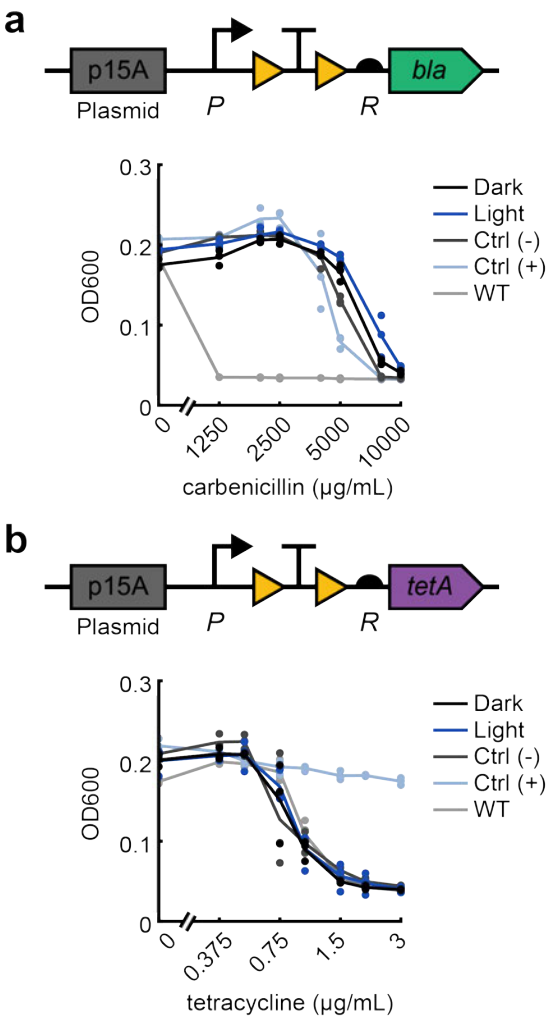

Figure AII-1. Nonfunctional resistance constructs.

Optogenetic activation of **(a)** OptoCre-*bla* and **(b)** OptoCre-*tetA* on the p15A plasmid origin using promoter *P* and RBS *R*. MIC is quantified by OD600 after 18 hours (n = 3 biological replicates).

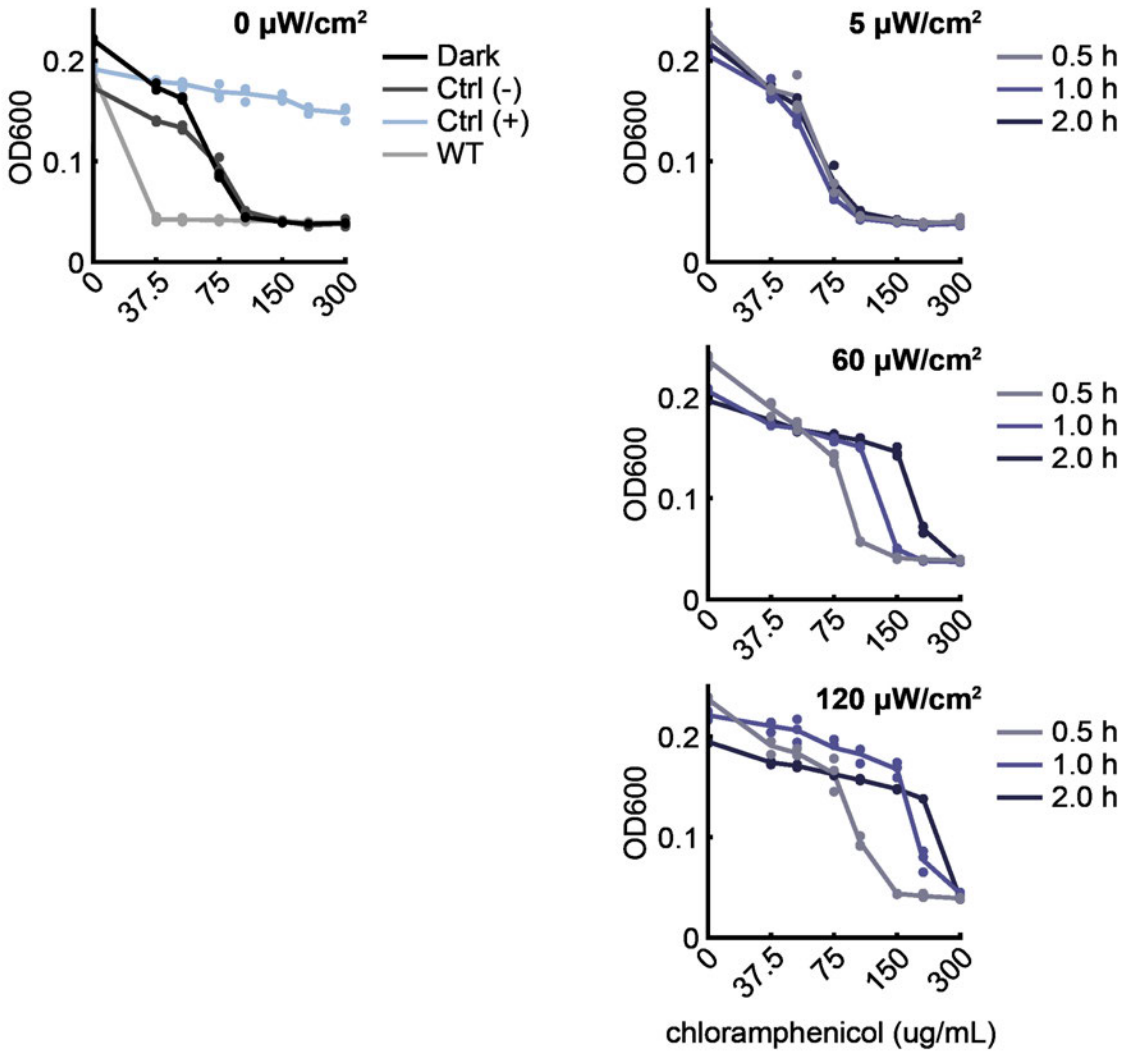

Figure AII-2. Impact of light intensity & duration on chloramphenicol resistance.

Tuning chloramphenicol resistance by changing light intensity and duration with p15A plasmid-based OptoCre-*cat* using cat_{T172A} with promoter P and RBS R. MIC is quantified by OD600 after 18 hours (n = 3 biological replicates).

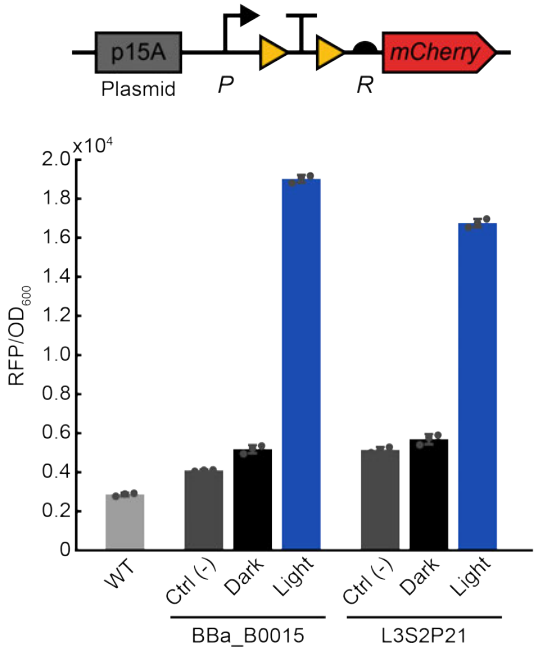

Figure AII-3. Characterization of alternate terminator sequence.

Characterization of synthetic terminators BBa_B0015 and L3S2P21 using *mCherry* fluorescence (n = 3 biological replicates). Terminator BBa_B0015 is used in all OptoCre antibiotic activation cassettes.

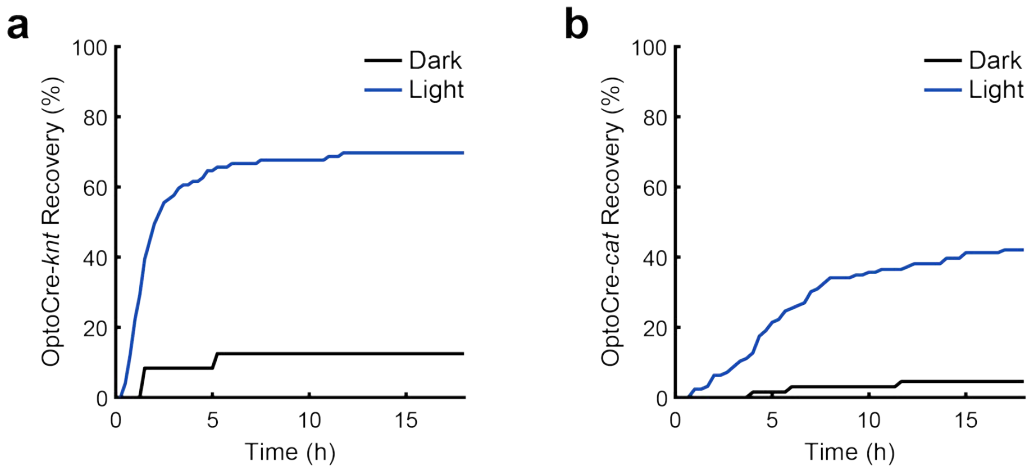

Figure AII-4. Growth recovery of cells from time-course microscopy.

Growth recovery of **(a)** chromosomal OptoCre-*knt* with promoter P* and RBS R on agarose pads containing 400 µg/mL kanamycin, and **(b)** p15A plasmid-based OptoCre-*cat* using cat_{T172A} with promoter P and RBS R on agarose pads containing 60 µg/mL chloramphenicol. Recovery is measured as percent cells present in the first frame that have divided at or before a given time point. Measurements are cumulative across three imaging positions for each condition.

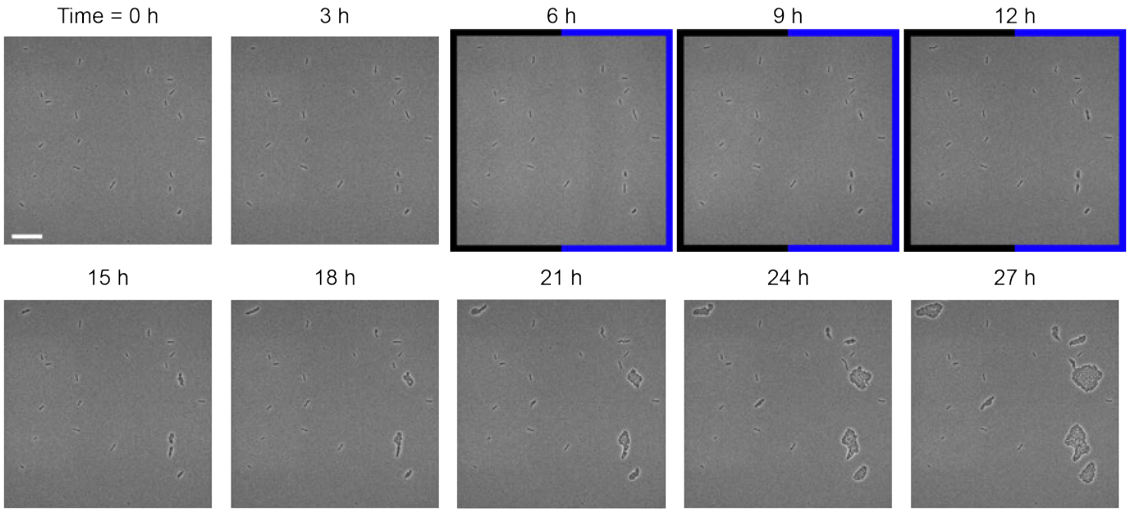

Figure AII-5. Single-cell time lapse microscopy of OptoCre-*cat* activated by DMD.

Single-cell time lapse microscopy of resistance induced by illuminating half of the field of view with a digital micromirror device (DMD). Activation of p15A plasmid-based OptoCre-*cat* using cat_{T172A} with promoter P and RBS R on agarose pads containing 60 µg/mL chloramphenicol (scale bar = 10 µm). DMD light activation was carried out on the right half of the frame from hours 6 to 12 of the experiment. This experiment was repeated three times on separate days, with similar results for all experiments.

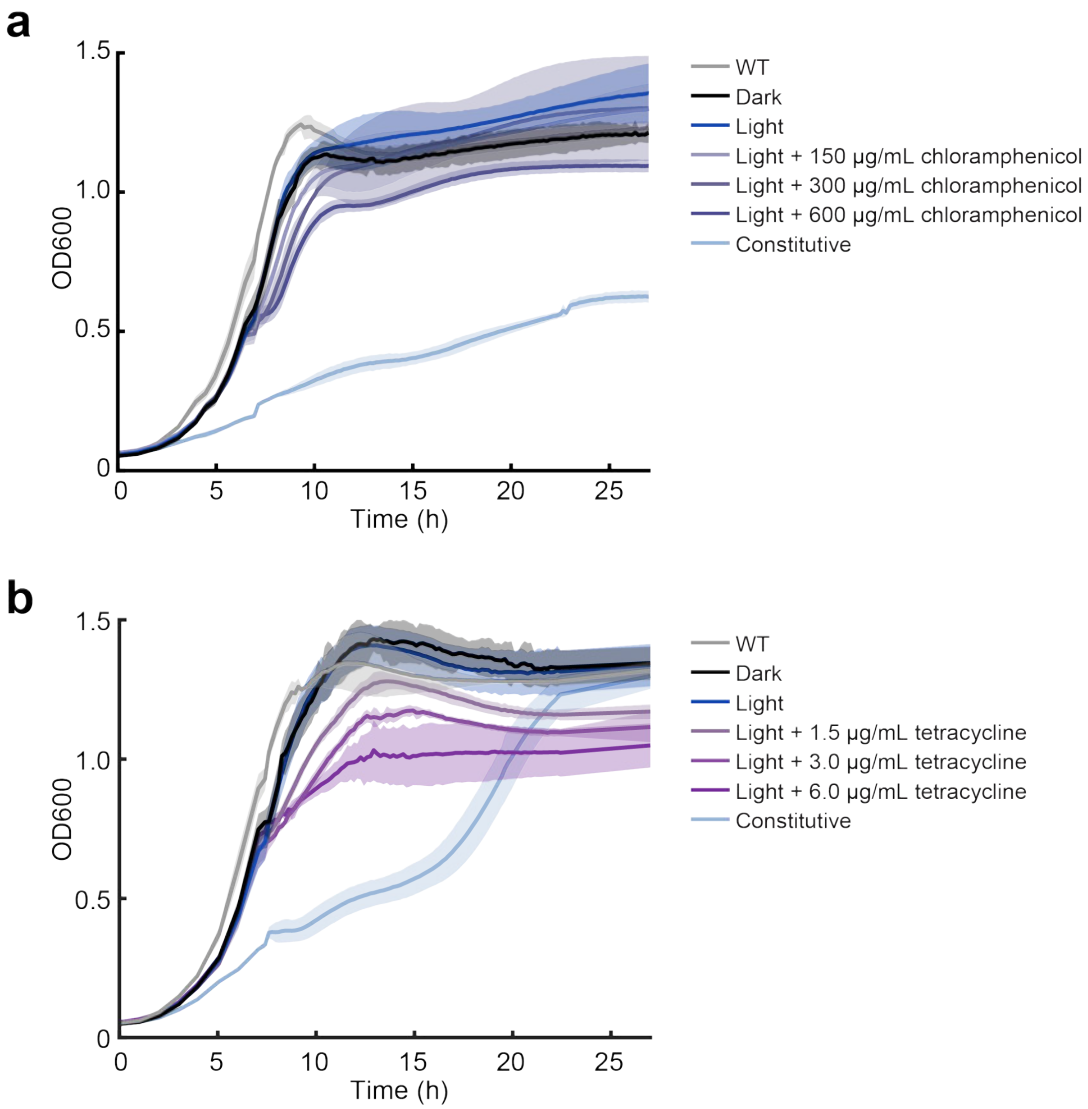

Figure AII-6. Growth time-course for octanoic acid production strains.

(a) Activation of p15A plasmid-based OptoCre-*cat* with promoter P and RBS R and cat_{T172A}, and RBS R' expressing *Cp*FatB1. Light induction was from 4.5-6.5 hours, with chloramphenicol added at 6.5 hours for the indicated strains. **(b)** Activation of p15A plasmid-based OptoCre-*tetA* with promoter P_{tet} and RBS R_{tet} expressing *tetA*, and RBS R' expressing *Cp*FatB1. Light induction was from 4-6 hours, with tetracycline added at 6 hours for indicated strains. Shaded error bars show standard deviation around the mean (n = 3 biological replicates).

Element	Assembly Method	Forward Primer	Reverse Primer
bla	Gibson	aagaaggagatatacatATGAGTATTCAACATTTCCG	tgccctggagatccctattaCCAATGCTTAATCAGTGAG
knt	Gibson	tttaagaaggagatatacatATGATTGAACAAGATGGATTGC	atgcctggagatccctattaTCAGAAGAACTCGTCAAGAAG
cat	Gibson	tttaagaaggagatatacatATGGAGAAAAAAATCACTGGAT	atgcctggagatccctattaTTACGCCCCGCCC
tetA (loxP-TT-loxP insertion)	GG	gtgactcgtctcgGCACGGCGAAATAACTTC	gtgactcgtctcgcgCTTCTTAAAATAACTTCGTATAATG
*Cp*FatB1	Gibson	gggcgtaataatagggatctTTTCAGAATTCAAAAGATCTTTT	atgcctggagatccctattaATGCCTGGAGATCCTTACTC
P*	GG	tacgctggtctccttGTCTTAAAGTCTAACCTATAGGATTCTTAC	tacgctggtctccgtCCCTCTCGATGGCTGTAAGA
P**	GG	tacgctggtctccttGTAATAAAGTCTAACCTATAGGATTTTTAC	tacgctggtctccgtCCCTCTCGATGGCTGTAAAA
R*	GG	gcatgaggtctcctaGCATACATTATACGAAGTTATATCACTCTACGG	cgatcaggtctcgaaTCATGTTTGCAGCTGGCCG
R’	GG	agtggaggtctcctcTCTTTTGTTTAATTACTAAGCGGGAGGTTAT	agtggaggtctcctcATAACCTCCCGCTTAGTAATTAAACAAA
L3S2P21	GG	gatgtccgtctccTCCTCGGTACCAAATTCCAGAAA	gatgtccgtctccGCAGGACCAAAACGAAAAAAGGC
Plasmid resistance swaps	Gibson	GATCTATCAACAGGAGTCCAAGC	GCGCAACGCAATTAATGTAAGT
FRT cassette (cassette)	Gibson	gttttgcgccattcgatggtGCAGCATTACACGTCTTGAG	acatcaccgatggggaagatcctgtcaaacatgagaattaattccg
FRT cassette (vector)	Gibson	ttaattctcatgtttgacaggatcttccccatcggtgatgtc	ctcaagacgtgtaatgctgcaccatcgaatggcgcaaaac

Table AII-1. Primers used for assembly of antibiotic resistance constructs.

Constructs assembled using either Gibson or Golden Gate (GG) method. Binding regions in uppercase.

BIBLIOGRAPHY

1. Mimee, M. *et al.* An ingestible bacterial-electronic system to monitor gastrointestinal health. *Science* **360**, 915–918 (2018).
2. Atkinson, J. T. *et al.* Real-time bioelectronic sensing of environmental contaminants. *Nature* **611**, 548–553 (2022).
3. Lalwani, M. A., Zhao, E. M. & Avalos, J. L. Current and future modalities of dynamic control in metabolic engineering. *Current Opinion in Biotechnology* **52**, 56–65 (2018).
4. Cohen, S. N., Chang, A. C. Y., Boyer, H. W. & Helling, R. B. Construction of Biologically Functional Bacterial Plasmids In Vitro. *Proceedings of the National Academy of Sciences of the United States of America* **70**, 3240–3244 (1973).
5. de Boer, H. A., Comstock, L. J. & Vasser, M. The tac promoter: a functional hybrid derived from the trp and lac promoters. *Proceedings of the National Academy of Sciences of the United States of America* **80**, 21–25 (1983).
6. Deisseroth, K. Optogenetics - Method of the Year. *Nature methods* **26**, 1–4 (2010).
7. Boyden, E. S. Optogenetics and the future of neuroscience. *Nature Neuroscience* **18**, 1200–1201 (2015).
8. Kim, S. *et al.* Whole-brain mapping of effective connectivity by fMRI with cortex-wide patterned optogenetics. *Neuron* (2023) doi:10.1016/j.neuron.2023.03.002.
9. Chen, W. *et al.* The Roles of Optogenetics and Technology in Neurobiology: A Review. *Frontiers in Aging Neuroscience* **14**, (2022).

10. Goglia, A. G. & Toettcher, J. E. A bright future: optogenetics to dissect the spatiotemporal control of cell behavior. *Current Opinion in Chemical Biology* **48**, 106–113 (2019).

11. Liu, Z. *et al.* Programming Bacteria With Light—Sensors and Applications in Synthetic Biology. *Frontiers in Microbiology* **9**, 2692 (2018).

12. Lindner, F. & DIepold, A. Optogenetics in bacteria – applications and opportunities. *FEMS Microbiology Reviews* **46**, 1–17 (2022).

13. Wei, J. & Jin, F. Illuminating bacterial behaviors with optogenetics. *Current Opinion in Solid State and Materials Science* **26**, 101023 (2022).

14. Chia, N., Lee, S. Y. & Tong, Y. Optogenetic tools for microbial synthetic biology. *Biotechnology Advances* 107953 (2022) doi:10.1016/J.BIOTECHADV.2022.107953.

15. Meyer, A. J., Segall-Shapiro, T. H., Glassey, E., Zhang, J. & Voigt, C. A. Escherichia coli “Marionette” strains with 12 highly optimized small-molecule sensors. *Nature Chemical Biology* **15**, 196–204 (2019).

16. Allen, J. Application of patterned illumination using a DMD for optogenetic control of signaling. *Nature Methods 2017 14:11* **14**, 1114–1114 (2017).

17. Huang, Y., Xia, A., Yang, G. & Jin, F. Bioprinting Living Biofilms through Optogenetic Manipulation. *ACS Synthetic Biology* **7**, 1195–1200 (2018).

18. Levskaya, A., Weiner, O. D., Lim, W. A. & Voigt, C. A. Spatiotemporal control of cell signalling using a light-switchable protein interaction. *Nature* **461**, 997–1001 (2009).

19. Perkins, M. L., Benzinger, D., Arcak, M. & Khammash, M. Cell-in-the-loop pattern formation with optogenetically emulated cell-to-cell signaling. *Nature Communications* **11**, 1–10 (2020).

20. Levskaya, A. *et al.* Engineering Escherichia coli to see light. *Nature* **438**, 441–442 (2005).

21. Jayaraman, P. *et al.* Blue light-mediated transcriptional activation and repression of gene expression in bacteria. *Nucleic Acids Research* **44**, 6994–7005 (2016).

22. Ohlendorf, R., Vidavski, R. R., Eldar, A., Moffat, K. & Möglich, A. From Dusk till Dawn: One-Plasmid Systems for Light-Regulated Gene Expression. *Journal of Molecular Biology* **416**, 534–542 (2012).

23. Romano, E. *et al.* Engineering AraC to make it responsive to light instead of arabinose. *Nature Chemical Biology* **17**, 817–827 (2021).

24. Schmidl, S. R., Sheth, R. U., Wu, A. & Tabor, J. J. Refactoring and Optimization of Light-Switchable *Escherichia coli* Two-Component Systems. *ACS Synthetic Biology* **3**, 820–831 (2014).

25. Ong, N. T. & Tabor, J. J. A Miniaturized Escherichia coli Green Light Sensor with High Dynamic Range. *ChemBioChem* **19**, 1255–1258 (2018).

26. Huala, E. *et al.* Arabidopsis NPH1: a protein kinase with a putative redox-sensing domain. *Science* **278**, 2120–2123 (1997).

27. Lungu, O. I. *et al.* Designing photoswitchable peptides using the AsLOV2 domain. *Chemistry & Biology* **19**, 507–517 (2012).

28. Tague, N., Coriano-Ortiz, C., Sheets, M. B. & Dunlop, M. J. Light inducible protein degradation in E. coli with LOVtag. Preprint at https://doi.org/10.1101/2023.02.25.530042 (2023).

29. Baumschlager, A., Aoki, S. K. & Khammash, M. Dynamic Blue Light-Inducible T7 RNA Polymerases (Opto-T7RNAPs) for Precise Spatiotemporal Gene Expression Control. *ACS Synthetic Biology* **6**, 2157–2167 (2017).

30. Yu, Y. *et al.* Engineering a far-red light-activated split-Cas9 system for remote-controlled genome editing of internal organs and tumors. *Science Advances* **6**, eabb1777 (2020).

31. Hartsough, L. A. *et al.* Optogenetic control of gut bacterial metabolism to promote longevity. *eLife* **9**, 1–16 (2020).

32. Pu, L., Yang, S., Xia, A. & Jin, F. Optogenetics Manipulation Enables Prevention of Biofilm Formation of Engineered Pseudomonas aeruginosa on Surfaces. *ACS Synthetic Biology* **7**, 200–208 (2018).

33. Mukherjee, M., Hu, Y., Tan, C. H., Rice, S. A. & Cao, B. Engineering a light-responsive, quorum quenching biofilm to mitigate biofouling on water purification membranes. *Science Advances* **4**, eaau1459 (2018).

34. Vizoso, M. *et al.* A doxycycline- and light-inducible Cre recombinase mouse model for optogenetic genome editing. *Nature Communications* **13**, 6442 (2022).

35. Madisen, L. *et al.* A toolbox of Cre-dependent optogenetic transgenic mice for light-induced activation and silencing. *Nature Neuroscience* **15**, 793–802 (2012).

36. Weinberg, B. H. *et al.* Large-scale design of robust genetic circuits with multiple inputs and outputs for mammalian cells. *Nature Biotechnology* **35**, 453–462 (2017).

37. Kiwimagi, K. A. *et al.* Quantitative characterization of recombinase-based digitizer circuits enables predictable amplification of biological signals. *Communications Biology* **4**, 1–12 (2021).

38. Meinke, G., Bohm, A., Hauber, J., Pisabarro, M. T. & Buchholz, F. Cre Recombinase and Other Tyrosine Recombinases. *Chemical Reviews* **116**, 12785–12820 (2016).

39. Kawano, F., Okazaki, R., Yazawa, M. & Sato, M. A photoactivatable Cre–loxP recombination system for optogenetic genome engineering. *Nature Chemical Biology* **12**, 1059–1064 (2016).

40. Weinberg, B. H. *et al.* High-performance chemical- and light-inducible recombinases in mammalian cells and mice. *Nature Communications* **10**, (2019).

41. Witten, I. B. *et al.* Recombinase-Driver Rat Lines: Tools, Techniques, and Optogenetic Application to Dopamine-Mediated Reinforcement. *Neuron* **72**, 721–733 (2011).

42. Allen, M. E. *et al.* An AND-Gated Drug and Photoactivatable Cre-loxP System for Spatiotemporal Control in Cell-Based Therapeutics. *ACS Synthetic Biology* **8**, 2359–2371 (2019).

43. Aditya, C., Bertaux, F., Batt, G. & Ruess, J. A light tunable differentiation system for the creation and control of consortia in yeast. *Nature Communications* **12**, 1–10 (2021).

44. Hochrein, L., Mitchell, L. A., Schulz, K., Messerschmidt, K. & Mueller-Roeber, B. L-SCRaMbLE as a tool for light-controlled Cre-mediated recombination in yeast. *Nature Communications* **9**, 1931 (2018).

45. Duplus-Bottin, H. *et al.* A single-chain and fast-responding light-inducible Cre recombinase as a novel optogenetic switch. *eLife* **10**, e61268 (2021).

46. Wegner, S. A., Barocio-Galindo, R. M. & Avalos, J. L. The bright frontiers of microbial metabolic optogenetics. *Current Opinion in Chemical Biology* **71**, 102207 (2022).

47. Pouzet, S. *et al.* The Promise of Optogenetics for Bioproduction: Dynamic Control Strategies and Scale-Up Instruments. *Bioengineering (Basel)* **7**, 151 (2020).

48. Weber, W. & Fussenegger, M. Inducible product gene expression technology tailored to bioprocess engineering. *Current Opinion in Biotechnology* **18**, 399–410 (2007).

49. Liang, J.-Y. *et al.* Blue light induced free radicals from riboflavin on E. coli DNA damage. *Journal of Photochemistry and Photobiology B: Biology* **119**, 60–64 (2013).

50. Ding, Q. *et al.* Light-powered Escherichia coli cell division for chemical production. *Nature Communications* **11**, 2262 (2020).

51. Wu, P., Chen, Y., Liu, M., Xiao, G. & Yuan, J. Engineering an Optogenetic CRISPRi Platform for Improved Chemical Production. *ACS Synthetic Biology* **10**, 125–131 (2021).

52. Lalwani, M. A. *et al.* Optogenetic control of the lac operon for bacterial chemical and protein production. *Nature Chemical Biology* **17**, 71–79 (2021).

53. Zhao, E. M. *et al.* Light-based control of metabolic flux through assembly of synthetic organelles. *Nature Chemical Biology* **15**, 589–597 (2019).

54. Lalwani, M. A., Kawabe, H., Mays, R. L., Hoffman, S. M. & Avalos, J. L. Optogenetic Control of Microbial Consortia Populations for Chemical Production. *ACS Synthetic Biology* **10**, 2015–2029 (2021).

55. Gutiérrez Mena, J., Kumar, S. & Khammash, M. Dynamic cybergenetic control of bacterial co-culture composition via optogenetic feedback. *Nature Communications* **13**, 1–16 (2022).

56. Carrasco-López, C., García-Echauri, S. A., Kichuk, T. & Avalos, J. L. Optogenetics and biosensors set the stage for metabolic cybergenetics. *Current Opinion in Biotechnology* **65**, 296–309 (2020).

57. Hutchings, M. I., Truman, A. W. & Wilkinson, B. Antibiotics: past, present and future. *Current Opinion in Microbiology* **51**, 72–80 (2019).

58. Anderson, J. C. *et al.* BglBricks: A flexible standard for biological part assembly. *Journal of Biological Engineering* **4**, 1 (2010).

59. Sheth, R. U., Yim, S. S., Wu, F. L. & Wang, H. H. Multiplex recording of cellular events over time on CRISPR biological tape. *Science* **358**, 1457–1461 (2017).

60. Yim, S. S. *et al.* Robust direct digital-to-biological data storage in living cells. *Nature Chemical Biology* **17**, 246–253 (2021).

61. Dwidar, M. & Yokobayashi, Y. Riboswitch Signal Amplification by Controlling Plasmid Copy Number. *ACS Synthetic Biology* **8**(2), 245–250 (2019) https://doi.org/10.1021/acssynbio.8b00454

62. Kasari, M., Kasari, V., Kärmas, M. & Jõers, A. Decoupling Growth and Production by Removing the Origin of Replication from a Bacterial Chromosome. *ACS Synthetic Biology* **11**(8), 2610–2622 (2022) doi:10.1021/ACSSYNBIO.1C00618.

63. Rennig, M. *et al.* TARSyn: Tunable Antibiotic Resistance Devices Enabling Bacterial Synthetic Evolution and Protein Production. *ACS Synthetic Biology* **7**, 432–442 (2018).

64. Murray, C. J. *et al.* Global burden of bacterial antimicrobial resistance in 2019: A systematic analysis. *The Lancet* **399**, 629–655 (2022).

65. Jernigan, J. A. *et al.* Multidrug-Resistant Bacterial Infections in U.S. Hospitalized Patients, 2012–2017. *New England Journal of Medicine* **382**, 1309–1319 (2020).

66. Barcudi, D. *et al.* MRSA dynamic circulation between the community and the hospital setting: New insights from a cohort study. *Journal of Infection* **80**, 24–37 (2020).

67. Cook, M. A. & Wright, G. D. The past, present, and future of antibiotics. *Science Translational Medicine* **14**, eabo7793 (2022).

68. Årdal, C. *et al.* Antibiotic development — economic, regulatory and societal challenges. *Nature Reviews. Microbiology* **18**, 267–274 (2020).

69. Von Wintersdorff, C. J. H. *et al.* Dissemination of antimicrobial resistance in microbial ecosystems through horizontal gene transfer. *Frontiers in Microbiology* **7**, 173 (2016).

70. Thomas, C. M. & Nielsen, K. M. Mechanisms of, and barriers to, horizontal gene transfer between bacteria. *Nature Reviews. Microbiology* **3**, 711–721 (2005).

71. Huddleston, J. R. Horizontal gene transfer in the human gastrointestinal tract: Potential spread of antibiotic resistance genes. *Infection and Drug Resistance* **7**, 167–176 (2014).

72. Barlow, M. What antimicrobial resistance has taught us about horizontal gene transfer. *Methods in Molecular Biology* **532**, 397–411 (2009).

73. Hawkey, P. M. & Jones, A. M. The changing epidemiology of resistance. *The Journal of Antimicrobial Chemotherapy* **64 Suppl 1**, i3-10 (2009).

74. Nolivos, S. *et al.* Role of AcrAB-TolC multidrug efflux pump in drug-resistance acquisition by plasmid transfer. *Science* **364**, 778–782 (2019).

75. Cooper, R. M., Tsimring, L. & Hasty, J. Inter-species population dynamics enhance microbial horizontal gene transfer and spread of antibiotic resistance. *eLife* **6**, (2017).

76. Sulavik, M. C. *et al.* Antibiotic susceptibility profiles of Escherichia coli strains lacking multidrug efflux pump genes. *Antimicrobial Agents and Chemotherapy* **45**, 1126–1136 (2001).

77. Olson, E. J. & Tabor, J. J. Optogenetic characterization methods overcome key challenges in synthetic and systems biology. *Nature Chemical Biology* **10**, 502–511 (2014).

78. Mansouri, M., Strittmatter, T. & Fussenegger, M. Light-Controlled Mammalian Cells and Their Therapeutic Applications in Synthetic Biology. *Advanced Science* **6**, 1800952 (2019).

79. Kolar, K., Knobloch, C., Stork, H., Žnidarič, M. & Weber, W. OptoBase: A Web Platform for Molecular Optogenetics. *ACS Synthetic Biology* **7**, 1825–1828 (2018).

80. Fenno, L., Yizhar, O. & Deisseroth, K. The Development and Application of Optogenetics. *Annual Review of Neuroscience* **34**, 389–412 (2011).

81. Lugagne, J.-B. & Dunlop, M. J. Cell-machine interfaces for characterizing gene regulatory network dynamics. *Current Opinion in Systems Biology* **14**, 1–8 (2019).

82. Milias-Argeitis, A. *et al.* In silico feedback for in vivo regulation of a gene expression circuit. *Nature Biotechnology* **29**, 1114–1116 (2011).

83. Zhao, E. M. *et al.* Optogenetic regulation of engineered cellular metabolism for microbial chemical production. *Nature* **555**, 683–687 (2018).

84. Wang, Y. *et al.* Optogenetic regulation of artificial microRNA improves H2 production in green alga Chlamydomonas reinhardtii. *Biotechnology for Biofuels* **10**, 257 (2017).

85. Milias-Argeitis, A., Rullan, M., Aoki, S. K., Buchmann, P. & Khammash, M. Automated optogenetic feedback control for precise and robust regulation of gene expression and cell growth. *Nature Communications* **7**, 12546 (2016).

86. Sankaran, S., Becker, J., Wittmann, C. & del Campo, A. Optoregulated Drug Release from an Engineered Living Material: Self-Replenishing Drug Depots for Long-Term, Light-Regulated Delivery. *Small* **15**, 1804717 (2019).

87. Moser, F., Tham, E., González, L. M., Lu, T. K. & Voigt, C. A. Light-Controlled, High-Resolution Patterning of Living Engineered Bacteria Onto Textiles, Ceramics, and Plastic. *Advanced Functional Materials* **29**, 1901788 (2019).

88. Tabor, J. J., Levskaya, A. & Voigt, C. A. Multichromatic Control of Gene Expression in Escherichia coli. *Journal of Molecular Biology* **405**, 315–324 (2011).

89. Jayaraman, P., Yeoh, J. W., Zhang, J. & Poh, C. L. Programming the Dynamic Control of Bacterial Gene Expression with a Chimeric Ligand- and Light-Based Promoter System. *ACS Synthetic Biology* **7**, 2627–2639 (2018).

90. Han, T., Chen, Q. & Liu, H. Engineered Photoactivatable Genetic Switches Based on the Bacterium Phage T7 RNA Polymerase. *ACS Synthetic Biology* **6**, 357–366 (2017).

91. Nihongaki, Y. *et al.* CRISPR–Cas9-based photoactivatable transcription systems to induce neuronal differentiation. *Nature Methods* **14**, 963–966 (2017).

92. Siuti, P., Yazbek, J. & Lu, T. K. Synthetic circuits integrating logic and memory in living cells. *Nature Biotechnology* **31**, 448–452 (2013).

93. Jullien, N. Regulation of Cre recombinase by ligand-induced complementation of inactive fragments. *Nucleic Acids Research* **31**, 131e–1131 (2003).

94. Jung, H. *et al.* Noninvasive optical activation of Flp recombinase for genetic manipulation in deep mouse brain regions. *Nature Communications* **10**, 314 (2019).

95. Weinberg, B. H. *et al.* High-performance chemical and light-inducible recombinases in mammalian cells and mice. *bioRxiv* 747121 (2019) doi:10.1101/747121.

96. Meador, K. *et al.* Achieving tight control of a photoactivatable Cre recombinase gene switch: new design strategies and functional characterization in mammalian cells and rodent. *Nucleic Acids Research* **47**, e97 (2019).

97. Taslimi, A. *et al.* Optimized second-generation CRY2-CIB dimerizers and photoactivatable Cre recombinase. *Nature Chemical Biology* **12**, 425–430 (2016).

98. Kennedy, M. J. *et al.* Rapid blue-light-mediated induction of protein interactions in living cells. *Nature Methods* **7**, 973–975 (2010).

99. O'Brien, S. P. & DeLisa, M. P. Split-Cre recombinase effectively monitors protein-protein interactions in living bacteria. *Biotechnology Journal* **9**, 355–361 (2014).

100. Hoess, R. H. & Abremski, K. Mechanism of strand cleavage and exchange in the Cre-lox site-specific recombination system. *Journal of Molecular Biology* **181**, 351–362 (1985).

101. Zoltowski, B. D. *et al.* Conformational switching in the fungal light sensor Vivid. *Science* **316**, 1054–7 (2007).

102. Grusch, M. *et al.* Spatio-temporally precise activation of engineered receptor tyrosine kinases by light. *The EMBO Journal* **33**, 1713–1726 (2014).

103. Kawano, F., Suzuki, H., Furuya, A. & Sato, M. Engineered pairs of distinct photoswitches for optogenetic control of cellular proteins. *Nature Communications* **6**, 6256 (2015).

104. Gerhardt, K. P. *et al.* An open-hardware platform for optogenetics and photobiology. *Scientific Reports* **6**, 35363 (2016).

105. Cherepanov, P. P. & Wackernagel, W. Gene disruption in Escherichia coli: TcR and KmR cassettes with the option of Flp-catalyzed excision of the antibiotic-resistance determinant. *Gene* **158**, 9–14 (1995).

106. Yao, S. *et al.* RecV recombinase system for in vivo targeted optogenomic modifications of single cells or cell populations. *bioRxiv* 553271 (2019) doi:10.1101/553271.

107. Dagliyan, O. *et al.* Computational design of chemogenetic and optogenetic split proteins. *Nature Communications* **9**, 4042 (2018).

108. Gibb, B. *et al.* Requirements for catalysis in the Cre recombinase active site. *Nucleic Acids Research* **38**, 5817–5832 (2010).

109. DeLano, W. L. PyMOL. (2002).

110. Karplus, P. A. & Schulz, G. E. Prediction of chain flexibility in proteins. *Naturwissenschaften* **72**, 212–213 (1985).

111. Huang, F. & Nau, W. M. A Conformational Flexibility Scale for Amino Acids in Peptides. *Angewandte Chemie. International Edition* **42**, 2269–2272 (2003).

112. Pu, J., Zinkus-Boltz, J. & Dickinson, B. C. Evolution of a split RNA polymerase as a versatile biosensor platform. *Nature Chemical Biology* **13**, 432–438 (2017).

113. Lee, T. *et al.* BglBrick vectors and datasheets: A synthetic biology platform for gene expression. *Journal of Biological Engineering* **5**, 12 (2011).

114. Campbell, R. E. *et al.* A monomeric red fluorescent protein. *Proceedings of the National Academy of Sciences of the United States of America* **99**, 7877–7882 (2002).

115. Brunner, M. & Bujard, H. *Promoter recognition and promoter strength in the Escherichia coli system*. *The EMBO Journal* **6,** 3139–3144 (1987).

116. Gibson, D. G. *et al.* Enzymatic assembly of DNA molecules up to several hundred kilobases. *Nature Methods* **6**, 343–345 (2009).

117. Datsenko, K. A. & Wanner, B. L. One-step inactivation of chromosomal genes in Escherichia coli K-12 using PCR products. *Proceedings of the National Academy of Sciences of the United States of America* **97**, 6640–5 (2000).

118. Stylianidou, S., Brennan, C., Nissen, S. B., Kuwada, N. J. & Wiggins, P. A. *SuperSegger*: robust image segmentation, analysis and lineage tracking of bacterial cells. *Molecular Microbiology* **102**, 690–700 (2016).

119. Nadler, D. C., Morgan, S. A., Flamholz, A., Kortright, K. E. & Savage, D. F. Rapid construction of metabolite biosensors using domain-insertion profiling. *Nature Communications* **7**, 1–11 (2016).

120. Cain, A. K. *et al.* A decade of advances in transposon-insertion sequencing. *Nature Reviews Genetics* **21**, 526–540 (2020).

121. Sankaran, S. *et al.* Toward Light-Regulated Living Biomaterials. *Advanced Science* **5**, 1800383 (2018).

122. Lamanna, J. *et al.* Digital microfluidic isolation of single cells for -Omics. *Nature Communications* **11**, 1–13 (2020).

123. Luro, S., Potvin-Trottier, L., Okumus, B. & Paulsson, J. Isolating live cells after high-throughput, long-term, time-lapse microscopy. *Nature Methods* **17**, 93 (2020).

124. Koganezawa, Y., Umetani, M., Sato, M. & Wakamoto, Y. History-dependent physiological adaptation to lethal genetic modification under antibiotic exposure. *eLife* **11**, (2022).

125. Sun, D., Jeannot, K., Xiao, Y. & Knapp, C. W. Editorial: Horizontal gene transfer mediated bacterial antibiotic resistance. *Frontiers in Microbiology* **10**, 1933 (2019).

126. Laskey, A. *et al.* Mobility of β-Lactam Resistance Under Bacterial Co-infection and Ampicillin Treatment in a Mouse Model. *Frontiers in Microbiology* **11**, 1591 (2020).

127. Fox, Z. R. *et al.* Enabling reactive microscopy with MicroMator. *Nature Communications* **13**, 1–8 (2022).

128. Tandar, S. T., Senoo, S., Toya, Y. & Shimizu, H. Optogenetic switch for controlling the central metabolic flux of Escherichia coli. *Metabolic Engineering* **55**, 68–75 (2019).

129. Moreno Morales, N., Patel, M. T., Stewart, C. J., Sweeney, K. & McClean, M. N. Optogenetic Tools for Control of Public Goods in Saccharomyces cerevisiae. *mSphere* **6**, (2021).

130. Wang, Z.; *et al.* A Single-Component Blue Light-Induced System Based on EL222 in Yarrowia lipolytica. *International Journal of Molecular Sciences* **23**, 6344 (2022).

131. Herzig, L. M., Elamri, I., Schwalbe, H. & Wachtveitl, J. Light-induced antibiotic release from a coumarin-caged compound on the ultrafast timescale. *Physical Chemistry Chemical Physics* **19**, 14835–14844 (2017).

132. Baumschlager, A., Rullan, M. & Khammash, M. Exploiting natural chemical photosensitivity of anhydrotetracycline and tetracycline for dynamic and setpoint chemo-optogenetic control. *Nature Communications* **11**, 1–10 (2020).

133. Sheets, M. B., Wong, W. W. & Dunlop, M. J. Light-Inducible Recombinases for Bacterial Optogenetics. *ACS Synthetic Biology* **9**(2), 227–235 (2020) doi:10.1021/acssynbio.9b00395

134. Tian, X. & Zhou, B. Strategies for site-specific recombination with high efficiency and precise spatiotemporal resolution. *Journal of Biological Chemistry* **296**, 100509 (2021).

135. Sawa, T., Kooguchi, K. & Moriyama, K. Molecular diversity of extended-spectrum β-lactamases and carbapenemases, and antimicrobial resistance. *Journal of Intensive Care* **8**, 1–13 (2020).

136. Mulvey, M. R. & Simor, A. E. Antimicrobial resistance in hospitals: How concerned should we be? *CMAJ: Canadian Medical Association Journal* **180**, 408–415 (2009).

137. Pedersen, L. C., Benning, M. M. & Holden, H. M. Structural Investigation of the Antibiotic and ATP-Binding Sites in Kanamycin Nucleotidyltransferase. *Biochemistry* **34**, 13305–13311 (1995).

138. Shaw, W. V. Chloramphenicol Acetyltransferase: Enzymology and Molecular Biology. *CRC Critical Reviews in Biochemistry* **14**, 1–46 (1983). https://doi.org/10.3109/10409238309102789

139. Stavropoulos, T. A. & Strathdee, C. A. Expression of the tetA(C) tetracycline efflux pump in Escherichia coli confers osmotic sensitivity. *FEMS Microbiology Letters* **190**, 147–150 (2000).

140. Chopra, I. & Roberts, M. Tetracycline Antibiotics: Mode of Action, Applications, Molecular Biology, and Epidemiology of Bacterial Resistance. *Microbiology and Molecular Biology Reviews* **65**, 232–260 (2001).

141. Sarria, S., Kruyer, N. S. & Peralta-Yahya, P. Microbial synthesis of medium-chain chemicals from renewables. *Nature Biotechnology* **35**, 1158–1166 (2017).

142. Yan, Q. & Pfleger, B. F. Revisiting metabolic engineering strategies for microbial synthesis of oleochemicals. *Metabolic Engineering* **58**, 35–46 (2020).

143. Burg, J. M. *et al.* Large-scale bioprocess competitiveness: the potential of dynamic metabolic control in two-stage fermentations. *Current Opinion in Chemical Engineering* **14**, 121–136 (2016).

144. Hartline, C. J., Schmitz, A. C., Han, Y. & Zhang, F. Dynamic control in metabolic engineering: Theories, tools, and applications. *Metabolic Engineering* **63**, 126–140 (2021).

145. Salverda, M. L. M., de Visser, J. A. G. M. & Barlow, M. Natural evolution of TEM-1 β-lactamase: experimental reconstruction and clinical relevance. *FEMS Microbiology Reviews* **34**, 1015–1036 (2010).

146. Andreani, V., You, L., Glaser, P. & Batt, G. A model-based approach to characterize enzyme-mediated response to antibiotic treatments: going beyond the SIR classification. *bioRxiv* 2021.07.16.452741 (2021) doi:10.1101/2021.07.16.452741.

147. Meredith, H. R. *et al.* Applying ecological resistance and resilience to dissect bacterial antibiotic responses. *Science Advances* **4**, (2018).

148. Olins, P. O., Devine, C. S., Rangwala, S. H. & Kavka, K. S. The T7 phage gene 10 leader RNA, a ribosome-binding site that dramatically enhances the expression of foreign genes in Escherichia coli. *Gene* **73**, 227–235 (1988).

149. Cetnar, D. P. & Salis, H. M. Systematic Quantification of Sequence and Structural Determinants Controlling mRNA stability in Bacterial Operons. *ACS Synthetic Biology* **10**, 318–332 (2021).

150. Shao, B. *et al.* Single-cell measurement of plasmid copy number and promoter activity. *Nature Communications* **12**, 1–9 (2021).

151. Shaw, W. V. *et al.* Primary structure of a chloramphenicol acetyltransferase specified by R plasmids. *Nature* **282**, 870–872 (1979).

152. Ciechonska, M. *et al.* Emergent expression of fitness-conferring genes by phenotypic selection. *PNAS Nexus* **1**, 1–13 (2022).

153. Lewendon, A. & Shaw, W. V. Transition state stabilization by chloramphenicol acetyltransferase. Role of a water molecule bound to threonine 174. *Journal of Biological Chemistry* **268**, 20997–21001 (1993).

154. Chen, Y. J. *et al.* Characterization of 582 natural and synthetic terminators and quantification of their design constraints. *Nature Methods* **10**, 659–664 (2013).

155. Hudson, A. J. & Wieden, H.-J. Rapid generation of sequence-diverse terminator libraries and their parameterization using quantitative Term-Seq. *Synthetic Biology* **4**, (2019).

156. Ho, J. M. L., Miller, C. A., Parks, S. E., Mattia, J. R. & Bennett, M. R. A suppressor tRNA-mediated feedforward loop eliminates leaky gene expression in bacteria. *Nucleic Acids Research* **49**, e25–e25 (2021).

157. Greco, F. V., Pandi, A., Erb, T. J., Grierson, C. S. & Gorochowski, T. E. Harnessing the central dogma for stringent multi-level control of gene expression. *Nature Communications* **12**, 1–11 (2021).

158. Wang, T. & Simmel, F. C. Riboswitch-inspired toehold riboregulators for gene regulation in Escherichia coli. *Nucleic Acids Research* **50**, 4784–4798 (2022).

159. Espah Borujeni, A., Zhang, J., Doosthosseini, H., Nielsen, A. A. K. & Voigt, C. A. Genetic circuit characterization by inferring RNA polymerase movement and ribosome usage. *Nature Communications* **11**, 1–18 (2020).

160. Li, B. *et al.* Real-Time Study of Rapid Spread of Antibiotic Resistance Plasmid in Biofilm Using Microfluidics. *Environmental Science and Technology* **52**, 11132–11141 (2018).

161. van Gestel, J. *et al.* Short-range quorum sensing controls horizontal gene transfer at micron scale in bacterial communities. *Nature Communications* **12**, 1–11 (2021).

162. Alexander, H. K. & Craig MacLean, R. Stochastic bacterial population dynamics restrict the establishment of antibiotic resistance from single cells. *Proceedings of the National Academy of Sciences of the United States of America* **117**, 19455–19464 (2020).

163. Sheets, M. B., Tague, N. & Dunlop, M. J. An optogenetic toolkit for light-inducible antibiotic resistance. *Nature Communications* **14**, 1034 (2023).

164. Hernández Lozada, N. J. *et al.* Highly Active C 8 -Acyl-ACP Thioesterase Variant Isolated by a Synthetic Selection Strategy. *ACS Synthetic Biology* **7**, 2205–2215 (2018).

165. Yurtsev, E. A., Chao, H. X., Datta, M. S., Artemova, T. & Gore, J. Bacterial cheating drives the population dynamics of cooperative antibiotic resistance plasmids. *Molecular Systems Biology* **9**, 683 (2013).

166. Sattayawat, P., Sofian Yunus, I. & Jones, P. R. Bioderivatization as a concept for renewable production of chemicals that are toxic or poorly soluble in the liquid phase. *Proceedings of the National Academy of Sciences of the United States of America* **117**, 1404–1413 (2020).

167. Engler, C., Kandzia, R. & Marillonnet, S. A one pot, one step, precision cloning method with high throughput capability. *PLoS ONE* **3**, e3647 (2008).

168. Ledermann, R., Strebel, S., Kampik, C. & Fischer, H. M. Versatile vectors for efficient mutagenesis of Bradyrhizobium diazoefficiens and other alphaproteobacteria. *Applied and Environmental Microbiology* **82**, 2791–2799 (2016).

169. Salis, H. M., Mirsky, E. A. & Voigt, C. A. Automated design of synthetic ribosome binding sites to control protein expression. *Nature Biotechnology* **27**, 946–950 (2009).

170. Wiegand, I., Hilpert, K. & Hancock, R. E. W. Agar and broth dilution methods to determine the minimal inhibitory concentration (MIC) of antimicrobial substances. *Nature Protocols* **3**, 163–175 (2008).

171. CLSI. *M07. Methods for Dilution of Antimicrobial Susceptibility Tests for Bacteria That Grow Aerobically.* (11th edition) (2018). Clinical and Laboratory Standards Institute

172. Sieuwerts, S., De Bok, F. A. M., Mols, E., De Vos, W. M. & Van Hylckama Vlieg, J. E. T. A simple and fast method for determining colony forming units. *Letters in Applied Microbiology* **47**, 275–278 (2008).

173. O'Connor, O. M., Alnahhas, R. N., Lugagne, J. B. & Dunlop, M. J. DeLTA 2.0: A deep learning pipeline for quantifying single-cell spatial and temporal dynamics. *PLoS Computational Biology* **18**, e1009797 (2022).

174. Lugagne, J.-B., Blassick, C. M. & Dunlop, M. J. Deep model predictive control of gene expression in thousands of single cells. *bioRxiv* 2022.10.28.514305 (2022) doi:10.1101/2022.10.28.514305.

175. Zhang, F. *et al.* Enhancing fatty acid production by the expression of the regulatory transcription factor FadR. *Metabolic Engineering* **14**, 653–660 (2012).

176. Sarria, S., Bartholow, T. G., Verga, A., Burkart, M. D. & Peralta-Yahya, P. Matching Protein Interfaces for Improved Medium-Chain Fatty Acid Production. *ACS Synthetic Biology* **7**, 1179–1187 (2018).

177. Pédelacq, J.-D., Cabantous, S., Tran, T., Terwilliger, T. C. & Waldo, G. S. Engineering and characterization of a superfolder green fluorescent protein. *Nature Biotechnology* **24**, 79–88 (2006).

178. Shaner, N. C. *et al.* Improved monomeric red, orange and yellow fluorescent proteins derived from Discosoma sp. red fluorescent protein. *Nature Biotechnology* **22**, 1567–1572 (2004).

179. Gadella, T. W. J. *et al.* mScarlet3: a brilliant and fast-maturing red fluorescent protein. *Nature Methods* **20**, 541–545 (2023).

180. Elowitz, M. B. & Leibier, S. A synthetic oscillatory network of transcriptional regulators. *Nature* **403**, 335–338 (2000).

181. Kim, S. W. *et al.* Outer membrane vesicles from β-lactam-resistant Escherichia coli enable the survival of β-lactam-susceptible E. coli in the presence of β-lactam antibiotics. *Scientific Reports* **8**, 1–13 (2018).

182. Bielaszewska, M. *et al.* In Vivo Secretion of β-Lactamase-Carrying Outer Membrane Vesicles as a Mechanism of β-Lactam Therapy Failure. *Membranes* **11**, 806 (2021).

183. Liu, Z. *et al.* Systematic comparison of 2A peptides for cloning multi-genes in a polycistronic vector. *Scientific Reports* **7**, 2193 (2017).

184. Wen, X., Langevin, A. M. & Dunlop, M. J. Antibiotic export by efflux pumps affects growth of neighboring bacteria. *Scientific Reports* **8**, 1–9 (2018).

185. Wang, P. *et al.* Robust Growth of Escherichia coli. *Current Biology* **20**, 1099–1103 (2010).

186. Lugagne, J.-B., Lin, H. & Dunlop, M. J. DeLTA: Automated cell segmentation, tracking, and lineage reconstruction using deep learning. *PLoS Computational Biology* **16**, e1007673 (2020).

187. Bergmiller, T. *et al.* Biased partitioning of the multidrug efflux pump AcrAB-TolC underlies long-lived phenotypic heterogeneity. *Science* **356**, 311–315 (2017).

188. Si, F. *et al.* Mechanistic Origin of Cell-Size Control and Homeostasis in Bacteria. *Current Biology* **29**, 1760-1770.e7 (2019).

189. Chait, R., Ruess, J., Bergmiller, T., Tkačik, G. & Guet, C. C. Shaping bacterial population behavior through computer-interfaced control of individual cells. *Nature Communications* **8**, 1535 (2017).

190. Dal Co, A., van Vliet, S., Kiviet, D. J., Schlegel, S. & Ackermann, M. Short-range interactions govern the dynamics and functions of microbial communities. *Nature Ecology & Evolution* **4**, 366–375 (2020).

191. Yang, Y. S. & Hughes, T. E. Cre Stoplight: A Red/Green Fluorescent Reporter of Cre Recombinase Expression in Living Cells. *BioTechniques* **31**, 1036–1041 (2001).

192. Ash, C., Dubec, M., Donne, K. & Bashford, T. Effect of wavelength and beam width on penetration in light-tissue interaction using computational methods. *Lasers in Medical Science* **32**, 1909–1918 (2017).

193. Zhou, Y. *et al.* A small and highly sensitive red/far-red optogenetic switch for applications in mammals. *Nature Biotechnology* **40**, 262–272 (2022).

194. Buchholz, F., Angrand, P.-O. & Stewart, A. F. Improved properties of FLP recombinase evolved by cycling mutagenesis. *Nature Biotechnology* **16**, 657–662 (1998).

195. Raymond, C. S. & Soriano, P. High-Efficiency FLP and ΦC31 Site-Specific Recombination in Mammalian Cells. *PLoS ONE* **2**, e162 (2007).

196. Raghavan, A. R., Salim, K. & Yadav, V. G. Optogenetic Control of Heterologous Metabolism in E. coli. *ACS Synthetic Biology* **9**, 2291–2300 (2020).

197. Kuwasaki, Y. *et al.* A red light–responsive photoswitch for deep tissue optogenetics. *Nature Biotechnology* **40**, 1672–1679 (2022).

198. Velappan, N., Sblattero, D., Chasteen, L., Pavlik, P. & Bradbury, A. R. M. Plasmid incompatibility: more compatible than previously thought? *Protein Engineering, Design and Selection* **20**, 309–313 (2007).

199. Zoltowski, B. D. & Crane, B. R. Light Activation of the LOV Protein Vivid Generates a Rapidly Exchanging Dimer. *Biochemistry* **47**, 7012–7019 (2008).

200. Wang, X., Chen, X. & Yang, Y. Spatiotemporal control of gene expression by a light-switchable transgene system. *Nature Methods* **9**, 266–269 (2012).

201. Zoltowski, B. D., Vaccaro, B. & Crane, B. R. Mechanism-based tuning of a LOV domain photoreceptor. *Nature Chemical Biology* **5**, 827–834 (2009).

202. Zhang, Z. & Lutz, B. Cre recombinase-mediated inversion using lox66 and lox71: method to introduce conditional point mutations into the CREB-binding protein. *Nucleic Acids Research* **30**, e90 (2002).

203. Schnütgen, F. *et al.* A directional strategy for monitoring Cre-mediated recombination at the cellular level in the mouse. *Nature Biotechnology* **21**, 562–565 (2003).

204. Green, A. A., Silver, P. A., Collins, J. J. & Yin, P. Toehold switches: de-novo-designed regulators of gene expression. *Cell* **159**, 925–939 (2014).

205. Zadeh, J. N. *et al.* NUPACK: Analysis and design of nucleic acid systems. *Journal of Computational Chemistry* **32**, 170–173 (2011).

206. Kim, J. *et al.* De novo-designed translation-repressing riboregulators for multi-input cellular logic. *Nature Chemical Biology* **15**, 1173–1182 (2019).

207. Galarneau, A., Primeau, M., Trudeau, L.-E. & Michnick, S. W. β-Lactamase protein fragment complementation assays as in vivo and in vitro sensors of protein–protein interactions. *Nature Biotechnology* **20**, 619–622 (2002).

208. Yu, Y. & Lutz, S. Circular permutation: a different way to engineer enzyme structure and function. *Trends in Biotechnology* **29**, 18–25 (2011).

209. Higgins, S. A., Ouonkap, S. V. Y. & Savage, D. F. Rapid and Programmable Protein Mutagenesis Using Plasmid Recombineering. *ACS Synthetic Biology* **6**, 1825–1833 (2017).

210. Dolberg, T. B. *et al.* Computation-guided optimization of split protein systems. *Nature Chemical Biology* **17**, 531–539 (2021).

CURRICULUM VITAE